

journal
of **ENGINEERING
SCIENCE**



TECHNICAL UNIVERSITY OF MOLDOVA

JOURNAL OF ENGINEERING SCIENCE

**Technical and applied scientific publication founded in 9 February 1995
Alternative title: Meridian ingineresc**

**2020
Vol. XXVII (1)**

**ISSN 2587-3474
eISSN 2587-3482**

**TECHNICAL UNIVERSITY OF MOLDOVA (PUBLISHING HOUSE)
„TEHNICA UTM” (PRINTING HOUSE)**

According to the Decision of the NAQAER No. 19 from 06.12.2019, JES is classified as B+ journal

Main subjects areas of the Journal of Engineering Science:

A. Industrial Engineering

- Mechanical Engineering and Technologies
- Applied Engineering Sciences and Management
- Materials Science and New Technologies
- Electrical Engineering and Power Electronics
- Energy systems
- Light Industry, New Technologies and Design
- Industrial and Applied Mathematics
- Vehicle and Transport Engineering

B. Electronics and Computer Science

- Electronics and Communication
- Microelectronics and Nanotechnologies
- Biomedical Engineering
- Computers and Information Technology
- Automation

C. Architecture, Civil and Environmental Engineering

- Architecture, Urbanism and Cadaster
- Civil Engineering and Management
- Energy Efficiency and New Building Materials
- Environmental Engineering

D. Food Engineering

- Food Technologies and Food Processes
- Food Industry and Management
- Biotechnologies, Food Chemistry and Food Safety
- Equipment for Food Industries

The structure of the journal corresponds to the classification of scientific publications:
Engineering, Multidisciplinary.

How to publish a paper:

1. Send the manuscript and information about the author to the **Editorial Board address:**
jes@meridian.utm.md
2. Manuscripts are accepted only in English, by e-mail, in template file (www.jes.utm.md)
3. After a review, you will be notified of the editorial board's decision.
4. After the Journal has been published, we will send it to you immediately by mail.

Editor-in-Chief

Dr. hab. prof. univ. Viorel BOSTAN

Technical University of Moldova

viorel.bostan@adm.utm.md

Editorial Board

Abdelkrim Azzouz, Dr. Ing., Professor, Quebec University of Montreal, Canada
Adrian Gheorghe, PhD, Professor Old Dominion University, Norfolk, Virginia, 23529, USA
Adrian Graur, PhD, Professor University „Ștefan cel Mare”, Suceava, Romania
Cornel Ciupan, PhD, Professor Technical University of Cluj Napoca, Romania
Cristoph Ruland, PhD, Professor, University of SIEGEN, Germany
Dimitr P. Karaivanov, Dr.Sc., PhD, Professor University of Chemical Technology and Metallurgy, Sofia, Bulgaria
Dumitru Mnerie, PhD, Professor „Politehnica”University of Timișoara, Romania
Dumitru Olaru, PhD, Professor Technical University „Gh. Asachi”, Iași, Romania
Florin Ionescu, PhD, Professor University Steinbes, Berlin, Germany
Frank Wang Professor of Future Computing, University of Kent, U.K.
Gabriel Neagu Profesor Institutul Național de Cercetare-Dezvoltare în Informatică București,
George S. Dulikravich, PhD, Florida International University, U.S.A.
Gheorghe Badea, Ph.Dr. in Engineering, Professor, Technical University of Civil Engineering Bucharest, Romania
Gheorghe Manolea, PhD, Professor University of Craiova, Romania
Grigore Marian, Dr.Sc., PhD, Professor Agrarian State University of Moldova, Chișinău, Republic of Moldova
Hai Jiang, Ph.D. Professor, Department of Computer Science, Arkansas State University, U.S.A.
Heinz Frank, PhD, Professor Reinhold Würth University, Germany
Hidenori Mimura, Professor, Research Institute of Electronics, Shizuoka University, Japan
Ion Bostan, Dr.hab., Acad. Academy of Science, Republic of Moldova
Ion Paraschivoiu, PhD, Professor Universite Technologique de Montreal, Canada
Ion Rusu, Dr. hab. Professor, Technical University of Moldova
Ion Tighineanu, Dr.hab., Acad. Academy of Science, Moldova
Ion Vișa, PhD, Professor University Transilvania of Brașov, Romania
Jorj. Ciumac, Dr., Professor, Technical University of Moldova
Laurențiu Slătineanu, PhD, Professor Technical University „Gh. Asachi”, Iași, Romania
Lee Chow, PhD, Professor, University of Central Florida, USA
Leonid Culiuc, Dr.hab., Acad. ASM, Institute of Applied Physic
Livia Nistor-Lopatenco, Ph.Dr. in Engineering, Associate Professor, Technical University of Moldova
Mardar Maryna, Doctor of Technical Science, Professor, Odessa National Academy of Food Technologies, Odessa, Ukraine
Mircea Bernic, Dr. hab., Professor, Technical University of Moldova
Mitrofan Ciobanu, academic MAS, Dr.Sc.,PhD, Professor Tiraspol State University, Chișinău, Republic of Moldova
Natalia Tislinschi, Dr., Ass. Professor, Technical University of Moldova
Oleg Lupan Dr.hab. Professor, Technical University of Moldova
Pavel Tatarov, Dr. hab., Professor, Technical University of Moldova
Pavel Topală, Dr.Sc., PhD, Professor, State University „Aleco Russo” from Bălți, Republic of Moldova
Peter Lorenz, PhD, Professor University of Applied Science Saar, Saarbrucken, Germania
Petru Cașcaval, PhD, Professor, ”Gheorghe Asachi” Technical University of Iasi, Romania

Petru Stoicev, Dr.Sc., PhD, Professor, Technical University of Moldova, Chişinău, Republic of Moldova
Polidor Bratu, PhD, academic RATS, president ICECON S.A. Bucureşti, Romania
Radu Munteanu, PhD, Professor Technical University of Cluj Napoca, Romania
Radu Sorin Văcăreanu, Dr. hab. Professor, Technical University of Civil Engineering Bucharest, Romania
Sergiu Zaporojan Dr., Professor, Technical University of Moldova
Spiridon Creţu, PhD, Professor Technical University „Gh. Asachi”, Iaşi, Romania
Eden Mamut, PhD, Professor University „Ovidius” Constanţa, România
Stanislav Legutko, PhD, Professor Poznan University of Technology, Poland
Rafał Gołębski, Dr., Ass. Professor, Czestochowa University of Technology, Poland
Stefan Tvetanov, Dr., Professor, University of Food Technologies, Bulgaria
Ştefan-Gheorghe Pentiuc, Dr., Professor, University “Stefan cel Mare” of Suceava, Romania
Svetlana Albu, Dr. hab. Professor, Technical University of Moldova
Thomas Luhmann, Dr-Ing. habil. Dr. h.c. Professor, Jade University of Applied Sciences, Germany
Tudor Ambros, Dr.Sc., PhD, Professor, Technical University of Moldova, Chişinău, Republic of Moldova
Valentin Arion, Dr.Sc., PhD, Professor, Technical University of Moldova, Chişinău, Republic of Moldova
Valentina Bulgaru, PhD, Assoc. professor, Technical University of Moldova, Chişinău, Republic of Moldova
Valeriu Dulgheru, Dr.Sc., PhD, Professor, Technical University of Moldova, Chişinău, Republic of Moldova
Vasile Tronciu Dr.hab. Professor, Technical University of Moldova
Victor Ababii, Dr. Professor, Technical University of Moldova
Victor Şontea Dr. Professor, Technical University of Moldova
Vilhelm Kappel, PhD, Institute of Research INCDIE ICPE-CA, Bucharest, Romania
Vladimir Zavialov, Dr. hab., Professor, National University of Food Technology, Ukraine
Vladislav Resitca, Dr., Ass. Professor, Technical University of Moldova
Yogendra Kumar Mishra, Dr. habil., Kiel University, Germany
Yuri Dekhtyar, Professor, Riga Technical University, Riga, Latvia

Responsible Editor:

Dr. hab. Rodica STURZA
Technical University of Moldova
rodica.sturza@chim.utm.md

Editorial Production:

Dr. Nicolae Trifan
Dr. Svetlana Caterenciuc
Rodica Cujba

CONTENT

Abstracts	6
A. Industrial Engineering		
Badri Narayan Mohapatra, Rashmita Kumari Mohapatra	<i>Application of DC motor as speed and direction control</i>	17
B. Electronics and Computer Science		
Alisa Maşnic	<i>Birefringence and exciton spectra of CuAlSe₂ and CuAlS₂ crystals</i>	23
Titu - Marius I. Băjenescu	<i>3D Micropackaging of integrated circuits</i>	28
C. Architecture, Civil and Environmental Engineering		
Sergii Kroviakov, Lidiia Dudnyk, Michael Zavoloka	<i>Properties of structural lightweight expanded clay concrete with different types of porous sands</i>	36
Eugeniu Braguța	<i>Grounds stabilized with organic binders.....</i>	43
Diana Antonova, Michael Zavoloka, Vasyl Karpiuk, Irina Karpiuk, Ion Rusu	<i>Strength, crack resistance and deformativity of reinforced concrete beams damaged by through cracks, reinforced carbon fiber.....</i>	50
D. Food Engineering		
Mihail Balan, Mircea Bernic, Natalia Țislinscaia	<i>Drying installation for granular products in the suspension layer.....</i>	64
Oxana Radu	<i>Peculiarities of walnut oil state in some food emulsions.....</i>	69
Angela Gurev, Veronica Dragancea, Svetlana Haritonov	<i>Microalgae – non-traditional sources of nutrients and pigments for functional foods</i>	75
Natalia Vladei	<i>Influence of maceration duration on Viorica wines quality.....</i>	99
Antoanela Patras, Alina Loredana Baetu, Marius Baetu	<i>Stability of ascorbic acid during the technological processes of apricot compote fabrication</i>	107

DOI: 10.5281/zenodo.3713354
CZU 621.331.2

APPLICATION OF DC MOTOR AS SPEED AND DIRECTION CONTROL

Badri Narayan Mohapatra^{1*}, ORCID ID: 0000-0003-1906-9932,
Rashmita Kumari Mohapatra²

¹Savitribai Phule Pune University, AISSMS IOIT, Pune, INDIA

²Mumbai University, TCET, Mumbai, INDIA

*Corresponding author: Badri Narayan Mohapatra,
badri1.mohapatra@gmail.com

Received: 01. 23. 2020

Accepted: 03. 12. 2020

Abstract. Motion control plays a vital role in industrial atomization. Application wise variety type of motors like DC, AC, stepper or servo are used. Because of easier control DC motors are very popular to the users, its application is oriented very useful for rotation and speed. As speed depends on voltage applied to the terminal, smoothly can be controlled down to zero and again accelerated opposite way without using power CKT and switching CKT. Hence, if voltage across motor terminal is varied, then speed can also be varied. One of the best controlling method for DC motor is armature voltage control method using PWM. Speed of the motors depends on the variation of the duty cycles. Direction control can be achieved by the same microcontroller using slight modifications in its programming language. Depending on the application speed range vary in DC motor. Analysis and design of any system in real time can be easily implemented by hardware technology also by smart software. A motor driver IC is interfaced to the microcontroller for receiving PWM signals and delivering desired output for speed control of a small DC motor. The combination provides smooth speed control in both clockwise as well as anticlockwise direction.

Keywords: *DC motor, PWM signal, Proteus simulation, PIC 18F4550, speed and direction control.*

Rezumat. Controlul mișcării joacă un rol esențial în atomizarea industrială. Se folosesc tipuri variate de motoare precum DC, AC, stepper sau servo. Datorită controlului ușor de realizat, motoarele DC sunt foarte populare printre utilizatori. Aplicația lor este orientată foarte util pentru rotire și viteză. Viteza depinde de tensiunea aplicată terminalului și poate fi controlată până la zero și din nou accelerată în sens invers, fără a folosi puterea CKT și comutarea CKT. Prin urmare, dacă tensiunea pe terminalul motorului variază, viteza poate fi, de asemenea, variată. Una dintre cele mai bune metode de control pentru motorul DC este metoda de control a tensiunii armăturii folosind PWM. Viteza motoarelor depinde de variația ciclurilor de serviciu. Controlul direcției poate fi realizat de același microcontroler folosind ușoare modificări în limbajul său de programare. În funcție de aplicație, intervalul de viteză variază în motorul DC. Analiza și proiectarea oricărui sistem în timp real poate fi pusă în aplicare cu ușurință de tehnologia hardware, de asemenea, prin software inteligent. Un driver de motor IC este interfațat cu microcontrolerul pentru primirea semnalelor PWM și furnizarea de ieșire dorită pentru controlul vitezei unui mic motor DC. Combinația asigură un control lin al vitezei atât în sensul acelor de ceasornic, cât și în sensul contrar acelor de ceasornic.

Cuvinte cheie: *motor DC, semnal PWM, simulare Proteus, PIC 18F4550, control de viteză și direcție.*

DOI: 10.5281/zenodo.3713358
CZU 535.343.2+544.22

BIREFRINGENCE AND EXCITON SPECTRA OF CuAlSe_2 AND CuAlS_2 CRYSTALS

Alisa Maşnic*

Technical University of Moldova, 168, Stefan cel Mare bd. Chisinau, Republic of Moldova

*alisa.masnic@tlc.utm.md

Received: 01. 14. 2020

Accepted: 03. 16. 2020

Abstract. The excitonic reflection spectra of CuAlS_2 and CuAlSe_2 crystals were measured at the temperature of 10 K for polarizations $E||c$ and $E\perp c$. Ground and excited states of the excitons were found out in the investigated spectra. Symmetries of the observed excitons were determined. The shapes of ground states lines of Γ_4 and Γ_5 excitons were calculated by means of the Kramers-Kronig relations. Exciton parameters and values of energetic gaps ($\Gamma_7-\Gamma_6$, $\Gamma_6-\Gamma_6$, and $\Gamma_7-\Gamma_6$) were determined. Optical reflection spectra in the depth of absorption band ($E_g - 6$ eV) were measured at 80 K for $E||c$ and $E\perp c$ polarizations. Optical constants were calculated from measured reflection spectra by Kramers-Kronig analysis. The phase in the excitonic region was determined. Transmission spectra of CuAlSe_2 single crystals deposit in crossed polarizers demonstrate a birefractive effect. In the case of parallel polarizers interference due to birefracton was observed. The isotropic point was determined.

Keywords: *absorption and reflection spectra, excitons, polaritons, birefringence.*

Rezumat. Spectrele excitonice de reflecție ale cristalelor CuAlS_2 și CuAlSe_2 au fost măsurate la temperatura de 10 K pentru polarizările $E || c$ și $E \perp c$. În spectrele cercetate au fost descoperite stări de bază și nivelele excitonice. S-au determinat simetriile excitonilor observați. Formele liniilor stărilor de bază ale excitonilor Γ_4 și Γ_5 au fost calculate prin intermediul relațiilor Kramers-Kronig. S-au determinat parametrii și valorile excitonului lacunelor energetice ($\Gamma_7-\Gamma_6$, $\Gamma_6-\Gamma_6$ și $\Gamma_7-\Gamma_6$). Spectrele de reflecție optică în adâncimea benzii de absorbție ($E_g - 6$ eV) au fost măsurate la 80 K pentru polarizările $E || c$ și $E \perp c$. Constanțele optice au fost calculate din spectrele de reflecție măsurate prin analiza Kramers-Kronig. Faza în regiunea excitonică a fost determinată. Spectrele de transmisie ale compusului CuAlSe_2 în polarizatoare încrucișate demonstrează un efect birefractiv. În cazul polarizatorilor paraleli s-a observat interferența datorată birefracției. A fost determinat punctul izotrop al cristalelor.

Cuvinte cheie: *spectre de absorbție și reflecție, excitoni, polaritoni, birefringență.*

DOI: 10.5281/zenodo.3713360
CZU 621.3.049.77

3D MICROPACKAGING OF INTEGRATED CIRCUITS

Titu-Marius I. Băjenescu*, ORCID ID: 0000-0002-9371-6766

Swiss Technology Association, Electronics Group Switzerland

**tmbajenesco@gmail.com*

Received: 01. 15. 2020

Accepted: 03. 05. 2020

Abstract. A major paradigm change, from 2D IC to 3D IC, is occurring in microelectronic industry. Joule heating is serious in 3D IC, and vertical interconnect is the critical element to be developed. Also, reliability concerns will be extremely important: electromigration and stress-migration. This paper presents some actual problems and reliability challenges in 3D IC packaging technology. It shows how different architectures have evolved to meet the specific needs of different markets: Multi Chip Module (MCP); Multipackage module (MPM); Embedded SIP modules; SIP package-on-package (PoP) modules; EMIB (Embedded Multi-die Interconnect Bridge); Silicon-based SIP-Module; 3D-TSV stacked module; SIP variants with combinations of wideband and flip-chip interconnects. Causes of blockages and failure mechanisms, as well as problems with predictive reliability, which will need to be developed in the coming years, are analysed.

Keywords: *prototypage virtuel, Moore's Law, analyse des compromis, reliability.*

Rezumat. O modificare majoră de paradigmă, de la 2D IC la 3D IC, se produce în industria microelectronică. Încălzirea Joule este gravă în 3D IC, iar interconectarea verticală este elementul critic care trebuie dezvoltat. De asemenea, preocupările privind fiabilitatea vor fi extrem de importante: electromigrare și migrare la stres. Această lucrare prezintă unele probleme reale și provocări de fiabilitate în tehnologia de ambalare 3D IC. Este aratat cum au evoluat diferite arhitecturi pentru a satisface nevoile specifice pentru diferite piețe. Este prezentat modul în care diferite arhitecturi au evoluat pentru a răspunde nevoilor specifice ale pieței: Multi Chip Module (MCP); Modul multipackage (MPM); Module SIP încorporate; Module SIP package-on-package (PoP); EMIB (podul de interconectare multi-die încorporat); Modul SIP bazat pe silicon; Modul stivuit 3D-TSV; Variante SIP cu combinații de interconectări cu bandă largă și flip-chip. Sunt analizate cauzele blocajelor și mecanismele de eșec, precum și probleme legate de fiabilitatea predictivă, care va trebui să fie dezvoltată în anii următori.

Cuvinte cheie: *prototipaj virtual, legea Moore, analiza de compromis, fiabilitate.*

DOI: 10.5281/zenodo.3713362
CZU 666.973

PROPERTIES OF STRUCTURAL LIGHTWEIGHT EXPANDED CLAY CONCRETE WITH DIFFERENT TYPES OF POROUS SANDS

Sergii Kroviakov*, ORCID ID: 0000-0002-0800-0123,
Lidiia Dudnyk, ORCID ID: 0000-0002-9969-8941,
Michael Zavoloka, ORCID ID: 0000-0002-2080-1230

Odessa State Academy of Civil Engineering and Architecture, str. Didrichsona, 4, Odessa, Ukraine

*Corresponding author: Sergii Kroviakov, *skrovyakov@ukr.net*

Received: 02. 18. 2020

Accepted: 03. 24. 2020

Abstract. In this work, the strength, water tightness and average density of modified expanded clay lightweight on different types of sands were investigated. Quartz sand, expanded clay sand and sand from granulated foam glass were used. It is shown that structural lightweight expanded clay concrete on light sand from granular foam glass is effective for thin-walled structures of hydraulic structures, if necessary, to reduce their weight. It was established that the average density of lightweight expanded clay concrete on a mixture of quartz sand and granulated foam glass is 1400-1440 kg/m³, water tightness is W10-W12, compressive strength up to 21 MPa, tensile strength in bending up to 5 MPa. Interstitial partitions of foam glass have an amorphous vitreous structure. The lightweight expanded clay concrete with sand of granulated foam glass has a high-water resistance and sufficient strength for thin-walled structures.

Keywords: *concrete, density, expanded clay, foam glass, sand, water tightness.*

Rezumat. În lucrare au fost cercetate rezistența, etanșeitatea față de apă și densitatea medie a betonului ușor din argilă expandată modificată pe diferite tipuri de nisip. S-au utilizat nisip de cuarț, nisip argilos expandat și nisip din sticlă cu spumă granulată. A fost demonstrat, că betonul din argilă expandată pe nisip ușor din sticlă granulată este eficient pentru structurile hidraulice cu pereți subțiri, pentru a reduce greutatea acestora. S-a stabilit, că densitatea medie a betonului ușor din argilă expandată pe un amestec de nisip de cuarț și sticlă cu spumă granulată este de 1400-1440 kg/m³, etanșeitatea la apă - W10-W12, rezistența la compresiune până la 21 MPa, rezistență la tracțiune de îndoire până la 5 MPa. Partițiile interstițiale ale spumei de sticlă au o structură vitroasă amorfă. Betonul ușor din lut expandat cu nisip din spumă de sticlă granulată are o rezistență sporită la apă și o rezistență suficientă pentru structurile cu pereți subțiri.

Cuvinte cheie: *beton, densitate, argilă expandată, spumă de sticlă, nisip, etanșare la apă.*

DOI: 10.5281/zenodo.3713364
CZU 524.131.5

GROUNDS STABILIZED WITH ORGANIC BINDERS

Eugeniu Braguța*, ORCID ID: 0000-0001-9579-1033

Technical University of Moldova, 168, Stefan cel Mare Bd., Chisinau, Republic of Moldova

*eugeniu.braguta@dmmc.utm.md

Received: 02. 05. 2020

Accepted: 03. 22. 2020

Abstract. The paper presents the enzymatic stabilizers effect on grounds in the compaction process by vibration. It has been intended, by specific rheological modeling of the ground mixtures with organic additives, as well as by laboratory or "in situ" tests, to highlight the increased effect of elasticity longitudinal modulus and volumetric elasticity. Also, based on experiments it was determined the rheological evolution of the bulk modulus in relation to time up to the asymptotic stabilization specific to the final parametric values of the structure resistance and stability. The analytic assessment performed by modeling, as well as the experimental results significantly highlight the enzyme stabilizer effect. Thus, it is distinguished that by the pore size and the enzyme content modification, as a result of the recycled ground dynamic behavior, the Poisson's ratio increases considerably, reaching the value of 0.485. The experimental results confirm the possibility to increase the resistance and stability of ground road structures stabilized with enzymes. In this context, the compaction process by vibrations has to be performed in the optimal dynamic regime for the substantial modification of the material porosity.

Keywords: *Organic additives, longitudinal modulus of elasticity and volumetric elasticity, recycled ground dynamic behavior, enzyme stabilizer, Poisson's ratio.*

Rezumat. În lucrare este analizat efectul stabilizatorilor enzimatici asupra solurilor în procesul de compactare prin vibrații. Prin modelare reologică specifică și încercări de laborator „in situ” a amestecurilor de soluri cu adaosuri organice a fost urmărit efectul de mărire a modulului de elasticitate longitudinală și volumică. A fost determinată evoluția reologică a modulului volumic în timp până la stabilizarea asimptotică specifică valorilor parametrice finale ale rezistenței și stabilității structurii. Atât evaluarea analitică prin modelare, cât și rezultatele experimentale evidențiază efectul stabilizatorului enzimatic. Astfel, se distinge că prin mărirea porilor și modificarea conținutului de enzime, ca urmare a comportamentului dinamic al solului reciclat, raportul Poisson crește considerabil, atingând valoarea de 0,485. Rezultatele experimentale confirmă posibilitatea creșterii rezistenței și stabilității structurilor rutiere de la sol stabilizate cu enzime. În acest context, procesul de compactare prin vibrații trebuie efectuat în regim dinamic optim pentru modificarea substanțială a porozității materialului.

Cuvinte cheie: *Aditivi organici, modul de elasticitate longitudinală și volumică, comportare dinamică a pământurilor reciclate, stabilizatori enzimatici, raport Poisson.*

DOI: 10.5281/zenodo.3713366
CZU 624.012.45

STRENGTH, CRACK RESISTANCE AND DEFORMATIVITY OF REINFORCED CONCRETE BEAMS DAMAGED BY THROUGH CRACKS, REINFORCED CARBON FIBER

Diana Antonova^{1*}, ORCID: 0000-0001-9021-857X,
Michael Zavoloka¹, ORCID: 0000-0002-2080-1230,
Vasyl Karpiuk¹, ORCID: 0000-0002-4088-6489,
Irina Karpiuk¹, ORCID: 0000-0003-3437-5882,
Ion Rusu², ORCID ID: 0000-0002-7507-638X

¹Odessa State Academy of Civil Engineering and Architecture, Didrichson street, 4, Odessa, Ukraine

²Technical University of Moldova, 168, Bd. Stefan cel Mare, Chisinau, Moldova

*Corresponding author: Diana Antonova, antonova.dv@ukr.net

Received: 01. 14. 2020

Accepted: 03. 19. 2020

Abstract. The article deals with the main results of experimental studies of strength, crack resistance and informational content of the diagonal and normal sections of common damaged and brought to the critical state of the first group r. c. - beams reinforced with carbon fibre sheet in the lower tensioned zone and on the support area. According to the adopted methodology, an experiment was conducted on the four-factor three-level Box-Benkin B4 plan. The average relative deformation values of the compressed concrete in the middle part of beams after their stabilization under low-cycle static loading have been evaluated. Tests of prototypes were carried out according to the scheme of single-track free-beam, alternately loaded from above, then from below by two concentrated forces without changing its position.

Keywords: *concrete, reinforcement, carbon fibre-reinforced polymer sheet, reinforced concrete beam, transverse loading, strength, deformations.*

Rezumat. În articol sunt prezentate principalele rezultate ale studiilor experimentale privind rezistența la fisurare și conținutul informațional al secțiunilor diagonale și normale ale părților deteriorate și aduse la starea critică din primul grup r. c.- grinzi întărite cu tablă din fibră de carbon în zona tensionată inferioară și pe zona de sprijin. Conform metodologiei adoptate, un experiment a fost realizat pe planul B4 Box-Benkin B4 cu trei factori. Au fost evaluate valorile medii de deformare relativă a betonului comprimat în partea de mijloc a grinzilor după stabilizarea lor în condiții de încărcare statică cu ciclu scăzut. Testele de prototipuri au fost efectuate conform schemei cu fascicul liber cu o singură cale, încărcate alternativ de sus, apoi de jos de două forțe concentrate, fără schimb de poziție.

Cuvinte cheie: *beton, armare, foaie de polimer armat cu fibră de carbon, grindă din beton armat, încărcare transversală, rezistență, deformări.*

DOI: 10.5281/zenodo.3713368
CZU 66.047.75

DRYING INSTALLATION FOR GRANULAR PRODUCTS IN THE SUSPENSION LAYER

Mihail Balan*, ORCID ID: 0000-0002-7788-345X,
Mircea Bernic, ORCID ID: 0000-0001-6166-6947,
Natalia Țislinscaia, ORCID ID: 0000-0003-3126-5792

Technical University of Moldova, 168, Stefan cel Mare bd., Chișinău, Republic of Moldova

*Corresponding author: Mihail Balan, mihail.balan@pmi.utm.md

Received: 01. 09. 2020

Accepted: 03. 18. 2020

Abstract. One of the main problems of wet plant products drying processes is the long duration of thermal tartarization, which consequently leads to the diminution of the quality indices. This problem is exacerbated in the case of oil products drying, high in fatty acids receptive to oxidation processes. For such products, especially granulation, as grape seeds are, drying in a suspended layer with microwave application is beneficial. This method allows automatic selection of already dried particles from the seed table and removing them from the heating zone, thus ensuring a maximum reduction of heat treatment time, so also favorable conditions for oxidation of fatty acids. The paper presents the construction of a laboratory installation for the study of the kinetics of drying processes in suspended layer with microwave application. The installation allows the online recording of the temperature, speed and humidity of the air in oilseeds and out and periodic recording of the mass decrease of the product.

Keywords: *oilseeds, grape seeds, suspension layer, drying, internal heat source.*

Rezumat. Una dintre problemele principale ale proceselor de uscare a produselor vegetale umede este durata îndelungată a tartarizării termice, ceea ce duce la diminuarea indicilor de calitate. Această problemă este agravată în cazul uscării semințelor oleaginoase, bogate în acizi grași receptivi la procesele de oxidare. Pentru astfel de produse, în special granulate, așa cum sunt semințele de struguri, uscarea într-un strat suspendat cu aplicare cu microunde este benefică. Această metodă permite selectarea automată a particulelor deja uscate de pe masa de semințe și îndepărtarea lor din zona de încălzire, asigurând astfel o reducere maximă a timpului de tratament termic. Lucrarea prezintă construcția unei instalații de laborator pentru studiul cineticii proceselor de uscare în strat suspendat cu aplicare la microunde. Instalarea permite înregistrarea online a temperaturii, vitezei și umidității aerului în semințele oleaginoase și în afara și înregistrarea periodică a scăderii în masă a produsului.

Cuvinte cheie: *oleaginoase, semințe de struguri, strat suspendat, uscare, sursă internă de căldură.*

DOI: 10.5281/zenodo.3713370
CZU 664.3

PECULIARITIES OF WALNUT OIL STATE IN SOME FOOD EMULSIONS

Oxana Radu*, 0000-0001-9260-6314

Technical University of Moldova, 168, Stefan cel Mare bd., Chisinau, Republic of Moldova

*oxana.radu@sa.utm.md

Received: 12. 22. 2019

Accepted: 02. 24. 2020

Abstract. The replacing of traditional lipids with more health-promoting oils containing polyunsaturated fatty acids (PUFA) is a modern trend in food industry. The principles of emulsions formation containing walnut oil (up to 90% PUFA) were studied in order to accumulate information that would help to design new functional products. The phase diagrams of the state of three-component systems – *Walnut oil / Water / Ethanol* and *Walnut oil / Polyphenol extract / Water* were investigated. It was shown that walnut oil was more prone to form W/O emulsions than O/W ones, that can possibly be explained by the presence of natural surfactants in it. This property of walnut oil was used within the functional spread obtaining. It has been established that the elaborated product represents an emulsion, in which water micelles and air inclusions are dispersed in continuous lipid phase, consisting of solid lipids. Withal, the structure stability of spread rich in PUFA from walnut oil was ascertained being almost analogous to milk-based butter, retaining its functionality and high biological value within a month at the temperature regime up to 5°C.

Keywords: *polyunsaturated fatty acids, microstructure, phase diagrams, spread, aggregative stability.*

Rezumat. În industria alimentară se remarcă o tendință modernă de a înlocui lipidele tradiționale cu uleiurile benefice pentru organismul uman datorită conținutului înalt de acizi grași polinesaturați (AGPN). Principiile formării emulsiilor pe baza de ulei de nucă (până la 90% AGPN) au fost studiate pentru a acumula informații care ar ajuta la elaborarea produselor funcționale noi. Au fost cercetate diagramele de fază ale stării sistemelor tricomponente – *Ulei de nucă / Apă / Etanol* și *Ulei de nucă / Extract de polifenoli / Apă*. S-a demonstrat, că uleiul de nucă era mai predispus la formarea emulsiilor de tip A/U, decât la cele U/A, ceea ce poate fi explicat prin prezența agenților tensioactivi naturali în compoziția sa. Această proprietate a uleiului de nucă a fost utilizată la obținerea spread-ului funcțional. S-a stabilit, că produsul elaborat reprezintă o emulsie, în care micellele de apă și incluziunile de aer sunt dispersate în faza lipidică continuă, formată din lipide solide. În plus, stabilitatea structurii spread-ului, bogat în AGPN din uleiul de nucă, a fost constatată ca fiind aproape asemănătoare untului clasic, păstrându-și funcționalitatea sa și valoarea biologică înaltă în decurs de o lună la regimul de temperatură până la 5°C.

Cuvinte cheie: *acizi grași polinesaturați, microstructură, diagrame de fază, spread, stabilitate agregativă.*

DOI: 10.5281/zenodo.3713372

CZU 551.464.7:664

MICROALGAE – NON-TRADITIONAL SOURCES OF NUTRIENTS AND PIGMENTS FOR FUNCTIONAL FOODS

Angela Gurev*, ORCID ID: 0000-0001-8493-5257,
Veronica Dragancea, ORCID ID: 0000-0002-5938-0410,
Svetlana Haritonov, ORCID ID: 0000-0002-9244-8982

Technical University of Moldova, 168, Stefan cel Mare bd., Chisinau, Republic of Moldova

*Corresponding author: Angela Gurev, angela.gurev@chim.utm.md

Received: 12.18.2019

Accepted: 02.28.2020

Abstract. The aim of this review is to draw the attention of researchers and technological engineers from the Moldovan food industry towards the potential of microalgae as a non-traditional source of nutrients and biological active substances, such as proteins, essential amino acids, carotenoids, vitamins, polyunsaturated fatty acids ω_3 , phytosterols, polysaccharides, phenolic acids, microelements, etc., which can be used to increase the nutritional and functional value of conventional foods. The study synthesizes information regarding the profile of biologically active substances obtained from various microalgae species, analyses the nutritional value of microalgae biomass and their field of application. This review focuses on pigments contained in microalgae (carotenoids, chlorophylls and phycobiliproteins), deals with their biological activity and health benefits. It draws attention to the results of the recent research, which proves that microalgae pigments exhibit pronounced antioxidant properties, protect cells from the radiation, capture free radicals and reduce the oxidative stress in the body, prevent cancer, inflammation and cardiovascular diseases, modulate the immune system, prevent the macular degeneration, etc. Review describes in more detail the carotenoids class and elucidates the qualitative and quantitative content of carotenoids in some microalgae. It discusses the areas of use of the pigments accumulated in microalgae and their further application as natural food additives and dyes.

Keywords: *bioactive compounds, carotenoids, chlorophylls, health benefits, food additives, phycobiliproteins, phytonutrients, xanthophylls.*

Rezumat. Scopul studiului este de a atrage atenția cercetătorilor și inginerilor tehnologi din domeniul industriei alimentare asupra microalgeor ca sursa netradițională de fitonutrienți și substanțe biologic active cum sunt proteinele, aminoacizii esențiali, carotenoizii, vitaminele, acizii polinesaturați omega ω_3 , fitosterolii, polizaharidele, acizii fenolici, microelementele, etc., care pot fi aplicați pentru sporirea valorii nutriționale și funcționale a alimentelor convenționale. Este sintetizată informația din 134 de surse bibliografice referitoare la profilul substanțelor biologic active, obținute din diferite specii de microalgae, analizată valoarea nutrițională a biomasei de microalgae și domeniile de utilizare ale acestora. Articolul este focusat pe pigmentii din microalgae (carotenoizi, clorofile și picobiliproteine), evidențiază activitatea biologică și beneficiile de sănătate ale acestora. Atrage atenția asupra rezultatelor cercetărilor recente, care demonstrează că pigmentii din microalgae manifestă proprietăți antioxidante pronunțate, protejează celulele de radiații, capturează radicalii liberi și reduc stresul oxidativ din organism, previn cancerul, inflamațiile și bolile cardiovasculare, modulează sistemul imunitar, previn degenerarea maculară, etc. Este descrisă detaliat clasa carotenoizilor, elucidat conținutul de carotenoizi în unele microalgae și oportunitatea utilizării pigmentilor din microalgae în calitate de aditivi și coloranți alimentari naturali.

Cuvinte cheie: *substanțe bioactive, carotenoizi, clorofile, beneficii de sănătate, aditivi alimentari, picobiliproteine, fitonutrienți, xantofile.*

DOI: 10.5281/zenodo.3713374
CZU 663.2:66.063.4(478)

INFLUENCE OF MACERATION DURATION ON VIORICA WINES QUALITY

Natalia Vladei*, ORCID: 0000-0003-1094-6812

Technical University of Moldova, 168, bd. Stefan cel Mare, Chisinau, Republic of Moldova

**natalia.furtuna@adm.utm.md*

Received: 01, 15, 2020

Accepted: 03, 18, 2020

Abstract. The subject of the research refers to experimental wines obtained from local selection grape variety Viorica, which were macerated for 4, 8 or 12 hours at 10, 15 and 20 °C. The maceration duration had a positive influence on the general characteristics of the studied wines. The analysis of terpenic compounds by spectro-photometric method showed that increasing the contact time of the must with the solid phase from 4 to 8 hours increases by about 20 % the amount of free terpenes, while decreasing the amount of bound terpenes by 15 %. Once the duration is increased, the concentration of the non-reducing extract is also increased. Considering the increase in the intensity of the color and the REDOX potential with the duration of maceration, the macerated wines for 8 and 12 hours were defined as having oxidation notes with decrease of the sensory quality. Therefore, the maceration regimes for optimal extraction of terpenic compounds were concluded to be at the temperature of 15 °C for 4 hours, thereby increasing the aromatic potential of the local selection grape variety Viorica.

Keywords: *aroma, flavor, local selection variety, maceration, terpenes, wine.*

Rezumat. Obiectul cercetării a fost reprezentat de nouă variante experimentale de vin obținute din soiul de struguri de selecție autohtonă Viorica, care au fost macerate timp de 4, 8 sau 12 ore la 10, 15 și 20 °C. Macerarea a avut o influență pozitivă asupra caracteristicilor generale ale vinurilor studiate. Analiza compușilor terpenici prin metoda spectrofotometrică a demonstrat că odată cu creșterea timpului de contact al mustului cu faza solidă de la 4 la 8 ore crește cu aproximativ 20% cantitatea de terpeni liberi, în timp ce scade cantitatea de terpeni legați cu 15%. Totodată are loc mărirea concentrației extractului nereducător. Având în vedere creșterea intensității culorii și a potențialului REDOX odată cu macerarea, vinurile macerate timp de 8 și 12 ore au fost definite ca având note de oxidare cu diminuarea calității senzoriale. Prin urmare, regimurile de macerare pentru extracția optimă a compușilor terpenici au fost stabilite a fi la temperatura de 15 °C timp de 4 ore, crescând astfel potențialul aromatic al soiului de struguri de selecție autohtonă Viorica.

Cuvinte cheie: *aromă, soi de struguri de selecție autohtonă, macerare, terpeni, vin.*

DOI: 10.5281/zenodo.3713376
CZU 577.164.2:664.8.036:634.21

STABILITY OF ASCORBIC ACID DURING THE TECHNOLOGICAL PROCESSES OF APRICOT COMPOTE FABRICATION

Antoanela Patras*, ORCID: 0000-0002-4054-4884,
Alina Loredana Baetu, Marius Baetu

"Ion Ionescu de la Brad" University of Agricultural Sciences and Veterinary Medicine, 3, Mihail Sadoveanu Alley, Iași, 700490, Romania

*Corresponding author: *Antoanela Patras, apatras@uaiasi.ro*

Received: 02. 18. 2020

Accepted: 03. 24. 2020

Abstract. Apricots are fruits with a short period of fresh-consumption and the compote fabrication is a usual method for their preservation. The present research is studying the changes in total vitamin C content, as well as the transformations between ascorbic acid and dehydroascorbic acid in four different phases of the technological flow of apricot compote fabrication. The ascorbate oxidase activity was also evaluated. The studied samples are represented by different stages of apricots during the technological flow of compote fabrication: raw material, washed fruits, after blanching (at 70 °C for 3 min), and finished product (after pasteurisation by maintaining at 95 °C the inside temperature of filled and closed jar for 15 min). Also, the ascorbic acid content after 3 months of compote preservation in the dark at 10 °C and respectively, 25 °C was measured. Three analytical methods were used: HPLC, reflectometry (using the Reflectoquant), and titrimetry (using 2, 6-dichlorophenol indophenol). The results proved that thermal processes seriously decreased the ascorbic acid content and increased the dehydroascorbic acid. The 3 months preservation at both temperatures has slight influence on the content of ascorbic acid, but at 25 °C the diminution of ascorbic acid and the increase of dehydroascorbic acid were more significant than at 10 °C.

Keywords: *ascorbate oxidase, blanching, dehydroascorbic acid, pasteurisation, preservation, technological flow, temperature, vitamin C.*

Rezumat. Caisele sunt fructe cu perioadă scurtă de consum în stare proaspătă, iar fabricarea compotului este o metodă uzuală pentru a le conserva. Cercetarea prezintă abordează modificările conținutului total de vitamina C, precum și transformările între formele acid ascorbic și acid dehidroascorbic, în patru etape diferite ale procesului tehnologic de fabricare a compotului de caise. Activitatea ascorbat oxidazei a fost deasemenea evaluată. Probele studiate sunt reprezentate de caise în diferite stadii ale procesului tehnologic de fabricare a compotului: materie primă, fructe spălate, după blanșare (3 min la 70 °C) și produs finit (după pasteurizarea borcanului umplut și închis, prin menținerea 15 min a temperaturii interne de 95 °C). Deasemenea, a fost măsurat conținutul de acid ascorbic după 3 luni de păstrare a compotului la întuneric, la 10 °C și respectiv, 25 °C. Au fost folosite trei metode analitice: HPLC, reflectometrică (folosind Reflectoquant-ul) și titrimetrică (folosind 2,6-diclorfenolindofenolul). Rezultatele au dovedit că procesele termice au scăzut serios conținutul de acid ascorbic și au crescut acidul dehidroascorbic. Păstrarea 3 luni la 10 °C a influențat puțin, în timp ce la 25 °C, diminuarea acidului ascorbic și creșterea acidului dehidroascorbic au fost importante.

Cuvinte cheie: *ascorbat oxidază, albire, acid dehidroascorbic, pasteurizare, conservare, flux tehnologic, temperatură, vitamina C.*

DOI: 10.5281/zenodo.3713354
CZU 621.331.2



APPLICATION OF DC MOTOR AS SPEED AND DIRECTION CONTROL

Badri Narayan Mohapatra^{1*}, ORCID ID: 0000-0003-1906-9932,
Rashmita Kumari Mohapatra²

¹Savitribai Phule Pune University, AISSMS IOIT, Pune, INDIA

²Mumbai University, TCET, Mumbai, INDIA

*Corresponding author: Badri Narayan Mohapatra,
badri1.mohapatra@gmail.com

Received: 01. 23. 2020

Accepted: 03. 12. 2020

Abstract. Motion control plays a vital role in industrial atomization. Application wise variety type of motors like DC, AC, stepper or servo are used. Because of easier control DC motors are very popular to the users, its application is oriented very useful for rotation and speed. As speed depends on voltage applied to the terminal, smoothly can be controlled down to zero and again accelerated opposite way without using power CKT and switching CKT. Hence, if voltage across motor terminal is varied, then speed can also be varied. One of the best controlling method for DC motor is armature voltage control method using PWM. Speed of the motors depends on the variation of the duty cycles. Direction control can be achieved by the same microcontroller using slight modifications in its programming language. Depending on the application speed range vary in DC motor. Analysis and design of any system in real time can be easily implemented by hardware technology also by smart software. A motor driver IC is interfaced to the microcontroller for receiving PWM signals and delivering desired output for speed control of a small DC motor. The combination provides smooth speed control in both clockwise as well as anticlockwise direction.

Keywords: *DC motor, PWM signal, Proteus simulation, PIC 18F4550, speed and direction control.*

Introduction

In both industries and domestic, the use of DC motor is very high. Domestic sense like mixer, zero machine, hair dryer, elevator similarly in industry point of view like traction and in elevator. These applications demand accuracy high-speed control, and good dynamic responses. Most of the home appliances, washers, dryers and compressors are good examples of speed control. In automotive, electronic steering control, engine control, fuel pump control, and electric vehicle control are good examples of these. In aerospace technology, there are a lot of applications, such as pumps, robotic arm controls, centrifuges, gyroscope controls and so on.

Depending on the application speed range varies in DC motor. Both industries and domestic, the use of DC motor is very high. Domestic sense like mixer, zero machine, hair

dryer, elevator similarly in industry point of view like traction and in elevator. For practical application of view DC motor is very useful [1].

12v dc will generate by driving circuit without changing load, one can able to control the DC motor with desired speed. For this one can use PIC18F4550 microcontroller device which is also very low cost and best low-cost device for ECG measurement [2] and this also is used for data Acquisition process [3].

Whenever we think then programmable devices like embedded technology comes fast in mind. The embedded systems are nowadays very much popular and most of the product are developed with Microcontroller based embedded technology. The advantages of using the microcontroller is the reduction of the cost and also the use of extra hardware such as the use of timer RAM and ROM can be avoided. This technology is very fast thereby controlling of multiple parameters is possible; also, the parameters are field programmable by the user. Here we are using Programmable embedded microcontroller for PWM based speed control of DC motor. The scope of this project includes using MPLAB IDE to program microcontroller PIC 18F4550, build hardware for the system, and interface the hardware to computer by using RS232 serial port communication. DC motor, programming one can use assembly language [4].

Block Diagram

By use of digital technology, there has been interesting in DC motor control, either in terms of direction or in terms of speed. This will be perfect only when code is run on the actual hardware.

The principal of electromagnetism will play an important role when current will pass through DC motor. Axle, stator, commutator, rotor, field magnet and brushes are six parts of DC motor [5].

Basically, the motor speed depends on supply voltage, if supply will be one fourth then speed will be reduced to twenty-five percentage of the original speed. Figure 1 represents the basic block diagram of the proposed system.

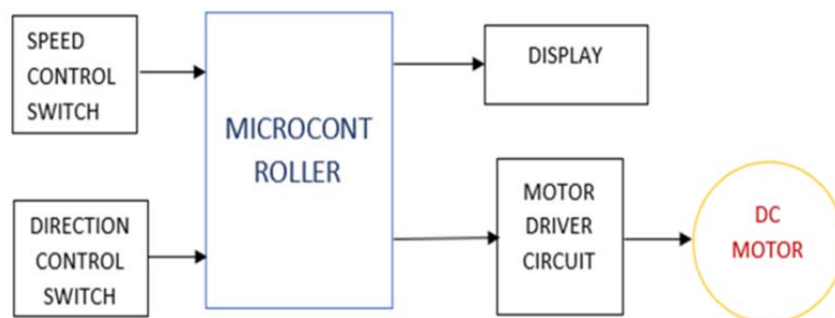


Figure 1. Block diagram of proposed system.

Hardware Implementation

Motor Basically it is used for encoding of amplitude of require signal and sometimes used as a carrier signal. Basically, it is used in AC/DC motors and control the power of various electrical devices. It is possible to control the average power delivered to load; DC voltage chopping can be possible with regular interval. Due to high and low pulse speed can be increased or decreased by the motor. As per the applications speed of the controller requirement is important. This requirement may demand the accuracy and good dynamic response. Desired speed makes able to change speed slower, faster, slower up, faster down

all can possible. Here the basic pin diagrams of PIC18F4550 is shown in figure 2. Figure 3 indicates Motor driver circuit, which is a monolithic, high current, high voltage is designed to accept TTL logic.

Internal clamp diodes are included and a separate supply for allowing the logic operation with a suitable switching application. After all circuits to be arranged properly, so one can tracking the copper layer just like in figure 4. PCB traces they may make or break the operation of electrical performance [6].

Figure 5 indicates the flow charts for speed and direction control and for this one has to assign the ports, variables and required connecting devices.

The main roll is the interrupt of delay, time, pulse and PWM module. PIC18F4550 microcontroller one can say the low cost and it is used to control advertising in LED system [7].

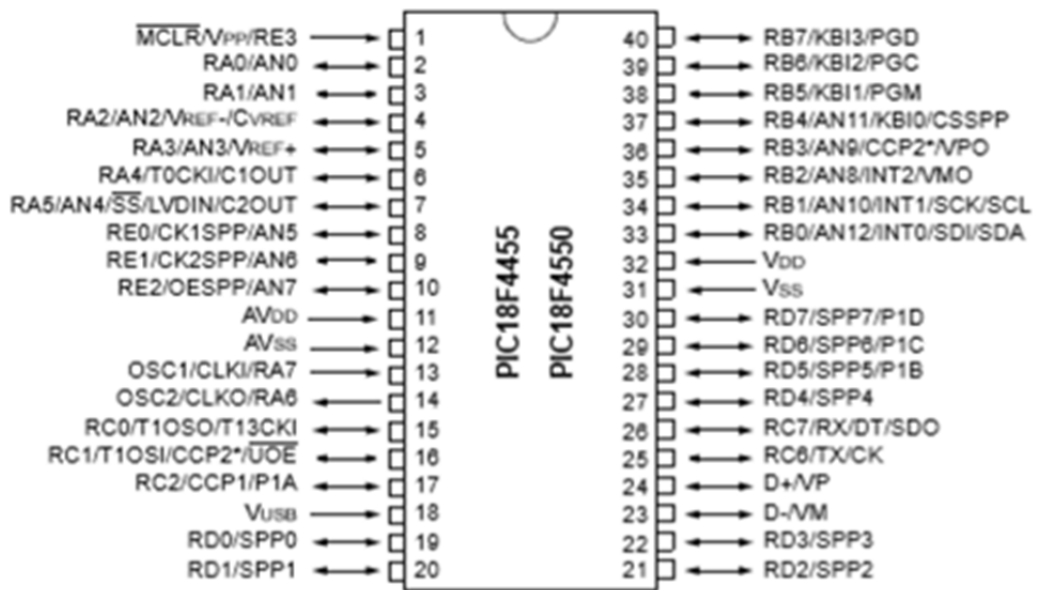


Figure 2. Pin diagram representation of PIC 18F4550.

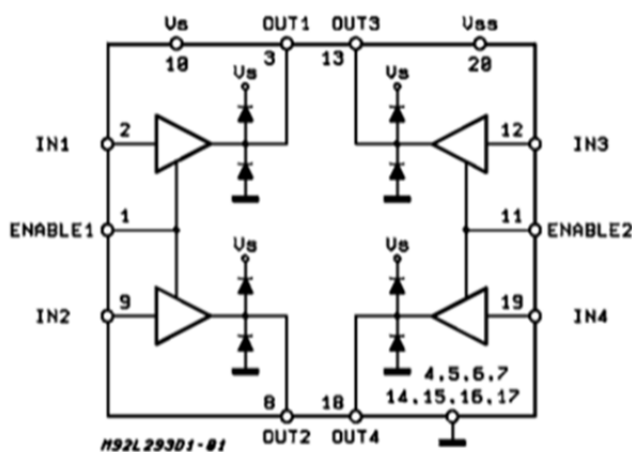


Figure 3. Representation of motor driver ckt block diagram.

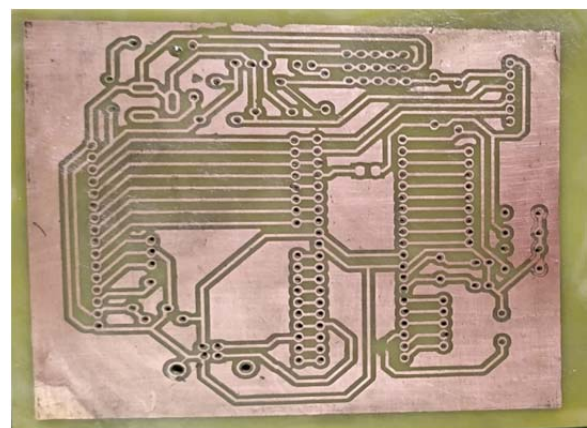


Figure 4. Circuit is arranged on a PCB with copper layer.

C programming can be easily programmable in PIC 18F series easily. System setup and calculation can implement in a flexible software like proteus [9]. It is also known as Electronic Design Automation (EDA) software [10].

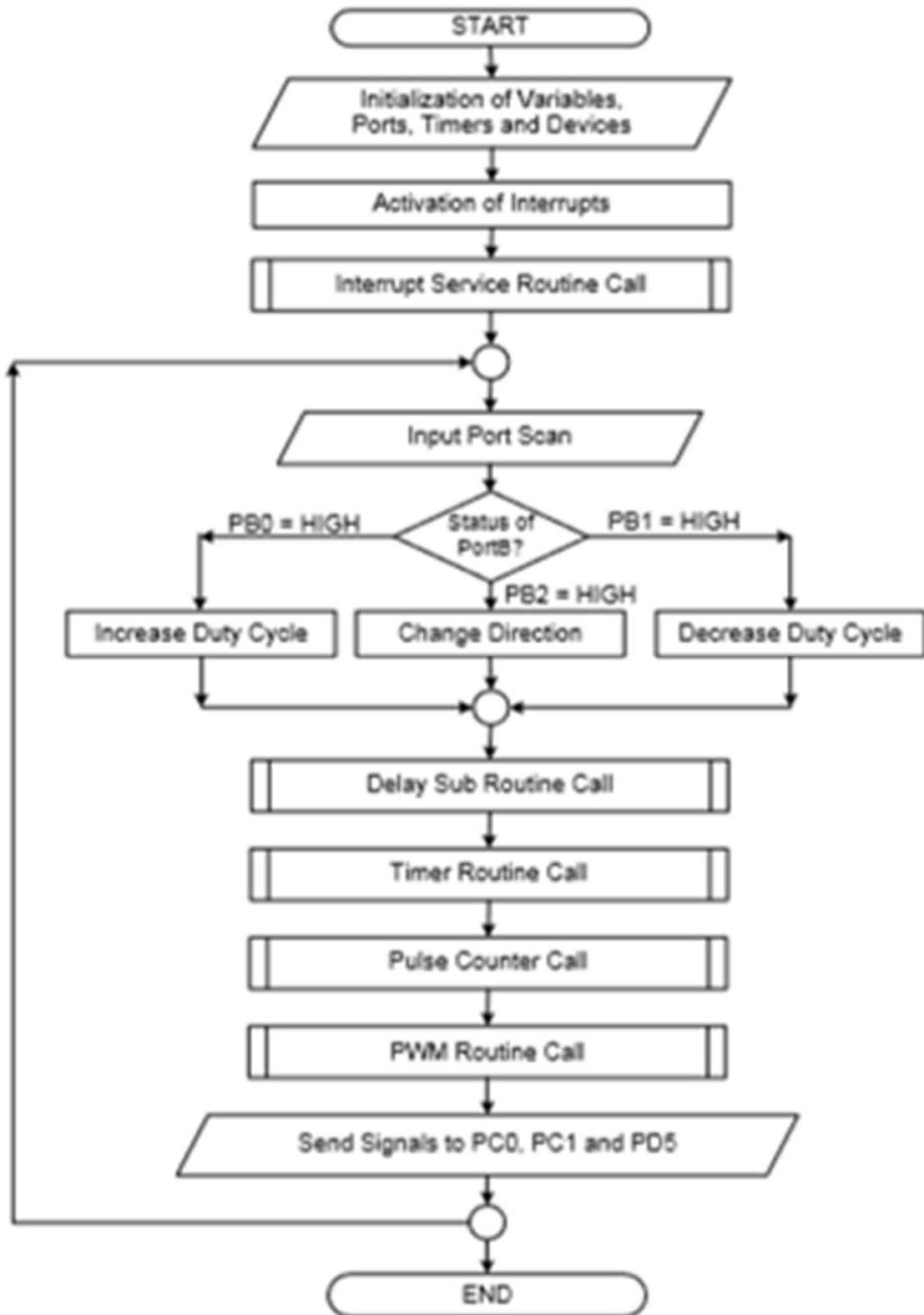


Figure 5. Flow chart of purposed system.

Basically, switches in H-bridge mainly controlled the speed and direction of DC motor. L293D IC is high current half H-drives [11]. A voltage of 4.5 v to 36 v and provide bidirectional drive current up to 600 mA. Hardware implementation is shown in figure 6 and figure 7 and indicates the software proteus simulation analysis on DC motor speed and direction control.

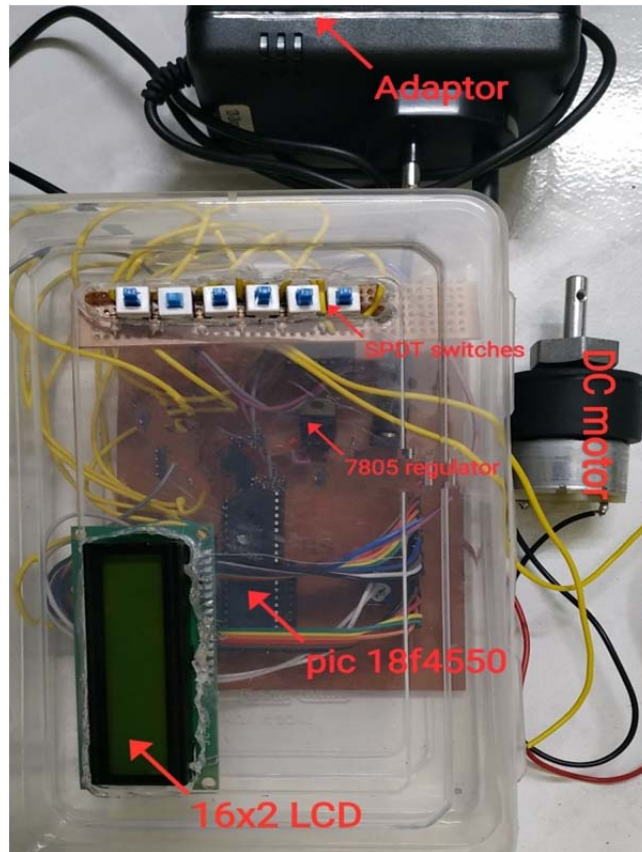


Figure 6. Hardware implementation.

Proteus Analysis

Due to low maintenance, good drive performance as well as low initiatory amount makes the dc motor more use in industry. DC motor has more features and utilized widely. PWM is also very common method and through PWM control of a DC motor used to drive the conveyor belt.

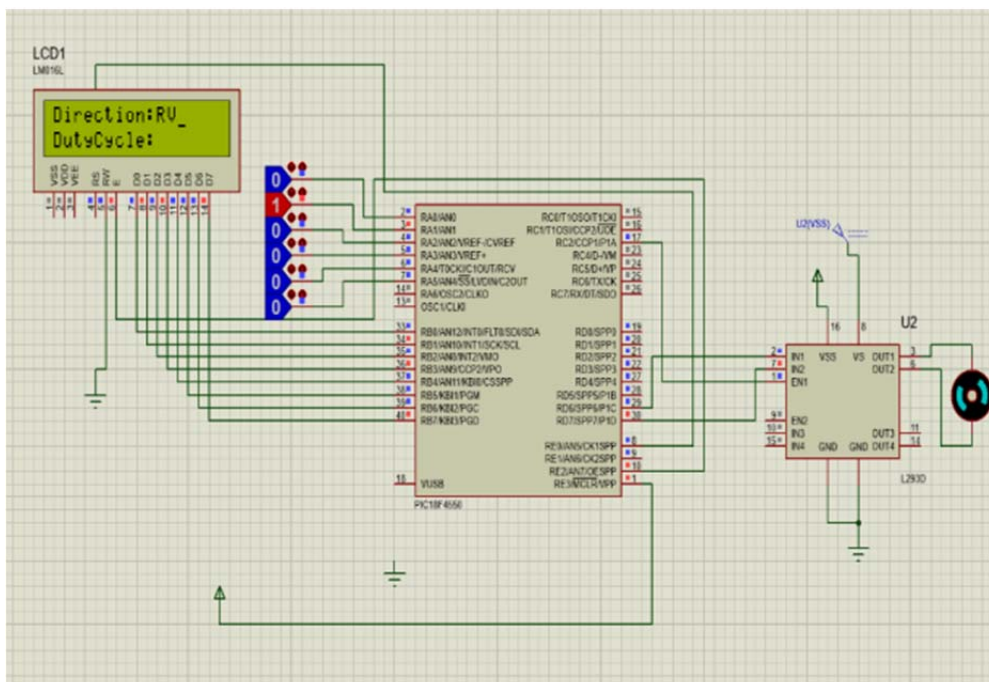


Figure 7. Analysis of control through simulation.

Depending on the programming of microcontroller the control on DC motor is faster and precise on its performance on operation. PWM signal can be changed due to changing in its duty cycle. That duty cycle can be control by H-bridge transistor.

Particularly, revolution per minute of DC motor changes as per controlled and one can make the programmed like increasing or decreasing the time interval. As a result, the motor rotation is maximum or minimum based on the duty cycle.

Conclusion

Continuous demand in electronics, instrumentation and electrical, this research idea gives a concise idea about design the low-cost technology for the control of speed and direction control. Pulse width modulation can switch the motor supply on and off very quickly. User can easily control can changes in speed and direction by reprogramming in microcontroller.

There may be chance of electric shock for conventional switching system. Both speed and direction control can easily be used in industrial as an automation system. So, the future direction is for mobile based or touch screen-based control the whole scenario so that it is free from danger and safer control can possible. For reliable and remarkable performance, future researcher can easily expand this work by implementing a mobile app application. Otherwise researcher can think of voice based controlled as a use of wireless network.

References

1. Egidio, L.N., Daiha, H.R., Deaecto, G.S. and Geromel, J.C., 2017, December. DC motor speed control via buck-boost converter through a state dependent limited frequency switching rule. In 2017 IEEE 56th Annual Conference on Decision and Control (CDC) (pp. 2072-2077). IEEE.
2. Sarkar, D. and Chowdhury, A., 2015, January. Low cost and efficient ECG measurement system using PIC18F4550 microcontroller. In 2015 International Conference on Electronic Design, Computer Networks & Automated Verification (EDCAV) (pp. 6-11). IEEE.
3. Hercog, D. and Gergič, B., 2014. A flexible microcontroller-based data acquisition device. *Sensors*, 14(6), pp.9755-9775.
4. Fahimi, B., Suresh, G. and Ehsani, M., 2000. Review of sensorless control methods in switched reluctance motor drives. In Conference Record of the 2000 IEEE Industry Applications Conference. Thirty-Fifth IAS Annual Meeting and World Conference on Industrial Applications of Electrical Energy (Cat. No. 00CH37129) (Vol. 3, pp. 1850-1857). IEEE.
5. Ghosh, M., Ghosh, S., Saha, P.K. and Panda, G.K., 2016. Semi-Analytical Dynamic Model of Permanent-Magnet Direct Current Brushed Motor Considering Slotting Effect, Commutation, and PWM-Operated Terminal Voltage. *IEEE Transactions on industrial electronics*, 64(4), pp.2654-2662.
6. Jones, D.L., 2004. PCB design tutorial. June 29th, pp.3-25.
7. Mujčić, E., Drakulić, U. and Škrgić, M., 2017. Advertising LED system using PIC18F4550 microcontroller and LED lighting. In *Advanced Technologies, Systems, and Applications* (pp. 311-321). Springer, Cham.
8. Ibrahim, D., 2011. *Advanced PIC microcontroller projects in C: from USB to RTOS with the PIC 18F Series*. Newnes.
9. Simonson, T., Gaillard, T., Mignon, D., Schmidt am Busch, M., Lopes, A., Amara, N., Polydorides, S., Sedano, A., Druart, K. and Archontis, G., 2013. Computational protein design: the Proteus software and selected applications. *Journal of computational chemistry*, 34(28), pp.2472-2484.
10. Aslam, S., Hannan, S., Sajjad, U. and Zafar, W., 2016. Implementation of PID on PIC24F series microcontroller for speed control of a DC motor using MPLAB and Proteus. *Advances in Science and Technology Research Journal*, 10(31).
11. Petru, L. and Mazen, G., 2015. PWM control of a DC motor used to drive a conveyor belt. *Procedia Engineering*, 100, pp.299-304.

DOI: 10.5281/zenodo.3713358
CZU 535.343.2+544.22



BIREFRINGENCE AND EXCITON SPECTRA OF CuAlSe_2 AND CuAlS_2 CRYSTALS

Alisa Maşnic*

Technical University of Moldova, 168, Stefan cel Mare bd. Chisinau, Republic of Moldova
*alisa.masnic@tlc.utm.md

Received: 01. 14. 2020

Accepted: 03. 16. 2020

Abstract. The excitonic reflection spectra of CuAlS_2 and CuAlSe_2 crystals were measured at the temperature of 10 K for polarizations $E||c$ and $E\perp c$. Ground and excited states of the excitons were found out in the investigated spectra. Symmetries of the observed excitons were determined. The shapes of ground states lines of Γ_4 and Γ_5 excitons were calculated by means of the Kramers-Kronig relations. Exciton parameters and values of energetic gaps ($\Gamma_7-\Gamma_6$, $\Gamma_6-\Gamma_6$, and $\Gamma_7-\Gamma_6$) were determined. Optical reflection spectra in the depth of absorption band ($E_g - 6$ eV) were measured at 80 K for $E||c$ and $E\perp c$ polarizations. Optical constants were calculated from measured reflection spectra by Kramers-Kronig analysis. The phase in the excitonic region was determined. Transmission spectra of CuAlSe_2 single crystals deposit in crossed polarizers demonstrate a birefractive effect. In the case of parallel polarizers interference due to birefractance was observed. The isotropic point was determined.

Keywords: absorption and reflection spectra, excitons, polaritons, birefringence.

1. Introduction

CuAlSe_2 and CuAlS_2 compounds, as well as their solid solutions belonging to the III-VI₂ materials crystallize in the chalcopyrite structure with the $I42d - D_{2d}^{12}$ space group. Stimulated emission and second harmonic generation at 10.6 μm as well as generation of infrared (IR) radiation in the region of 4.6 and 12 μm was realized in these compounds [1-4]. Biexcitons [5], interference of additional waves [6], resonance Raman scattering [7-9] and intense emission due to exciton polaritons and bound excitons [10-12] have been observed in these crystals. Optoelectronic devices and solar cells are developed on the basis of these materials [13-18]. The photoluminescence properties of CuAlSe_2 crystals doped with Er^{3+} ions [15] as well as the photoelectrical properties of surface barrier structures on the basis of CuAlSe_2 have been studied [17, 18]. These materials possess a strong anisotropy of optical properties in the visible and infrared spectral ranges which is very important for the development of polarized optoelectronic devices.

The goal of this paper is to investigate the main exciton parameters as well as the energy gaps at the center of the Brillouin zone as a function of composition of $\text{CuAl}_{1-x}\text{Ga}_x\text{Se}_2$ solid solutions. The energy position of $n=1$ and 2 lines of the $\Gamma_4(\text{A})$, $\Gamma_5(\text{B})$ and $\Gamma_5(\text{C})$ exciton series, as well as the $\Gamma_7(\text{V}_1) - \Gamma_6(\text{C}_1)$, $\Gamma_6(\text{V}_2) - \Gamma_6(\text{C}_1)$, $\Gamma_7(\text{V}_3) - \Gamma_6(\text{C}_1)$ energy intervals, are determined from wavelength modulated optical reflectivity spectra. The

effective electron mass (m_{c1}^*), and hole masses (m_{v1}^* , m_{v2}^* , m_{v3}^*), are estimated from the analysis of exciton reflectivity spectra according to a single-oscillator model of dispersion relations. The asymmetry parameters of reflectivity spectra are determined.

2. Experimental details

CuAlSe₂ and CuAlS₂ crystals in the form of platelets with 2.5 × 1.0 cm² mirror-like surfaces and thicknesses of 300–400 μm were grown by chemical vapor transport [16]. The surface plane of the platelets contains the C -axis. The optical reflectivity and wavelength modulated spectra were measured using a MDR-2 (LOMO, Russia) spectrometer. For low-temperature measurements, the samples were mounted on the cold station of a LTS-22 C 330 optical cryogenic system.

3. Experimental results and discussion

3.1. Excitonic spectra of CuAlS₂ crystals

According to theoretical calculations of the band structure [3 – 6], the minimum of interband gap is formed by direct electronic transitions at the center of Brillouin zone for CuAlS₂ crystals. The lower conduction band possesses Γ_6 symmetry and the upper valence bands V_1 , V_2 , V_3 possess Γ_7 , Γ_6 and Γ_7 symmetries, respectively. The interaction of electrons from the conduction band Γ_6 with holes from Γ_7 is determined by the product of irreducible representations $\Gamma_1 \times \Gamma_6 \times \Gamma_7 = \Gamma_3 + \Gamma_4 + \Gamma_5$. As a result of this interaction, the Γ_4 exciton allowed in E||c polarization, Γ_5 exciton allowed in E⊥c polarization and Γ_3 exciton forbidden in both polarizations are formed in the long-wavelength part of the spectrum. The interaction of electrons from the conduction band C_1 of Γ_6 symmetry with holes from the valence band V_2 with Γ_6 symmetry leads to the appearance of three excitonic series Γ_1 , Γ_2 , and Γ_5 . According to the selection rules, Γ_5 excitons are allowed, while Γ_1 and Γ_2 excitons are forbidden for E⊥c polarization.

The lines $n = 1$ ($\omega_t = 3.543$ eV, $\omega_l = 3.546$ eV) and $n = 2$ (3.565 eV) of the hydrogen-like Γ_4 exciton series were revealed in the reflection spectra of CuAlS₂ crystals measured at 10 K in E||c polarization [7]. The reflection spectra in the $n = 1$ region has a typical form with a 3.543 eV maximum and a 3.546 eV minimum. These peculiarities are explained by the presence of transversal and longitudinal excitons. The longitudinal-transverse splitting energy of Γ_4 excitons estimated on the basis of these data equals 3 meV. A Rydberg constant of 32 meV is determined for Γ_4 excitonic series from the energetic position of $n = 1$ and $n = 2$ lines (fig. 1). The continuum energy (E_g , $n = \infty$) is 3.575 eV. The energy values discussed above for the ground ($n = 1$) and excited ($n = 2$) excitonic states are satisfactorily correlating with the 3.534 eV and 3.665 eV values previously obtained at 77 K [8].

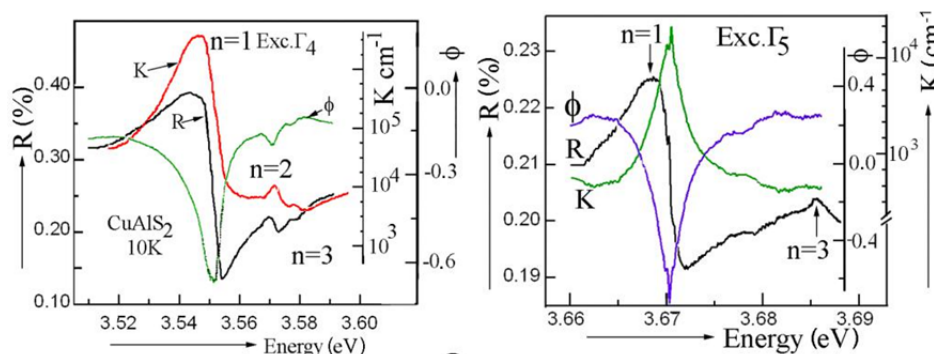


Figure 1. Spectral dependence of absorption coefficient (K) and of phase (Φ) of the reflected beam calculated from the measured reflection spectra (R) in CuAlS₂ crystals.

A maximum at 3.668 eV (transversal exciton) and a minimum at 3.670 eV (longitudinal exciton) related to Γ_5 excitonic series are revealed in $E \perp c$ polarization (Fig. 1). The transverse-longitudinal splitting of Γ_5 exciton equals 2.0 meV. An excited state $n = 2$ is revealed at 3.687 eV. The exciton binding energy of Γ_5 excitons is 25 meV, and the convergence limit of the series is 3.693 eV. The C exciton is revealed at 3.813 eV ($n=1$) in the same polarization [7]. The reflection coefficient for the B-excitonic series is 21% at 3.6 eV, and the dielectric constant ϵ_b is 7.2. A value of the effective mass μ equal to $0.09m_0$ is derived for a binding energy of 25 meV.

The phase φ of the reflected beam and the magnitude of the absorption coefficient K in the resonance region of Γ_4 and Γ_5 excitons are obtained from the calculations of reflection spectra by means of Kramers-Kronig relations (Fig. 1). It is known that the amplitude of the reflection coefficient R is related to the phase φ of the reflected beam according to the following expression:

$$r = \sqrt{R}e^{-i\varphi} \quad (1)$$

The optical functions n , k , R , φ , ϵ_1 , ϵ_2 are related to each other by the following correlations:

$$\left\{ \begin{array}{l} r = \frac{N-1}{N+1} = \frac{n+ik-1}{n+ik+1} \\ r = \sqrt{R}e^{-i\varphi} = \sqrt{R}(\cos\varphi - i\sin\varphi) \end{array} \right. \quad (2) \quad \left\{ \begin{array}{l} n = \frac{1-R}{1-2\sqrt{R}\cos\varphi+R} \\ k = \frac{2\sqrt{R}\sin\varphi}{1-2\sqrt{R}\cos\varphi+R} \end{array} \right. \quad (3)$$

The phase $\varphi \approx \varphi(\omega)$ is calculated for each wavelength value by using the Kramers-Kronig integrals on the basis of experimentally measured amplitude values of the reflection coefficient $R \approx R(\omega)$. The phase of the reflected beam is related to the amplitude according to the following expression:

$$\varphi(\omega_0) = \frac{\omega_0}{\pi} \int_0^{\infty} \frac{\ln R(\omega)}{\omega_0^2 - \omega^2} d\omega \quad (4)$$

The spectral dependences of the phase of the reflected beam and the absorption magnitudes in the region of excitonic resonances Γ_4 and Γ_5 are also shown in Fig. 1. It is evident from the calculated results that the phase of the reflected beam changes in the same way for both excitonic resonances, reaching the lowest values at frequencies near ω^L . A difference is observed in the contours of the absorption spectra for Γ_4 and Γ_5 excitons. For the Γ_4 excitons, the absorption maximum nearly corresponds to the transversal exciton frequency ω^T , while for Γ_5 excitons it is shifted towards the frequency of longitudinal exciton ω^L .

3.2. Birefringence in crystals and interference of CuAlSe₂ single crystals

When the light waves pass through a thin crystal with plane parallel surfaces, the waves reflected from the first and second surfaces interfere. The condition of interference is the following:

$$2\pi nd\lambda^{-1} = N\pi + \pi/2 \quad (5)$$

From the spectral position of two neighboring maxima (minima) λ_a , λ_b of the transmission or reflection spectra one can determine the refractive index, if the thickness d of the sample is known. The transmission or reflection spectra are measured separately for the $E \parallel c$ and $E \perp c$ polarizations, and the refractive indices n_{\parallel} and n_{\perp} are determined, respectively:

$$n_{||} = 1/2d(\lambda_{a||}^{-1} - \lambda_{b||}^{-1}) \text{ for the } E||c \text{ polarization,}$$

$$n_{\perp} = 1/2d(\lambda_{a\perp}^{-1} - \lambda_{b\perp}^{-1}) \text{ for the } E\perp c \text{ polarization,}$$

where n is the refractive index, d is crystal thickness, and λ_a and λ_b are the wave length of maxima in the transmission spectrum.

The difference of the refractive indices can be determined from measurements with cross-oriented (or parallel-oriented) polarizers. In a crystal situated between the two polarizers the light waves with polarizations $E||c$ and $E\perp c$ gain a difference of phases and interfere, producing a series of bands. The difference in phase is acquired due to different light velocities for the waves with different polarizations, i.e. due to different values of $n_{||}$ and n_{\perp} . As shown in the lower part of figure 2, a narrow transmission band with very weak side bands is observed at the wavelength λ_0 in the spectrum of a thick sample ($d= 570 \mu\text{m}$) placed between two cross-oriented polarizers (band-pass mode) [19]. A narrow absorption band is observed for the crystal with this thickness placed between two parallel-oriented polarizers (not shown in this figure). For a thinner crystal ($d= 15 \mu\text{m}$) placed between two parallel-oriented polarizers, a series of bands 1–10 are produced on the short-wavelength side of the isotropic point, while the bands a1–a7 are produced on the long-wavelength side of λ_0 (upper part of figure 2). The emergence of these side bands is due to the small thickness of the sample. The number of bands is determined by the thickness of the sample and the difference $\Delta n = n_o - n_e$. The value of Δn is determined from the position of interference bands and the thickness of the crystal. The method with two polarizers for measuring the birefringence is more sensitive and efficient compared to the method using separate polarizers for the determination of n_o and n_e refractive indices: $\Delta n = N_{\perp} \lambda / d$, where $N_{\perp} = 0, \pm 1, \pm 2, \dots$

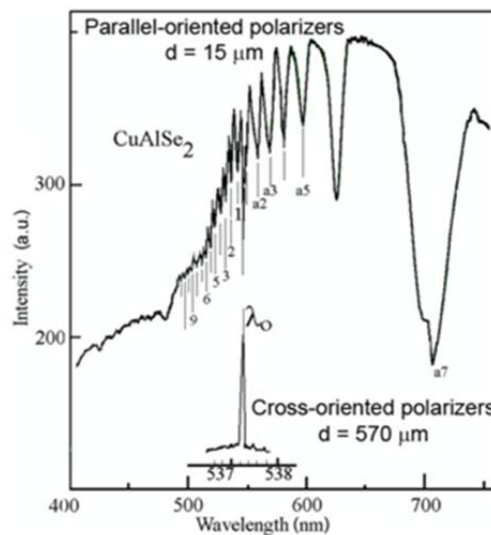


Figure 2. Transmission spectrum of CuAlSe_2 crystals measured with cross-oriented and parallel-oriented polarizers.

4. Conclusions

The results of this study demonstrate that CuAlSe_2 crystals possess a strong anisotropy of optical properties in the region of excitonic transitions. The parameters of Γ_4 and Γ_5 excitons were determined by Kramers-Kronig calculations of the reflection spectra, and the energy interval between the $\Gamma_7-\Gamma_6$, $\Gamma_6-\Gamma_6$ and $\Gamma_7-\Gamma_6$ bands were found to be of 3.575, 3.693, and 3.963 eV, respectively.

References

1. Shay J L and Wernick J H 1975 *Ternary Chalcopyrite Semiconductors: Growth, Electronic Properties, and Applications* (Oxford: Pergamon).
2. Birkmire R W and Eser E 1997 *Annu. Rev. Mater. Sci.* 27 625.
3. Ramanathan K *et al* 2003 *Prog. Photovolt.* 11 225.
4. Jin M-S, Yoon C-S and Kim W-T 1996 *J. Phys. Chem. Solids* 57 1359.
5. Bodnar I V, Rudi V Yu and Rudi Yu V 1994 *Fiz. Tekh. Poluprov.* 28 1755.
6. Zaretskaya E, Gremenok V, Zalesski V, Schorr S, Rud V and Rud Yu 2009 *Phys. Status Solidi c* 6 1278.
7. Chichibu S, Mizutani T, Murakami K, Shioda T, Kurafuji T, Nakanishi H, Niki S, Fons P J and Yamada A 1998 *J. Appl. Phys.* 83 3678.
8. Alonso M I, Wakita K, Pascual J, Garriga M and Yamamoto N 2001 *Phys. Rev. B* 63 075203.
9. Schuler S, Siebentritt S, Nishiwaki S, Rega N, Beckmann J, Brehme S and Lux-Steiner M Ch 2004 *Phys. Rev. B* 69 045210.
10. Siebentritt S, Beckers I, Riemann T, Christen J, Hoffmann A and Dworzak M 2005 *Appl. Phys. Lett* 89 091909.
11. Durante Rinc on´ C A, Hern´andez E, Alonso M I, Garriga M, Wasim S M, Rinc on´ C and Le on´ M 2001 *Mater. Chem. Phys.* 70 300.
12. Kawashima T, Adachi S, Miyake H and Sugiyama K 1998 845202n *J. Appl. Phys.* 84 5202.
13. Shirakata S, Ogawa A, Isomura S and Kariya T 1993 *Japan. J. Appl. Phys. Suppl.* 32–394.
14. Syrbu N N, Bogdanash M, Tezlevan V E and Stamov I G 1997 *J. Phys.: Condens. Matter* 9 1217.
15. Syrbu N N, Tiginyanu I M, Ursaki V V, Tezlevan V E, Zalamai V V and Nemerenco L L 2005 *Physica B* 365 43.
16. Arushanov E, Siebentritt S, Schedel-Niedrig T and Lux-Steiner M Ch 2006 *J. Appl. Phys.* 100 063715.
17. Levchenko S, Syrbu N N, Tezlevan V E, Arushanov E, Merino J M and Le on´ M 2008 *J. Phys. D: Appl. Phys.* 41 0055403.
18. Levchenko S, Syrbu N N, Tezlevan V E, Arushanov E, Doka-Yamigno S, Schedel-Niedrig Th and Lux-Steiner M C 2007 *J. Phys.: Condens. Matter* 19 456222.
19. Susaki M, Yamamoto N and Horinaka H 1994 *Japan. J. Appl. Phys.* 33 1561.

DOI: 10.5281/zenodo.3713360
CZU 621.3.049.77



3D MICROPACKAGING OF INTEGRATED CIRCUITS

Titu-Marius I. Băjenescu*, ORCID ID: 0000-0002-9371-6766

Swiss Technology Association, Electronics Group Switzerland
*tmbajenesco@gmail.com

Received: 01. 15. 2020

Accepted: 03. 05. 2020

Abstract. A major paradigm change, from 2D IC to 3D IC, is occurring in microelectronic industry. Joule heating is serious in 3D IC, and vertical interconnect is the critical element to be developed. Also, reliability concerns will be extremely important: electromigration and stress-migration. This paper presents some actual problems and reliability challenges in 3D IC packaging technology. It shows how different architectures have evolved to meet the specific needs of different markets: Multi Chip Module (MCP); Multipackage module (MPM); Embedded SIP modules; SIP package-on-package (PoP) modules; EMIB (Embedded Multi-die Interconnect Bridge); Silicon-based SIP-Module; 3D-TSV stacked module; SIP variants with combinations of wideband and flip-chip interconnects. Causes of blockages and failure mechanisms, as well as problems with predictive reliability, which will need to be developed in the coming years, are analysed.

Keywords: *prototypage virtuel, Moore's Law, analyse des compromis, reliability.*

Introduction

3D MCM (Multi Chip Module) introduces the IC chip 3D integration technology as well as multilayer interconnected technology of high-density chip, characterized by higher assembly density and capability, more system functions and I/O, lower power consuming and cost, and smaller size [1, 2]. As an important part of electronics devices, the packaging is responsible for the circuit support, protection, I/O connection, heat dissipation and shielding [3]. The new development of electronics devices is placing more new demands on the packages and on the development of packaging materials. The integration of microcircuit packaging trade-off analysis together with functional verification and architectural design results in a complete virtual prototyping solution for the optimization of complex electronic systems [4].

The main driver in today's commercial electronics market is time. Laptops, cell phones and a host of other complex high-density systems often have design cycles of less than a year and even shorter market windows [5]. The very existence of these products depends on finding fast design solutions to meet increasingly demanding performance and cost requirements.

A key to minimizing system cost without compromising time-to-market is to combine manufacturing information with application-specific design information early in the design

process. Including a manufacturing cost analysis in the system design methodology, we can avoid leaving money on the table at the end of development without increasing design time [7]. Common wisdom says that 80% of a product's cost, size and performance (timing, electrical synchronization, power dissipation and reliability) should be spent in the first 20% of the design cycle (Figure 1). Yet this is the part of the cycle for which we have the least mature methods and tools. This part includes requirements capture, specification, trade-off and partitioning. The 80%, which includes some detailed simulation and all physical design, refines and implements the design.

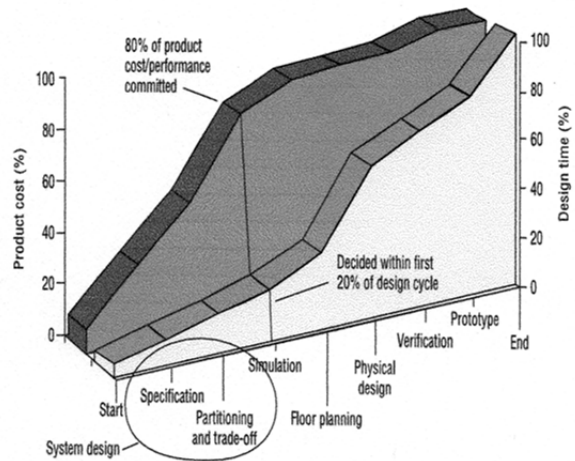


Figure 1. The first cycle of system design should focus on cost, performance, size, power dissipation and system reliability [7].

Moore's Law

In recent years, there has been speculation that Moore's Law is about to come to an end (Figure 2). However, this is not the end of the line. Moore's Law was never just about the number of transistors and nanometres. It was about the benefits of new processes and new models for PCs, data centers, cloud services, embedded products, mobile devices, etc. It was about the benefits of new processes and new models for the future. And the arrival of quantum computing elements, among other things, should give us more ways to achieve further gains [3, 8-10].

The role of trade-off analysis in microcircuit packaging

The future CMOS below 22 nm is delicate and one of the pathways for ultimate system integration is 3D integration requiring the development of via (Through Silicon Via TSV), thinning and substrate assembly technologies to stack chips and substrate levels on top of each other. It also requires the development of new materials for connections (carbon nanotubes, new insulation dielectrics) and new technologies for very low-pitch interconnections. In addition, these processes will have to be "low temperature" to be compatible with most of the structures to be interconnected. Stresses in TSVs, and therefore in the neighboring Si, arise from two sources: (1) growth stresses, that arise as a result of via-filling by electroplating, and (2) thermo-mechanical stresses that arise due to thermal expansion mismatch between Cu in

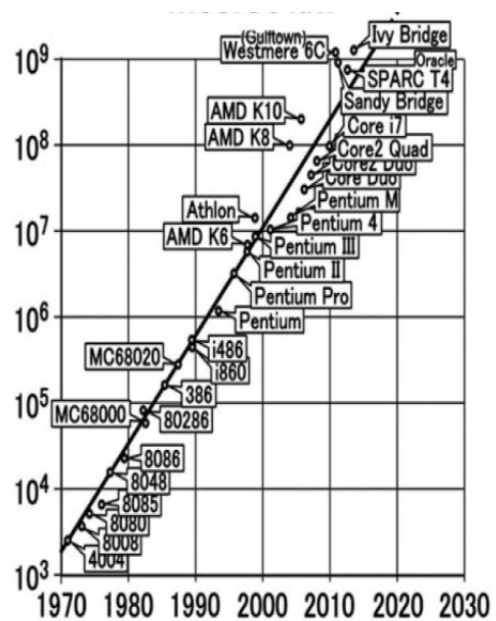


Figure 2. Moore's Law predicts exponential growth of ICs since 1970 (after [3]).

the via and the surrounding Si [11 - 19]. In addition to producing defects (e.g., voids) in TSVs, including complications in electrical performance and potentially causing interfacial and or dielectric fracture, induced stresses also give rise to a plasticity-related phenomenon commonly referred to as Cu pumping, which can have serious reliability implications.

The analysis of the packaging trade-off extends traditional virtual prototyping to include the determination of technology implementation details (Figure 3). The design horizon will depend on your virtual prototype, as you can define exactly how far the virtual prototype extends to describe the system details. Most of the electronics system design community (driven by microcircuit design) defines virtual prototyping as architectural design. Functional verification will provide evidence that the functionality of the system meets the customer's requirements.

The micro/nanopackaging

This is a key point concerning MEMS (Micro Electro-Mechanical System) which requires considering the system as a whole from the point of view of the elementary component, electrical connections, energy sources and storage components, interconnections and mechanical protection. Packaging represents 80% of the cost of the final product and 80% of the causes of failure. MEMS packaging is indeed a complex issue. Moving parts are mechanically very fragile and often require to operate in a relatively high vacuum ($< 10^{-2}$ mbar) in the case of vibrating systems.

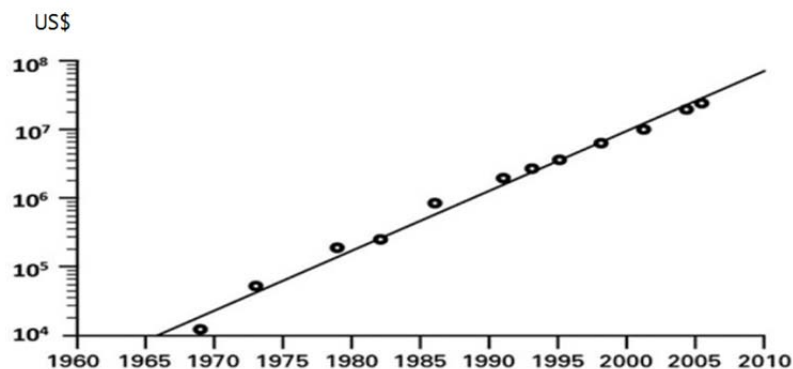


Figure 3. The exponential growth of the cost of lithographic equipment since 1966 [3].

The conventional method for maintaining Moore's Law is to reduce the dimensions of components by lithography - which is increasingly sophisticated and expensive [3]. 3D integration technology - which has been recognized as a technology for realizing future low-cost ICs - provides the third dimension to extend Moore's Law to an ever-higher density, with more functionality and better performance, at lower costs [7].

To realize a small form factor, 3D packaging is required. The market requirements for microelectronics form factor lead to 3D packages that are ultra-light, ultra-thin and with a small footprint. 3D silicon chips are typically 50 ... 100 μm thick and are about 90% thinner than conventional packages. The high-density interconnects in 3D packaging are in the order of 5 ... 20 μm in diameter and more than 90% smaller than those in 2D packaging. Thus, a huge reduction in size and weight could be achieved by replacing conventional packaging with 3D technology (Figure 4) [11]. A small form factor requires a small chip footprint, which is defined as the area of the printed circuit board occupied by the silicon chip.

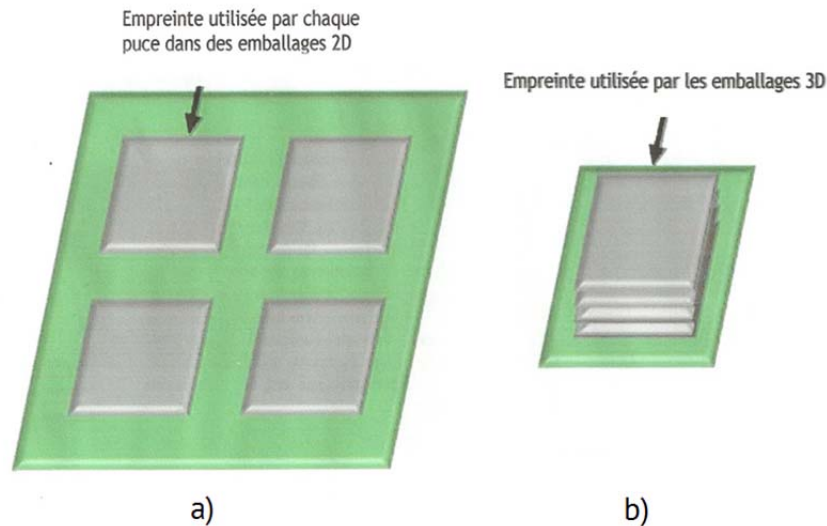


Figure 4. Schematic illustration of the difference footprint between conventional 2D packets (a) and 3D packages (b), (after [11]).

A high-level assembly process flow for a single component is illustrated in Figure 5 to show the typical points in the flow where the wafer, die, and assembled package are tested to check for manufacturing quality or performance.

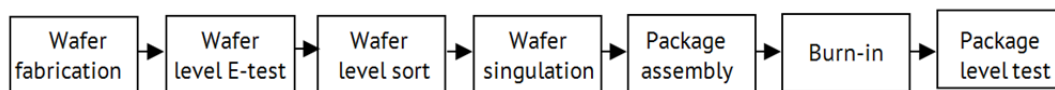
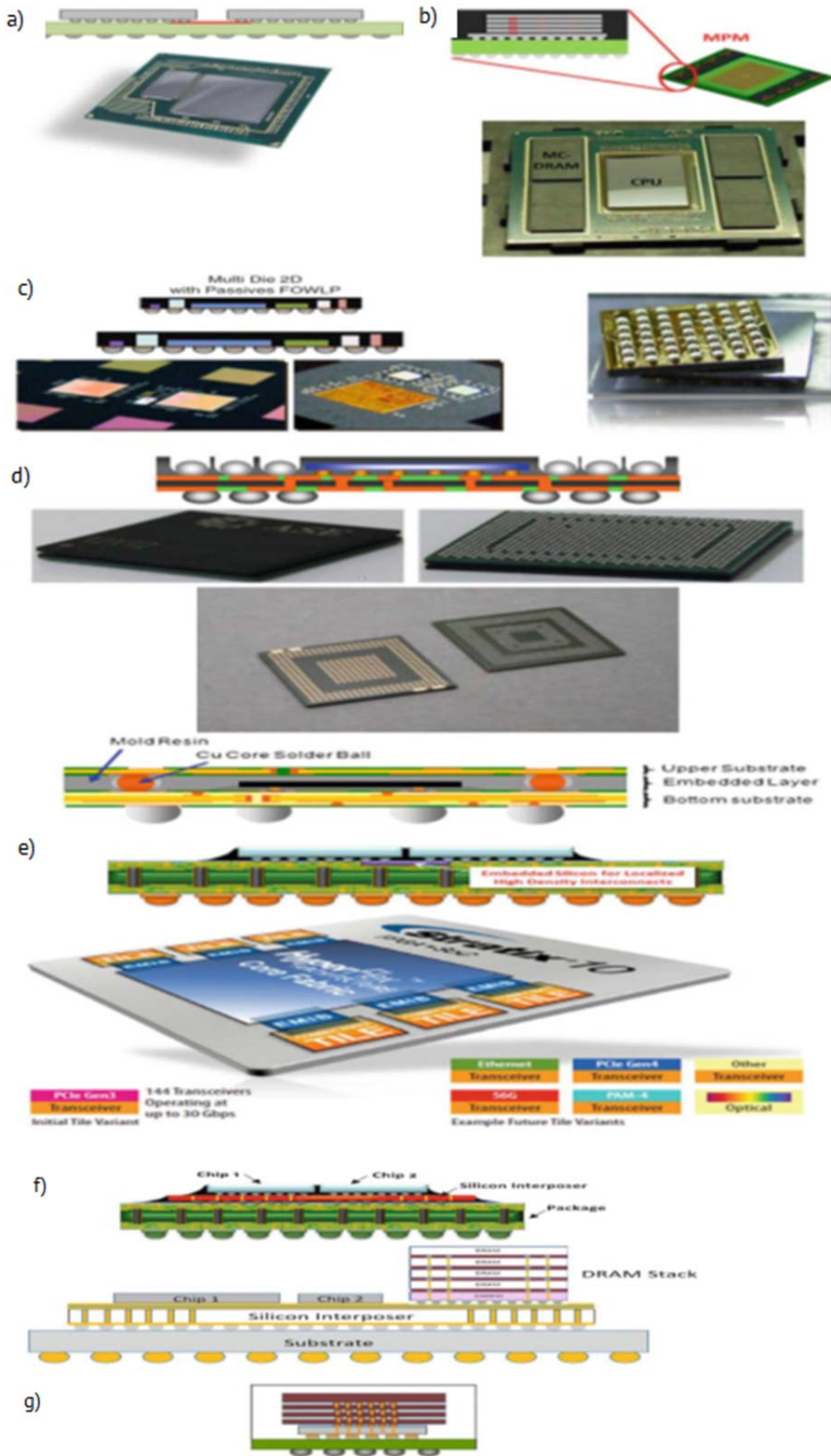


Figure 5. Key steps in a package assembly process.

Figure 6 illustrates how different architectures have evolved to meet specific needs for different markets (after [11, 20]).

- (a) Multi Chip Module (MCP) - Two or more chips are attached in a planar configuration to a packaging substrate (the red line in the schematic drawing indicates that the two or more chips are electrically connected using side interconnects on the package). The image shows the Intel Iris Pro processor with a CPU (the larger of the two chips) and a DRAM chip.
- (b) Multipackage module (MPM). One or more chips are packaged before being attached to the final package. The picture above shows the Intel Knight's Landing processor using the MC-DRAM memory module. The MC-DRAM memory module (a memory stack conforming to the Hybrid Memory Cube specification [1]) consists of four stacked memory chips connected by Through Silicon Vias (TSVs), placed on top of a logic chip.
- (c) Embedded SIP modules have seamless chip-to-package interconnections and are usually constructed using wafer levels or reconstituted panels [2, 3].

Two packages are stacked on top of each other and connected by peripheral interconnections. Peripheral interconnections can be made using solder balls, Cu rods or solder-coated copper balls. An example of a MCeP (Molded Core embedded Package) is shown in figure 6d. MCeP is the registered trademark of SHINKO electric industries, Co. Ltd. (SIP – a subset of the broader concept of System On Package (SOP) (figure 6e). Its refers to the on-package integration of multiple heterogeneous and/or homogenous ICs, each of which may be in the form of unpackaged die, individually packaged die, or packaged modules.



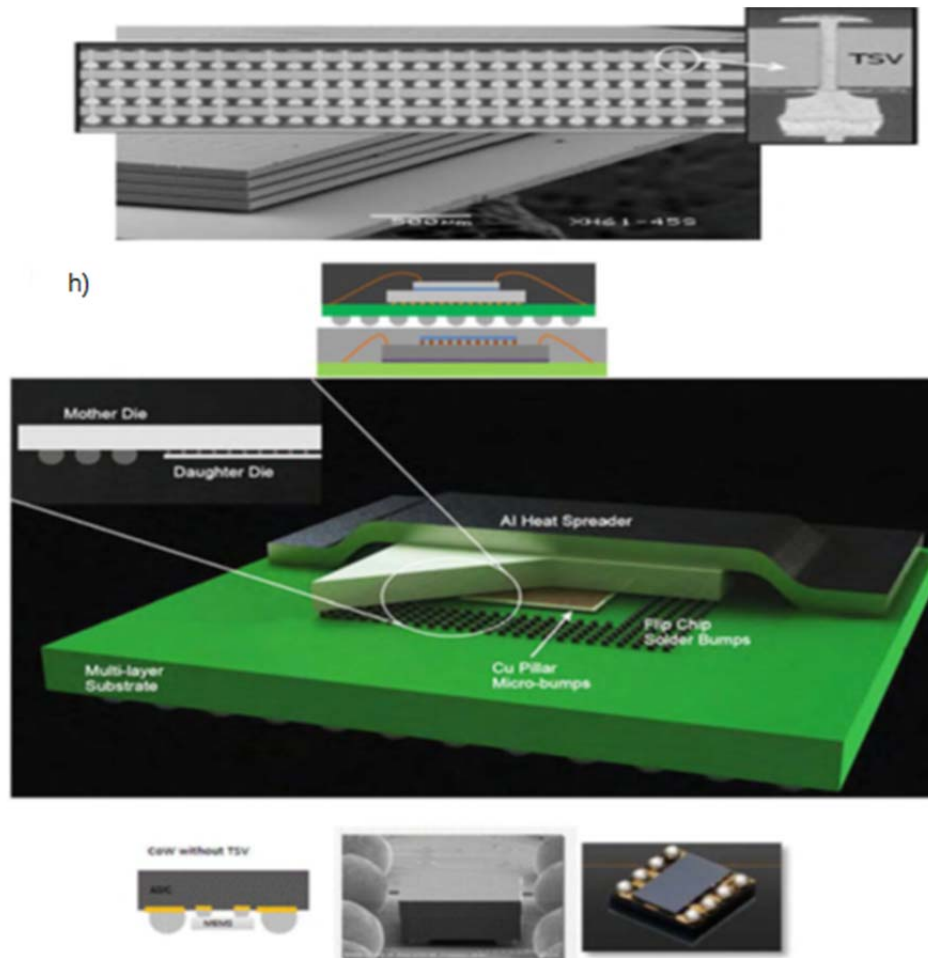


Figure 6. Specific architectures for different markets (after [4, 6, 11, 20]):
 (a) Multi Chip Module (MCP); (b) Multi Package module (MPM)
 (c) Embedded SIP modules; (d) SIP package-on-package (PoP) modules
 (e) EMIB (Embedded Multi-die Interconnect Bridge); (f) Silicon-based SIP-Module;
 (g) 3D-TSV stacked module; (h) SIP variants with combinations of wideband and flip-chip interconnects.

EMIB-based SIPs use embedded silicon for localized high-density interconnects. The figure 6e shows part of Altera's STRATIX-10 [5]. A silicon interposer is used for thin feature interconnects between different chips or chip stacks (figure 6 f). The interposer has TSVs to connect the chips to the packaging substrate [6]. Multiple chips are stacked using TSV-based interconnects (figure 6g). The figure 6h shows a Micron HMC memory stack. SIP variants include combinations of wideband and flip-chip interconnects. One class of SIP configurations that has driven the most significant technology changes is through silicon vias (TSV)-based SIP [21,22]. The most commonly used interconnect between stacked die for currently available products with TSVs is solder based with interconnect pitches as low as 40 μm (advantage: compliant, also more tolerant to misalignment and lack of coplanarity between bonded surfaces during assembly. However, as the joints become increasingly small, with decreasing interconnect pitches projected below 40 μm for future 3D stacks, the available solder volume will be reduced and a greater proportion of the solder joint will become intermetallic compounds, thus decreasing its compliance [23]. With shrinking interconnect pitch, there is an increasing risk of solder bridging during the assembly process since the joints are closer to each other.

Reliability of micro-nanosystems

A micro-nanosystem can be defined as a system in which at least one functional component is at the micro-nanometric scale [24]. The term "system" implies that one can interact in a controlled manner on its operation. The large initial tensile stress is caused by grain boundary elimination during self-annealing and device fabrication, and is undesirable from the reliability perspective, since this causes large stresses in Si. Because of the potentially serious reliability complications, the role of Cu pumping has been widely studied, and the effects of various process parameters (such as TSV spacing, diameter, Cu overburden after electroplating, and annealing conditions) have been noted [25 - 30]. Although electromigration (EM) is a significant reliability issue in metallic interconnects in electronics, TSVs are generally less susceptible to EM induced failures. Since EM induced interfacial sliding is non-symmetric (and unlike under thermal cycling conditions, it accrues continuously) it may pose a potentially serious reliability challenge, particularly as the current density through the vias increases with decreasing TSV diameter. Stacked packages utilize commercial-off-the-shelf (COTS) packaging which establishes the reliability baseline. The unique reliability issues with package stacking are assembly quality and mechanical shock and vibration effects [31 - 33]. MEMS reliability studies concern the development of knowledge of failure mechanisms and the use of this knowledge to establish predictive models. To date, this is the first brake on the industrialization of MEMS and even more so of NEMS [34 - 35]. The main difficulty comes from the very large diversity of materials and technological processes used (the characteristics of thin films depend on the techniques and conditions of elaboration and these characteristics may change during the device manufacturing process, but also over time or differ from one device to another) [36 - 37]. The lack of recognized techniques for the characterization of MEMS and the lack of standardization in terms of reliability are also important bottlenecks. Predictive reliability is, therefore, still in its infancy and will need to be developed at all costs in the coming years [38].

Conclusion

TSV-based 3D stacking has generated considerable interest, research and development effort in architecture and manufacturing has resulted in a detailed understanding of multiple aspects of the technology. The primary advantages of package stacking are the reduction in substrate area, decreased interconnection lengths and the ability to pre-test packages before stacking. The electrical interconnection length between packages in a stack is less than the length that could be achieved with individual packages arrayed in a planar configuration, decreasing propagation delay. A major advantage of this approach is the ability to pre-test and burn-in devices prior to stacking. Whether at home, in the office or on the move, modern life is increasingly dominated by electronics. For more than 50 years, the development of microelectronic (and now very often nanoelectronic) devices has revolutionized our way of life by offering a vast choice of products and services. Technological progress has made possible the realization of new objects and functions, some of which are giving rise to considerable markets. From safer and more environmentally friendly autonomous cars, to ever more sophisticated fixed and mobile communication systems, to increasingly powerful multimedia and computer equipment, to personal medical assistance systems and leisure activities, the range of applications continues to expand and diversify.

References

1. C. Lee, et al., *Proc. from the 66th Electronic Comp. and Techn. Conf. (ECTC)*, Las-Vegas, 31 May-3 June 2016, p. 1439.
2. R. R. Tummala, *Fundamentals of Microsystems Packaging*, McGraw-Hill, New York, 2001, pp. 4-41.
3. D. C. Brock, *Understanding Moore's Law: Four Decades of Innovation*, Chemical Heritage Foundation, Philadelphia, 2006, pp. 67-84.
4. Y. Li, P. K. Muthur Srinath, D. Goyal, *J. Electron. Mater.*, 45(1), 116(2016).
5. L. Li, et al., *Proc. from the 66th Electronic Comp. and Techn. Conf. (ECTC)*, Las Vegas, 31 May-3 June 2016, p. 1445
6. T.-M. Băjenescu, "Challenges in Nanotechnologies and Manufacturing Processes," *EEA* vol. 60 (2012), no. 1, pp. 75-79.
7. P. A. Sandborn, and M. Vertal, "Analyzing Packaging Trade-Offs During System Design," *IEEE Design and Test of Computers*, vol. 15, no. 3 (july-sept.), 10-19.
8. T.-M. Băjenescu, "MEMS and their Reliability," *EEA* vol. 58 (2010), no. 4, pp. 7-15
9. Zhiyong Ma and David G. Seiler, "Methodology and Diagnostic Techniques for Nanoelectronics," *Paul Stanford Publishing* 2016, pp. 1089-1119.
10. J. Q. Lu, *Proc. IEEE* 97(1), 18(2009).
11. S. F. Al-sarawi, D. Abott, P. D. Franzon, *IEEE Trans. Comp. Packag. Manufact. Technol.*, 21(1), 2(1998).
12. Yan Li, and Deepack Goyal (Eds.), *3D Microelectronic Packaging*, Springer, 2017.
13. N. Nabiollahi, et al., *Microelectronics Reliability*, 55(5), pp. 765-770, 2015.
14. C.-H. Liu, et al., *Proc. from the 66th Electronic Comp. and Techn. Conf. (ECTC)*, Las-Vegas, 26-29 May 2015, p. 1502.
15. C.-H. Liu, et al., *Proc. from the 64th Electronic Comp. and Techn. Conf. (ECTC)*, Las-Vegas, 26-29 May 2014, p. 1628.
16. R. Mahajan, et al., *Proc. from the 66th Electronic Comp. and Techn. Conf. (ECTC)*, Las-Vegas, 31 May-3 June 2016, p. 558.
17. K. Zoschke, et al., *Proc. from the 60th Electronic Comp. and Techn. Conf. (ECTC)*, Las-Vegas, 1-4 June 2010, p. 1385.
18. A. Eitan, K. Hung, *Proc. from the 65th Electronic Comp. and Techn. Conf. (ECTC)*, San Diego, 26-29 May 2015, p. 460.
19. T.-M. Băjenescu, "Some Reliability Problems of Electronic Packaging," *Meridian Ingineresc*, no. 4(2014), pp. 22-31.
20. R. Mahajan, and B. Sankman, "3D Packaging Architectures and Assembly Process Design," in Yan Li, and Deepack Goyal (Eds.), *3D Microelectronic Packaging*, Springer, 2017.
21. E. Jan Vardaman, "Foundry and assembly partnerships move the industry forward in tsv technology," http://www.semi.org/en/marketinfo /ctr_041176.
22. Packaging-key for system integration, 27 JUNE 2013, Vila Do Conde, Porto (Portugal).
23. D. P. LaPotin, T. R. Mazzawy, and M. L. White, "Early Package Analysis: Considerations and Case Study," *Computer*, vol. 26, no. 4, Apr. pp. 30-39.
24. T.-M. Băjenescu, "Reliability Aspects of MEMS and RF microswitches," *Meridian Ingineresc*, no. 4(2015), pp. 13-19.
25. K.-W. Lee, et al., *Proc. from the 64th Electronic Comp. and Techn. Conf. (ECTC)*, Orlando, 27-30 May 2014, p. 304.
26. G. Pares, et al., *Proc. from the 11th Electronics Packaging Conf. (EPTC)*, Singapore, 9-11 Dec. 2009, p. 772.
27. I. Szendiuch, *Radioengineering*, 20(1), 214(2011).
28. T. M. Bauer, et al., *Proc. from the 59th Electronic Comp. and Techn. Conf. (ECTC)*, San Diego, 26-29 May 2009, p. 1165.
29. K. N. Tu, "Reliability challenges in 3d ic packaging technology," *Microelectronic Reliability*, Vol. 51. No. 3, March 2011, PP. 517-523.
30. E. Jan Vardaman, "Foundry and assembly partnerships move the industry forward in tsv technology," http://www.semi.org/en/marketinfo /ctr_041176.
31. Packaging-key for system integration, 27 JUNE 2013, Vila Do Conde, Porto (Portugal).
32. D. P. La Potin, T. R. Mazzawy, and M. L. White, "Early Package Analysis: Considerations and Case Study," *Computer*, vol. 26, no. 4, Apr. pp. 30-39.
33. T.-M. Băjenescu, "Nano-electronics and Reliability," *EEA* vol. 59 (2011), no. 4, pp. 9-14.
34. T.-M. Băjenescu, "Micro-comutatoare RF MEMS: fiabilitate, moduri și mecanisme de defectare," *Meridian Ingineresc*, no. 3(2013), pp. 11-17.
35. T.-M. Băjenescu, "Some Reliability Problems of Electronic Packaging," *Meridian Ingineresc*, no. 4(2014), pp. 22-31.
36. T.-M. Băjenescu, "Reliability Aspects of MEMS and RF microswitches," *Meridian Ingineresc*, no. 4(2015), pp. 13-19.
37. T.-M. Băjenescu, "Crackings in Microelectronic Packaging," *EEA* vol. 65(2015), no. 2, pp. 15-24.
38. T.-M. Băjenescu, "Zuverlässige Bauelemente für elektronische Schaltungen," *Springer*, 2020.

DOI: 10.5281/zenodo.3713362
CZU 666.973



PROPERTIES OF STRUCTURAL LIGHTWEIGHT EXPANDED CLAY CONCRETE WITH DIFFERENT TYPES OF POROUS SANDS

Sergii Kroviakov*, ORCID ID: 0000-0002-0800-0123,

Lidiia Dudnyk, ORCID ID: 0000-0002-9969-8941,

Michael Zavoloka, ORCID ID: 0000-0002-2080-1230

Odessa State Academy of Civil Engineering and Architecture, str. Didrichsona, 4, Odessa, Ukraine

*Corresponding author: Sergii Kroviakov, skrovyakov@ukr.net

Received: 02. 18. 2020

Accepted: 03. 24. 2020

Abstract. In this work, the strength, water tightness and average density of modified expanded clay lightweight on different types of sands were investigated. Quartz sand, expanded clay sand and sand from granulated foam glass were used. It is shown that structural lightweight expanded clay concrete on light sand from granular foam glass is effective for thin-walled structures of hydraulic structures, if necessary, to reduce their weight. It was established that the average density of lightweight expanded clay concrete on a mixture of quartz sand and granulated foam glass is 1400-1440 kg/m³, water tightness is W10-W12, compressive strength up to 21 MPa, tensile strength in bending up to 5 MPa. Interstitial partitions of foam glass have an amorphous vitreous structure. The lightweight expanded clay concrete with sand of granulated foam glass has a high-water resistance and sufficient strength for thin-walled structures.

Keywords: *concrete, density, expanded clay, foam glass, sand, water tightness.*

Introduction

Structural expanded clay concrete and other lightweight concrete on artificial porous aggregates are often used in construction, including for thin-walled structures of hydraulic structures. Expanded clay lightweight concretes are the most promising materials for floating hydraulic structures, as they allow to increase the carrying capacity of these structures and have high durability [1]. The development of building technologies makes it possible to additionally increase the efficiency of expanded clay concrete and makes relevant research on the use of modern modifiers and new types of porous sands in their composition. In particular, granular foam glass [2, 3] is a promising porous filler. This aggregate has a low average density and at the same time practically does not permeable to water.

Problem formulation

The experience of using lightweight expanded clay concrete and light concrete similar to them showed high efficiency of these materials in civil, industrial and hydraulic

engineering. Due to the low average density of concrete, the load on the foundations and supports is reduced. For constructions that work in bending, the use of lightweight concrete reduces the mass of the full load, thereby allowing an increase in the length of the spans. For example, in Norway, in 1999, a "Stolmabridge" with a main span of 148 m was built from lightweight concrete of class LC-55 with an average density of 1900..1950 kg/m³ [4].

In reinforced concrete shipbuilding, lightweight concrete has shown high durability in the construction of oil and gas production platforms, floating docks, houses and hotels. These structures are operated in waters containing sulphates and chlorides, as well as exposed to freezing and thawing [1, 5]. Also, lightweight concrete allows you to increase the carrying capacity of reinforced concrete floating structures. In 1995, the International Federation for Structural Concrete (fib) recommended using only high-strength lightweight concrete in the construction of floating oil and gas platforms [6].

For the construction of reinforced concrete floating structures mainly lightweight concrete is used on ceramic aggregates with quartz sand. The average density of such lightweight expanded clay concrete and their analogs is usually from 1800 to 2000 kg/m³. But recently, the first time for the marine floating structure tripping complex MPU Heavy Lifter was used lightweight concrete, which included part of the light sand. The class of this concrete is LC 35/38, its average density is less than 1600 kg/m³ [7].

One of the relatively new types of light sand for lightweight expanded clay concrete is granulated foam glass [8]. Foam glass contains more than 90% of glass phase. Foam glass granules include small evenly distributed closed pores, separated by thin partitions. This type of aggregate is practically not permeable to water, therefore it is a promising component for light concrete of hydraulic structures, including floating reinforced concrete. When using a rational amount of granulated foam glass as a fine aggregate, lightweight expanded clay concrete with sufficient strength and durability can be obtained with a reduced average density.

Research methodology

For the manufacture of lightweight expanded clay concrete used:

- expanded clay gravel of a fraction of 5-10 mm produced by the Odessa expanded clay factory with a bulk density of 500 kg/m³;
- sulphate-resistant Portland cement CEM I 32.5 R/SR manufactured by Ivano-Frankivsk Cement Plant;
- polycarboxylate plasticizer Coral ExpertSuid-5.

Five different types of sands were used as fine aggregate for lightweight expanded clay concrete, which were obtained by mixing different types of sands previously scattered in fractions [9]:

Composition number 1 (№1). Quartz sand with a fraction ratio (in mm): 0.16-0.315 - 10%, 0.315-0.63 - 25%, 0.63-1.25 - 25%, 1.25-2.5 - 25%, 2.5-5 - 15%. The bulk density of this sand was 1580 kg/m³.

Composition number 2 (№2). Sand in which 50% of the fractions of 2.5-5 mm and 1.25-2.5 mm (coarse fractions) were replaced with expanded clay sand of the same fractions (the producer of expanded clay sand is Odessa Expanded clay Plant).

The density of sand particles in the fraction 2.5-5 mm - 605 kg/m³, in fractions 1.25-2.5 mm - 700 kg/m³. The bulk density of this artificial sand was 1430 kg/m³.

Composition number 3 (№3). Sand, in which 100% of the fractions of 2.5-5 mm and 1.25-2.5 mm was replaced with expanded clay sand of the same fractions. The bulk density of this sand was 1290 kg/m³.

Composition number 4 (№4). Sand, in which 50% of the fractions of 2.5-5 mm and 1.25-2.5 mm were replaced with granulated foam glass of the same fractions (foam glass manufacturer LLC «NPP Tekhnologiya», Shostka). The bulk density of granulated foam glass in the 2.5-5 mm fraction is 230 kg/m³, in the 1.25-2.5 mm fraction it is 270 kg/m³. The bulk density of this artificial sand was 1330 kg/m³.

Composition number 5 (№5). Sand in which 100% of the fractions of 2.5-5 mm and 1.25-2.5 mm was replaced by granulated foam glass of the same fractions. The bulk density of this sand was 1080 kg/m³.

Water absorption of expanded-clay granules per hour was about 16%, foam glass – 5..6%.

Also in the concrete undergone, the amount of plasticizer Coral ExpertSuid-5 was varied in the range from 0.4 to 1% by weight of cement.

All mixtures had equal mobility P5. The amount of Portland cement in all investigated lightweight expanded clay concrete was 500 kg/m³, the amount of expanded clay gravel was 675 l/m³. The amount of sand in the concrete was adjusted depending on the amount of water in the mixture ranged from 460 to 470 l/m³.

Results and discussion

Equal mobility of mixtures was provided by changing the amount of water, respectively, the W/C of the mixtures depended on their composition. Figure 1 shows the graphs of the effect of the amount of Coral ExpertSuid-5 plasticizer and the type of sand on the W/C of expanded clay lightweight concrete mixtures. Analysis of the graphs shows that with an increase in the amount of the plasticizer Coral ExpertSuid-5 from 0.4 to 0.6% of the W/C mixtures on all types of sand, it sharply decreases – by 11-13%. A further increase in the amount of plasticizer also reduces the W/C of the mixture, but less significantly.

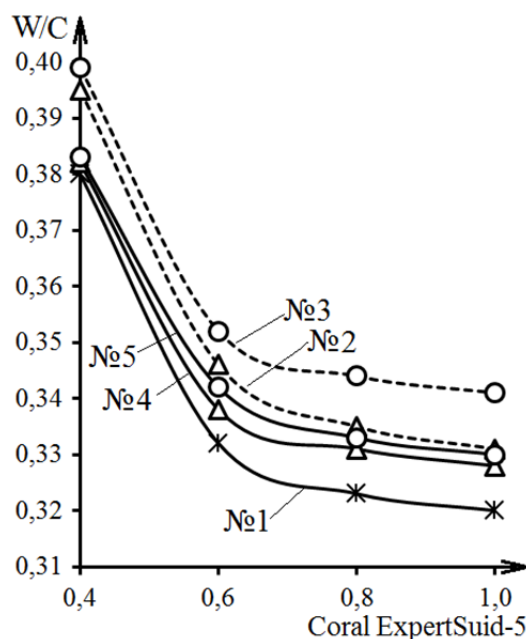


Figure 1. The influence of the amount of plasticizer and the type of sand on the W/C expanded clay lightweight concrete mixtures of equal mobility.

The smallest W/C are in mixtures on quartz sand (№ 1), the largest in expanded clay sand (№2, №3). Accordingly, when replacing 100% of the large fractions of quartz sand with light porous sand, the W/C grows more significantly than when replacing 50% of the fractions volume. Mixes with fine aggregate of granulated foam glass (№4, №5) have higher-grade aggregate with higher amounts of silica sand, but lower than lightweight expanded clay concrete mixes with expanded clay sand. This results from the fact that the granulated foam glass has mainly closed porosity, respectively low water absorption.

Figure 2 shows graphs of the effect of the amount of plasticizer and the type of sand on the strength of the lightweight expanded clay concrete was studied. Analysis of the graphs shows that the amount of plasticizer Coral ExpertSuid-5 significantly affects the strength of expanded clay concrete under compression (Figure 2, a), but less significantly on the tensile strength under bending (Figure 2, b). The strongest are lightweight expanded clay concrete with the amount of plasticizer Coral ExpertSuid-5 0.8% by weight of cement.

The type of sand has a more noticeable effect on the compressive strength of lightweight expanded clay concrete than on the tensile strength in bending.

Compressive strength of light concrete with expanded clay sand in large fractions (№ 2, №3) is 3-10% lower than the strength of expanded clay concrete with quartz sand (№1). The tensile strength in bending of expanded clay lightweight concrete data is 4-9% lower than the strength of expanded clay concrete with quartz sand.

During the use of granulated foam glass as a fine aggregate (№4, №5), the strength of lightweight expanded clay concrete under compression decreases by 17-32% compared to concrete on quartz sand (№ 1), and the tension in bending increases by 5-19%.

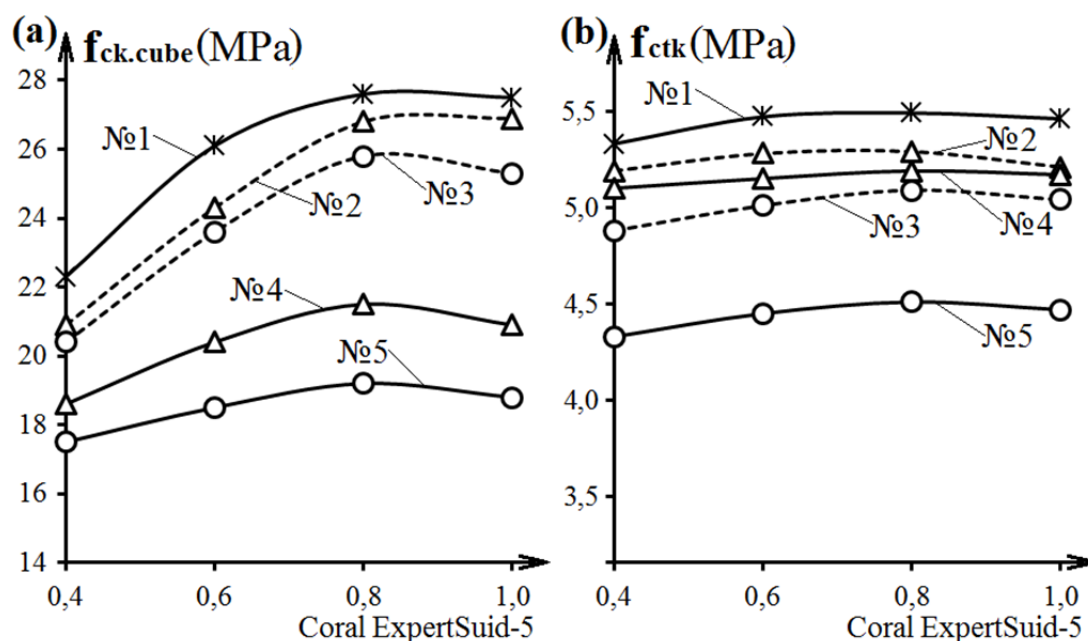


Figure 2. The effect of the amount of plasticizer and the type of sand on the strength of expanded clay lightweight concrete: a) in compression; b) tension in bending.

One of the most important quality indicators for concrete hydraulic structures is water tightness. It largely determines the durability of the material in thin-walled structures that are operated in contact with water. Accordingly, in the framework of this work, the water tightness of lightweight expanded clay concrete was investigated. Figure 3 shows the

effect of the amount of plasticizer and the type of sand on the water tightness of the expanded clay concrete was studied.

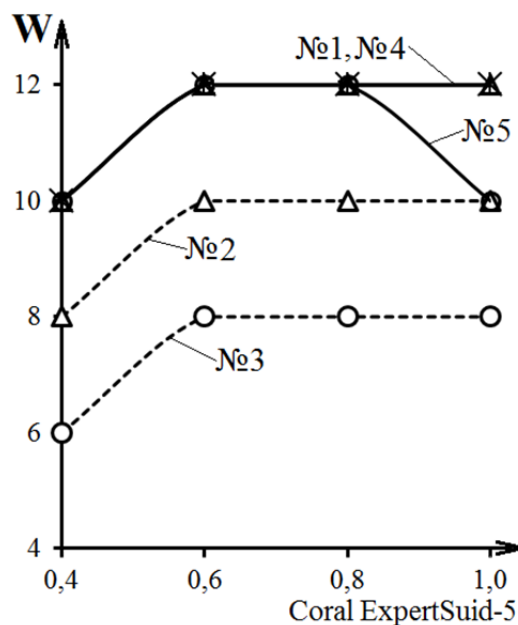


Figure 3. The effect of the amount of plasticizer and the type of sand on the water tightness of lightweight expanded clay concrete.

Analysis of the graphs shows that lightweight expanded clay concrete with foamed glass in large fractions of sand (№4, №5) are water tightness at virtually the level of expanded clay concrete on quartz sand. The water tightness of lightweight concrete with expanded clay sand in large fractions, respectively, is one (for №2) and two (for №3) grades lower than similar lightweight expanded clay concrete on quartz sand. This is due to the ability of this porous sand to pass water under hydrostatic pressure. By increasing the dosage of the Coral ExpertSuid-5 additive to 0.6-1.0%, the water tightness of the lightweight expanded clay concrete is increased by about the mark.

As noted above, the main purpose of the application of light sand in lightweight expanded clay concrete is to reduce their average density. The effect of the amount of plasticizer and the type of sand on the average density of expanded clay concrete is shown in Figure 4.

As can be seen in the graphs, with an increase in the dosage of the plasticizer due to a decrease in the W/C of the mixture, the average density of lightweight expanded clay concrete does not significantly increase. During the application of 50% (№2) and 100% (№3) of expanded clay sand in large fractions, the average density of lightweight concrete decreases, respectively, from 4-5% and 6-7% compared to expanded clay concrete on quartz sand.

Sand granulated foam glass has a lower bulk density, respectively, during the application of 50% (№4) and 100% (№5) of foam glass in large fractions, the average density of lightweight expanded clay concrete decreases by 7-8% and 13-14% compared to expanded clay concrete on quartz sand (№1). At the same time, the average density of lightweight expanded clay concrete with 100% sand from granulated foam glass in large fractions (№5) does not exceed 1440 kg/m³.

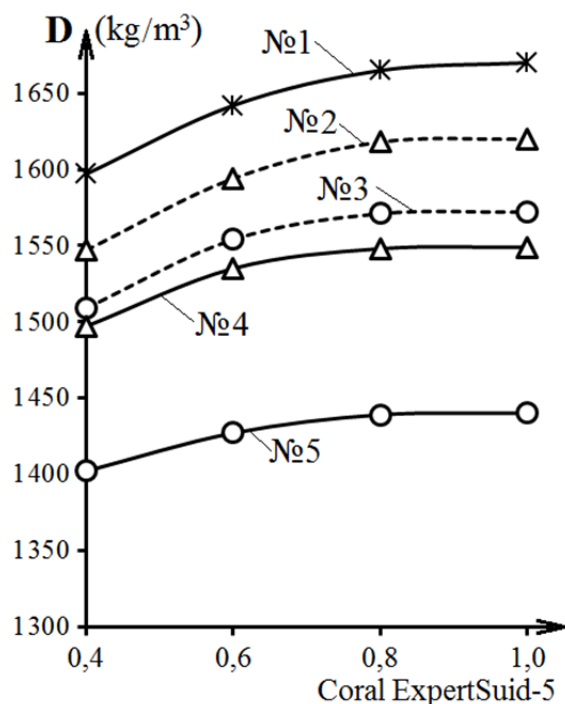


Figure 4. The effect of the amount of plasticizer and the type of sand on the average density of lightweight expanded clay concrete.

Figure 5 shows the photographs of the structure of the contact zone of the granules of foam glass and the cement-sand matrix, taken with an electron microscope at 5000×1 magnification. Interstitial partitions of foam glass have an amorphous vitreous structure, respectively, in the photo they look like solid.

As a conclusion, the cement-sand matrix has close contact with the foam glass granules, which is explained, in particular, by the low water absorption of these granules and, accordingly, by small deformations of the aggregate during wetting and drying.

The above features of the structure of expanded clay concrete with granulated foam glass as part of fine aggregate explain the high water tightness of these materials at their low density and confirm the prospects of using porous sand based on granular foam glass in lightweight concrete for thin-walled structures of hydraulic structures.

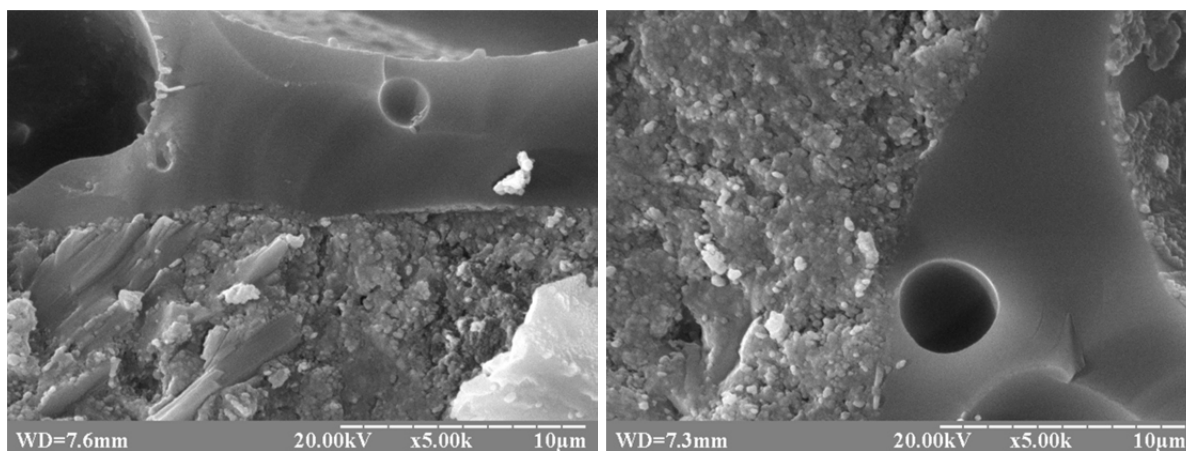


Figure 5. The structure of the contact zone of foam glass granules and cement-sand matrix, an increase of 5000×1.

Conclusions

Modified lightweight expanded clay concrete with light sand of granulated foam glass is an effective material for thin-walled structures, which is important to reduce weight while providing the necessary strength and high water tightness of the material. In particular, this type of lightweight concrete can be used in reinforced concrete shipbuilding to further increase the carrying capacity of floating structures.

The average density of lightweight expanded clay concrete on a mixture of quartz sand and granulated foam glass is 1400-1440 kg/m³, water tightness is W10-W12, compressive strength up to 21 MPa, tensile strength in bending up to 5 MPa. That is, lightweight expanded clay concrete with sand of granulated foam glass has a high water resistance and sufficient strength for many thin-walled structures.

References

1. Gerwick B. C. Jr. Construction of marine and offshore structures, Third Edition. Baton Rouge: Taylor & Francis, 2005.
2. Al-Sibahy A., Edwards R. Mechanical and thermal properties of novel lightweight concrete mixtures containing recycled glass and metakaolin. *Construction and Building Materials*, 2012, vol. 31, pp. 157–167.
3. Popov M., Zakrevskaya L., Vagano V., Hempel S., Mechtcherine V. Performance of lightweight concrete based on granulated foamglass. *IOP Conference Series: Materials Science and Engineering* (2015), Nr. 96 (1), S. Art. 012017
4. Helland S. Lightweight aggregate concrete in Norwegian bridges. *HPC BridgeViews*, Issue No. 11, Sept/Oct. 2000. pp. 2-3.
5. Benchmarking of deemed-to-satisfy provisions in standards: Durability of reinforced concrete structures exposed to chlorides. State-of-the-art report.fib:2015.191 p.
6. Lightweight aggregate concrete. Recommended extension to Model Code 90, Guide. Identification of research needs, technical report. Case Studies, State-of-art report.fib Bulletin No. 8, 2000. 118 p.
7. Liu G., Li H. Offshore platform integration and float over technology. Sciencepress, Beijing, China, 2017. 280 p.
8. Davidyuk A.N. Legkiye konstruktsionno-teploizolyatsionnyye betony na steklovidnykh poristykh zapolnitelyakh. M.: Krasnaya zvezda, 2008.
9. Krovyakov S. O., Dudnyk L. V. Porivnyannya vlastyvostryey modyfikovanykh keramzytobetoniv z riznymy typamy piskiv. *Resursoyekonomnímateriali, konstruktsií, budívlí ta sporudi*. Vıpusk 35. Rıvne: NUVGP, 2018. pp.18-25.

DOI: 10.5281/zenodo.3713364

CZU 524.131.5



GROUNDS STABILIZED WITH ORGANIC BINDERS

Eugeniu Braguța*, ORCID ID: 0000-0001-9579-1033

*Technical University of Moldova, 168, Stefan cel Mare Bd., Chisinau, Republic of Moldova***eugeniu.braguta@dmmc.utm.md*

Received: 02. 05. 2020

Accepted: 03. 22. 2020

Abstract. The paper presents the enzymatic stabilizers effect on grounds in the compaction process by vibration. It has been intended, by specific rheological modeling of the ground mixtures with organic additives, as well as by laboratory or "in situ" tests, to highlight the increased effect of elasticity longitudinal modulus and volumetric elasticity. Also, based on experiments it was determined the rheological evolution of the bulk modulus in relation to time up to the asymptotic stabilization specific to the final parametric values of the structure resistance and stability. The analytic assessment performed by modeling, as well as the experimental results significantly highlight the enzyme stabilizer effect. Thus, it is distinguished that by the pore size and the enzyme content modification, as a result of the recycled ground dynamic behavior, the Poisson's ratio increases considerably, reaching the value of 0.485. The experimental results confirm the possibility to increase the resistance and stability of ground road structures stabilized with enzymes. In this context, the compaction process by vibrations has to be performed in the optimal dynamic regime for the substantial modification of the material porosity.

Keywords: *Organic additives, longitudinal modulus of elasticity and volumetric elasticity, recycled ground dynamic behavior, enzyme stabilizer, Poisson's ratio.*

Introduction

As a rule, the Earth, as basic or actual building material, does not have the ideal form from the point of view of an engineer in the field. It is known, that this problem is exceeded through different specific procedures to improve soil quality, one of the most important and frequent actions on the soil is the densification being achieved by compaction.

For road structures, while using existing soils, additive materials are necessary, as well as appropriate technologies, in order to obtain the resistance and stability performances at the levels required by normative regulations. In this context, this paper highlights the effect of ground mixed with natural enzymes, mineral aggregates and additive materials. For certain categories of ground with large content of clay mixed with sand and mineral aggregates with an adequate treatment of enzyme stabilizers there were obtained remarkable experimental results.

Thus, the characteristics of the stabilized enzyme structures can be defined being based on mechanical strength σ_z of the vertically longitudinal elasticity modulus E_z , of the volumetric elasticity modulus E_v and rigidity coefficient k vertical direction [1].

The presence of enzymes in the mixture of material is remarked, under conditions of corresponding dosing, mixing and homogenization, by modifying the coefficient Poisson, noted with ν . In this case, by increasing values of ν towards the maxim limit $\nu_{\max} = 0,5$ it is found the increase of volumetric elasticity modulus, the increase of resistance as well as of the completed structure rigidity [2, 3].

The rigor of the processed stabilized ground structure

During the blending process, the mixture ground-mineral aggregates should assure the optimal dose of supply in atomized condition with enzymes or organic binders that would occupy the porous spaces by decreasing the water content from the natural porous network.

Present technologies with automatic control and computer monitoring are able to arrange a large variety of technical solutions [4, 14].

Therefore, the processed material in the form of stabilized earth with enzyme must have the porous network with high content of enzymes to expand Poisson coefficient and the rising resistance of freezing process (freezing-thaw).

In the field of elastic deformation for the vertically implemented road structure, as a consequence of compaction through vibration, rigidity can be measured as follows:

$$k = C_z \cdot S \quad (1)$$

Where k is rigidity coefficient, in the elastic field, C_z is the coefficient of uniform elastic contraction matching to the area S of the contact rectangular surface; for the coefficient of uniform elastic contraction the following relation is implemented [5].

$$C_z = \alpha \frac{E_z}{\sqrt{S}} \frac{1}{1-\nu^2} \quad (2)$$

Where α is the form coefficient of the real surface, which is materialized through a contact board, with values within the range $0,8 \div 1,5$.

In regard to „in situ” experiments for a certain ground type, one can use „test plate” with a rectangular surface of area S' , which permits the calculation of rigidity coefficient k' for the „test field” with the relation:

$$k' = \alpha \frac{E_z \sqrt{S'}}{1-\nu^2} \quad (3)$$

The rigidity coefficient k for the real surface S of rectangular shape (the contact spot) between the vibrating roller and the stabilized ground layer can be calculated using the formula:

$$k = \frac{\alpha E_z \sqrt{S}}{1-\nu^2} \quad (4)$$

From the relations (3) and (4) there can be measured the value of k in relation to the value of k' determined experimentally, as follows

$$k = k' \sqrt{\frac{S}{S'}} \quad (5)$$

For the test plate with $S = 4500 \text{ cm}^2$ the rigidity coefficient k' for different field categories was experimentally determined under dynamic regime of vibrations of resonance.

Table 1

Experimental values of rigidity k' with the dynamic teste plate

Nature of Stabilized Ground Layer	Rigidity Coefficient k' (MN/m)
Loose sandy soil Gravel (3 ÷ 7) mm with sand	44,0
Loose loamy fine sand Gravel (7 ÷ 15) mm with loamy sand	67,5
Medium grained and light loamy loose sand	90,0
Medium grained sand until the sea	95,6
Gravel (7 ÷ 15) mm with pre compacted ground Clay with compacted ground	120

Modulus of longitudinal elasticity

For a cylindrical sample derived from the stabilized/compacted layer, subjected to the uniaxial compression, according to the national standards the axial elastic modulus E_z is determined as follows:

$$E_z = \frac{4}{\pi} \frac{F_z}{d^2 - d_0^2} \frac{h_0}{\Delta h} \quad (6)$$

Where F_z is the axial force applied centrally;

d_0 - initial diameter of uncompressed sample;

h_0 - initial height of uncompressed sample;

d - final diameter of the median transversal section after compression;

h - final height remained, of the sample, after compression;

Δh - variation of height (compaction) of the sample under compression force, so that

$$\Delta h = h - h_0 < 0$$

Accordingly, based on 1500 of samples collected from the ground layer stabilized with enzymes and compacted with a vibrating roller, there were determined the values of the modulus E_z .

Regulated by the amount of enzyme mass, reported to 100 kg of milling, mixed, compacted ground, that is at the percentage dose ε , %, were achieved the values of longitudinal elastic modulus E_z given within the Table 2.

Table 2

Modulus E_z depending on the ε

ε , %	0,1	0,2	0,3	0,4	0,5	0,6
E_z , MN/m ²	5,81	6,50	7,80	8,78	9,15	10,21

Coefficient of Poisson

On condition of uniaxial compression under direction Z with the force F_z the process of axial deformation described through specific deformation $\varepsilon_z = \frac{h-h_0}{h_0} = \frac{\Delta h}{h_0}$ is logically accompanied by the transversal deformation from the median plan, expressed by $\varepsilon_y = \frac{d-d_0}{d_0} = \frac{\Delta d}{d_0}$, so that $\varepsilon_y = \nu \varepsilon_z$ [4, 6, 7]

Respectively, the coefficient of Poisson ν may be determined with the relation

$$\nu = \frac{h_0 \Delta d}{d_0 |\Delta h|} \quad (7)$$

The experimental conclusions have shown ν values of between 0.42 and 0.485 for the 1500 samples collected „in situ”. Table 3 presents the values of the coefficient of Poisson depending on the percentage dose ε of the enzyme stabilizer.

Table 3

Values of the coefficient of Poisson depending on the ε , %

ε , %	0,1	0,2	0,3	0,4	0,5	0,6
ν	0,421	0,442	0,453	0,465	0,475	0,485

Modulus of volumetric elasticity

For fields with large surfaces and wide spaces subjected to vibrations or undulating processed wave unidirectional propagation, the volumetric modulus E_v can be calculated as follows:

$$E_v = E_z \frac{1-\nu}{(1+\nu)(1-2\nu)} \quad (8)$$

It is demonstrated that by alteration the porosity and supply of voids with stable fluid like substances, the coefficient of Poisson rises until the limit value $\nu_{max} = 0,5$ (so that $\nu < \nu_{max}$) [1, 11].

Modulus of volumetric elasticity E_v during the module E_z and ν , determined experimentally is given in table 4.

Table 4

Modulus E_v depending on modulus E_z and ν

ν	0,421	0,442	0,453	0,465	0,475	0,485
$E_z, MN/m^2$	5,81	6,50	7,80	8,78	9,46	10,21
$E_v, MN/m^2$	14,96	21,83	31,25	45,86	67,26	117,80

The samples taken on layers of ground stabilized with enzymes within the dose $\varepsilon = 0,5\%$ were used for the purpose of being followed in time. The volumetric elastic modulus dynamic (deformation) measured „in situ” at 35 m from the compaction source through vibration, at certain time intervals, is shown in the Table 5 [3, 8, 12]

Table 5

Volumetric elasticity modulus E_v in time

Time, hours	0	16	24	48	72
$E_v, MN/m^2$	67,5	70,5	96,3	101,8	109

The rheological evolution with regard to time points out a stable asymptotic, as results from the experimental data contained within Table 2. Therefore, the rheological law established by the authors of the present paper is under form [9].

$$E_v(t) = \frac{0877+15t}{0,13t+0,013} \quad (9)$$

With $E_v(0) = 67,46 MN/m^2$ at the moment $t = 0$. The temporal variable t is expressed in hours.

For the results obtained experimentally, within Figure 1, it appears the curve of variation of the modulus $E_v(t)$ in relation to time.

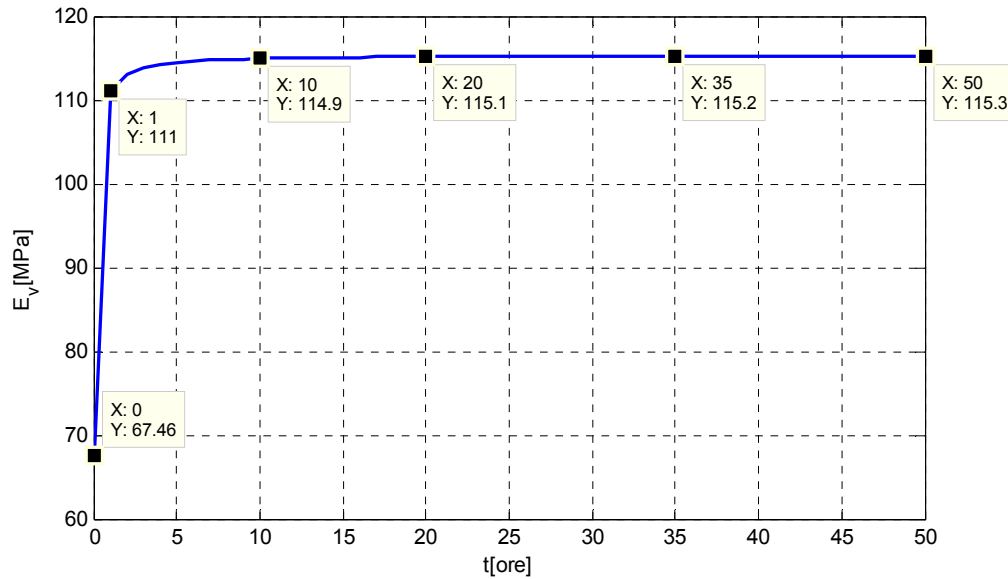


Figure 1. Variation of volumetric elasticity modulus in relation to time.

Californian index CBR

The Californian index of bearing capacity is indicated under the form of $CBR = \frac{F_p}{F_s}$ for the depth of penetration Δp , where F_p is the effective penetration force, and F_s is the standard force relating to the values $\Delta p = 2,5$ mm and $\Delta p = 5$ mm.

For grounds stabilized with enzymes there were obtained the values from Table 6 [8 - 15].

Table 6

Index CBR, % for stabilized ground

Sample Lot	Average Value of the Effective Penetration Force	CBR _{2,5} , $\Delta p = 2, 5$ mm $F_s = 13, 2$ KN	CBR ₅ , $\Delta p = 5$ mm $F_s = 20, 0$ KN
I	8,3	63	-
	11,0	-	53
II	7,5	56	-
	9,2	-	46
III	7,8	58	-

Continuation Table 6

	9,3	-	46
IV	9,45	71,5	-
	13,11	-	66
V	Index CBR, % for untreated ground		
	3,11	23,55	-
	3,86	-	19,32

Interpretation of experimental results

The experiments performed not only „in situ”, but also in the laboratory, aimed to highlight the modification of the parameters of deformability, elasticity and resistance of grounds stabilized with enzymes, based on a permanent procedure, being compared to the same grounds untreated with enzyme stabilizers, that is in the natural state.

- a) The modulus of longitudinal elasticity E_z determined at the request of axial compression, corresponding to relation 6, for stabilized grounds, it was evaluated for 1500 samples collected from the layer of stabilized ground for six mass doses ε of stabilizer, as results from Table 2. It is found that as the percentage quantity of stabilizer ε increases, also increases the modulus E_z .
- b) The coefficient of Poisson, which experimentally was determined based on relation 7, for stabilized grounds, in the percentage quantities ε of the stabilizer, it is found to be increasing according to Table 3.
- c) The volumetric modulus E_v depends not only on the coefficient of Poisson, but also on the modulus E_z . Therefore, as the modulus of Poisson and the dosage of stabilizer increases, it is found a pronounced increase of the volumetric modulus, according to the data from Table 4.
- d) The Californian index CBR, with the experimental results from Table 6, points out values correlated with the volumetric modulus E_v , being mentioned the fact that the values for the ground stabilized are 3 - 4 greater than the case of ground untreated with enzyme solutions.

Conclusions

The issue of stabilizing grounds with enzymes is an efficient opportunity to achieve the road structures by processing „in situ” local grounds, which are made better with mineral aggregates and treated with organic substances.

In this context, it is also inscribed the present work shows not only the theoretical aspect to modify the elasticity modulus by increasing the coefficient of Poisson, depending on the dose of stabilizer, as well as the experimental results obtained „in situ” on the polygon testing and in the laboratory. It is specified the fact that there were accomplished experimental stages „in situ” with equipment of milling, mixture and stabilizer atomization, the deposit of unprocessed ground layers as well as the dynamic compaction through vibration. The experiments consisted to sample the natural ground and the layers of stabilized ground. As well, the dynamic charges from the field permitted the determination of the elastic moduli and rigidities. The capacity of road structure resistance was measured „in situ” by determining the Californian index CBR:

Based on analytical and experimental results the following conclusions can be summarized:

- ✓ The enzyme stabilizers in atomized and homogenous mixture with the natural ground determine the significant modification of resistance, volumetric elastic modulus, coefficient of Poisson and Californian index CBR;
- ✓ The presence of stabilizer with enzymes in the porous structure of grounds leads to significant increases of modulus and Californian index.

As a conclusion, the ecological treatment with enzymes to earth assures the road layers accomplishment from ground with special performances.

References

1. Rahman F., Hossain M. and Romanoski S. A. Soil stiffness evaluation for compaction control cohesionless embankments, *Geotechnical Testing Journal*, Vol. 31, No. 5, pp. 442–451, 2008.
2. Braguța E. The dynamic compaction through vibration of road structures from stabilized soil with organic binders: Ph.D. Thesis. Galati (Romania): Dunarea de Jos" University from Galati, 2018.
3. Bratu P., Braguța E. Performanțe de rezistență a pământurilor stabilizate cu enzime, în procesul de compactare prin vibrații, *Consilox - 12*, "Știința materialelor oxidice în slujba dezvoltării durabile" 16-20 septembrie 2016, Sinaia, Romania.
4. Rolling M. P. and Rolling R. R. *Geotechnical materials in construction*, McGraw – Hill, 1996.
5. Pințoi R., Bordos R., Braguța E. Vibration Effects in the Process of Dynamic Compaction of Fresh Concrete and Stabilized Earth, *Journal of Vibration Engineering & Technologies* – Vol. 5, No.3, June 2017.
6. Nicolescu L., *Technology of stabilizing grounds*, Publishing House Ceres, Bucharest, 1980.
7. Nicoară S. V. Contributions to the compaction of porous media in construction retention. PhD thesis. University Politehnica, Timisoara, 2003.
8. Condrat A., Ababii A., Braguța E. Tehnologii noi și utilaje pentru stabilizarea pământurilor cu folosirea stabilizatorilor pe baza de compuși organici naturali polienzimici, Conferința Științifică Internațională de Cercetare și Administrare Rutieră, "CAR 2015" București, 9-11 iulie 2015.
9. Dobrescu C. F., Braguța E. Evaluation of strength and deformation parameters of soil based on laboratory tests, Multi-Conference on Systems & Structures (SysStruc 17) din Universitatea Eftimie Murgu din Reșița 9-11 noiembrie 2017.
10. Braguța E. Interacțiunea compactor teren în procesul de vibrare, conferința tehnico - științifică internațională „Probleme actuale ale urbanismului și amenajării teritoriului” 17-19 noiembrie 2016, Chișinău, ISBN 978-9975-71-854-9.
11. Bratu, P.; Ghinea, A. Perfecționarea constructivă și funcțională a mașinilor de compactat prin vibrare. *Rev. Mecanizarea construcțiilor* nr. 3/1981.
12. Dobrescu C. F., Braguța E. Optimization of Vibro-Compaction Technological Process Considering Rheological Properties, Acoustics and Vibration of Mechanical Structures—AVMS-2017, Proceedings of the 14th AVMS Conference, Timisoara, Romania, ISBN 978-3-319-69822-9, ISSN 0930-8989.
13. Dobrescu C.F. Analiza parametrică reologică a procesului de compactare dinamică a pământurilor în regim controlat de vibrații forțate, „Dezvoltarea durabilă favorabilă incluziunii” Sibiu, 6-7 Noiembrie 2014;
14. Dobrescu C.F. Highlighting the change of the dynamic response to discrete variation of soil stiffness in the process of dynamic compaction with roller compactors based on linear rheological modelling. *Appl. Mech. Mater.* 801, 242–248 (2015).
15. Dobrescu C. F., Braguța E. Evaluarea parametrilor de rezistență și deformabilitate ai terenului pe baza încercărilor de laborator, *Academia de Științe Tehnice din România și Universitatea Ovidius din Constanța*, ZASTR 2017 6-7 octombrie, ISSN 2066-6586.

DOI: 10.5281/zenodo.3713366

CZU 624.012.45



STRENGTH, CRACK RESISTANCE AND DEFORMATIVITY OF REINFORCED CONCRETE BEAMS DAMAGED BY THROUGH CRACKS, REINFORCED CARBON FIBER

Diana Antonova^{1*}, ORCID: 0000-0001-9021-857X,Michael Zavoloka¹, ORCID: 0000-0002-2080-1230,Vasyl Karpiuk¹, ORCID: 0000-0002-4088-6489,Irina Karpiuk¹, ORCID: 0000-0003-3437-5882,Ion Rusu², ORCID ID: 0000-0002-7507-638X¹Odessa State Academy of Civil Engineering and Architecture, Didrichson street, 4, Odessa, Ukraine²Technical University of Moldova, 168, Bd. Stefan cel Mare, Chisinau, Moldova*Corresponding author: Diana Antonova, antonova.dv@ukr.net

Received: 01. 14. 2020

Accepted: 03. 19. 2020

Abstract. The article deals with the main results of experimental studies of strength, crack resistance and informational content of the diagonal and normal sections of common damaged and brought to the critical state of the first group r. c. - beams reinforced with carbon fibre sheet in the lower tensioned zone and on the support area. According to the adopted methodology, an experiment was conducted on the four-factor three-level Box-Benkin B4 plan. The average relative deformation values of the compressed concrete in the middle part of beams after their stabilization under low-cycle static loading have been evaluated. Tests of prototypes were carried out according to the scheme of single-track free-beam, alternately loaded from above, then from below by two concentrated forces without changing its position.

Introduction

In the course of operation or armed hostilities the span r.c. structures are subject to substantial damage and considerable reduction of their bearing capacity, especially under low-cycle repeated loading. In this regard, there is a need to restore their performance and / or increase bearing capacity. However, in the current design standards there are no recommendations to determine the residual bearing capacity of such structures and calculate their gain. There are some known methods to restore performance and strengthen the structure by increasing the cross section and attaching additional metal or reinforced concrete elements. Still, the calculation methods of such reinforcement are also imperfect. It is proposed to renew operation capacity of such structures by strengthening their tensioned parts with CFRP; the performed experimental research will provide the basis to calculate bearing capacity of present structures with the aid of the deformation method improved by the authors.

Theoretical prerequisites, procedures and results of the research

Resistance of r.c. elements to the combined action of transverse forces and bending moments at low-cycle non-reversal high-level loads is one of the most significant and underexplored problems both in the r.c. theory and in actual design process [1]. Indefinite repetition in operation and a change of the reverse load can lead to the consequences that are qualitatively different from those obtained as a result of calculation for permanent loading of maximum intensity which actually is taken into account by the majority of effective design standards.

Existing design standards, even under constant load, are far from perfectionism. Significantly “lag behind” in this regard are methods to calculate strength of normal sections, when the influence of non-repeating cyclic signs of load on them is taken into account indirectly or not at all, especially at a higher level.

A survey of the available bibliography has proved that researchers still did not come to a single opinion about the impact of loads on the bearing capacity of the studied elements. Majority of authors indicate that such bearing capacity reduces under low-cycle loading. Other researchers [2, 3, 4] state that the infrequent cyclic loading of the operational level ($\eta \leq 0.70$) can lead up to 20% higher strength of the span r.c. elements, which needs additional clarifications and experimental confirmation.

Resistance of the span r.c. CFRP-strengthened structures subjected to low-cycle repeated high-level loading that have been damaged in operation or in military hostilities was not studied at all. Therefore, the research is important and up-to-date.

Research methodology

In accordance with the adopted methodology the in-situ test is accomplished with the use of 4-factor 3-level B4 plan of Box-Behnken. The factors have been varied according to the data elicited from the literature review which show that the most influential factor X1 is the value of the relative span of the section a/h_0 , which was varied at three levels: $a = h_0, 2h_0$ and $3h_0$.

The next influential by value factor is, as a rule, such design factor as the grade of heavy concrete: $X2 \rightarrow C16/20, C30/35, C40/55$, and the third factor – the value (quantity) of the transverse reinforcement in the support areas: $X3 \rightarrow \rho_{sw}=0.0016; 0.0029; \text{ and } 0.0044$. The fourth factor was assumed to be the external action factor X4 and a level of the reversal load: $\eta = \pm 0.50; \pm 0.65; \pm 0.80$ of the actual bearing capacity, i.e., the transverse load value where at the opening width of the diagonal cracks w_k exceeded 0.4 mm, and the span sag $f \geq 1/150$.

The tested beam samples were kept in normal thermal and humid conditions at the temperature $20 \pm 2^\circ\text{C}$ and almost 100% air humidity during 100...110 days.

Prior to testing the side surfaces of the beams were coated with a thin layer of lime solution in order to facilitate fixation of formation and development of normal and diagonal cracks, and afterwards these beams were dried until they reached the natural humidity.

Deformations of the concrete, reinforcement and bending of the test samples were measured with the aid of dial indicators having a division value 0.001 mm and 0.01mm accordingly. The samples were tested according to the pattern of a single span simply supported beam which was intermittently loaded from the top and from the bottom by two point forces without any changes in the beam position.

Before the main experiment the 25 test beams (twin beams) of the first series were tested in turn for action of a single-time short-period stage-wise increasing loading, practically, up to destruction, when the open width of the diagonal cracks and the sag exceeded the permissible values ($w_k > 0.8$ mm, $f \geq l/150$). After that, similar research beams of the second and third series were tested under the influence of alternating low-cycle transversal loads of the indicated levels in accordance with the test base $N = 20$ cycles, after which the sample was pumped to destruction or reaching the ultimate state, if this did not happen earlier on the previous ones cycles. The criteria for the destruction of the prototypes were the achievement of ultimate strain values in concrete or reinforcement, an excessively large opening (up to 1 mm) of inclined (more often) or normal (less often) cracks, a significant increase (up to 15 mm) in the deflection boom, no increase or decrease (by 15% and more) displays of the manometer of the power plant pumping station [5]. In the fourth series the tested sample beams of the 2nd series were brought to their limit state and then reinforced with a metal casing and tested by reversal and repeated loading.

After the tested samples of series 3 beams were brought to the limit state according to the 1st and 2nd groups, the damaged lower tensioned zone and almost destructed support areas were strengthened with CFRP sheets Sika® Wrap® -231C according to the Sika Russie [6] technology (series 5). The construction of this strengthening is shown in Figure 1.

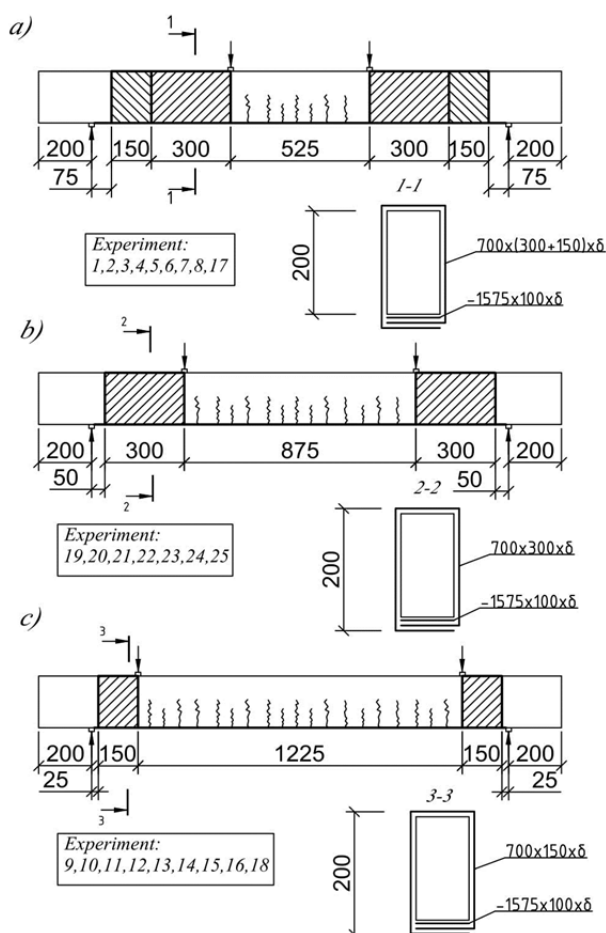


Figure 1. Patterns of strengthening the lower tensioned zones and support areas of the damaged r.c. beams of 3rd series with large (a), medium (b) and small (c) shear spans. The strengthened with external CFRP beams of series 5 were tested according to the same methodology as the beams of series 3.

Strength of the tested beam samples

As a result of processing the obtained experimental data of the first, third and fifth series, the removal of insignificant and recalculation of those coefficients that remained with the help of the effective COMPREX computer program were developed under the guidance of prof. Voznesensky V.A., that obtained adequate mathematical models of strength, i.e., destructive transverse V_u , i loads in natural or reduced to cross-sectional expressions that have sufficient informational benefit and show satisfactory convergence with experimental data and characterize the strength of research elements:

- reference (series1) with the stage-wise gradually increasing loading.

$$\hat{Y}(V_{u,1}) = 98 - 41x_1 + 12x_2 + 6x_3 + 16x_1^2 - 7x_2^2 - 5x_3^2 - 7x_1x_2, \text{ кН}, \nu=5.2\%$$

$$\text{Variability coefficient } \bar{U} = 5.2\%; \quad (1)$$

$$\hat{Y}\left(\frac{V_{u,1}}{bh_0}\right) = 5.60 - 2.3x_1 + 0.69x_2 + 0.34x_3 + 0.91x_1^2 - 0.40x_2^2 - 0.29x_3^2 - 0.40x_1x_2, \quad (1a)$$

- similar beams (series 3) with the low-cycle non-reversal high-level loading.

$$\hat{Y}(V_{u,3}) = 90 - 36x_1 + 10x_2 + 7x_3 - 3x_4 + 18x_1^2 - 6x_2^2 - 6x_3^2 - 2x_4^2 - 8x_1x_2 + 2x_1x_4, \text{ кН},$$

$$\text{Variability coefficient } \bar{U} = 5.1\%;(2)$$

$$\hat{Y}\left(\frac{V_{u,3}}{bh_0}\right) = 5.14 - 2.06x_1 + 0.57x_2 + 0.40x_3 - 0.17x_4 + 1.03x_1^2 - 0.34x_2^2 - 0.34x_3^2 - 0.11x_4^2 - 0.46x_1x_2 + 0.11x_1x_4, \text{ МПа} \quad (2a)$$

- 3 CFRP-strengthened beams (series 5) brought to the critical state according to the 1st group subject to similar loading.

$$\hat{Y}(V_{u,f}) = 153 - 69x_1 + 12x_2 + 4x_3 + 9x_1^2 - 8x_2^2 - 7x_1x_2,$$

$$\text{Variability coefficient } \bar{U} = 5.2\%;(3)$$

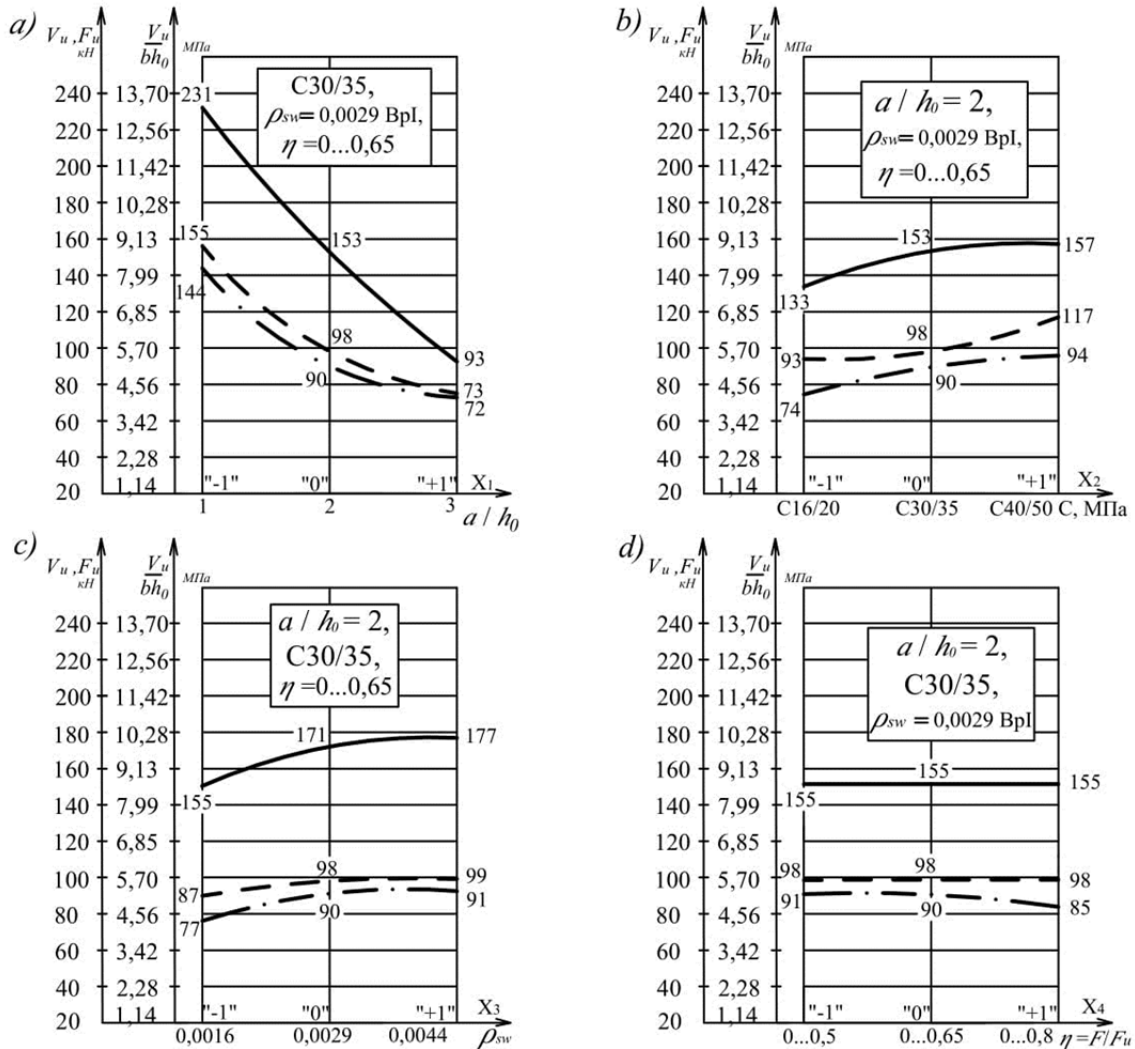
$$\hat{Y}\left(\frac{V_{u,f}}{bh_0}\right) = 8.74 - 3.94x_1 + 0.69x_2 + 0.23x_3 - 0.51x_1^2 - 0.46x_2^2 - 0.40x_1x_2, \text{ МПа} \quad (3a)$$

Mathematical models (1), (2) and (3) characterize the bearing capacity of the tested elements support zones in the natural form, and (1a), (2a) and (3a) reflect the strength of their oblique sections reduced to the dimensions of their cross sections only.

The presented adequate mathematical models have a significant advantage over other statistical dependencies that make possible to evaluate the influence of each research factor on the output parameter not only in particular, but also in interaction with each other, and also to compare the magnitude of this influence both in a single series and for all the indicated series together, that is a comprehensive analysis. A geometric interpretation of the actual and reduced bearing capacity of the supporting sections of the prototype beams is partially presented in Figure 2.

The concrete grade is the next factor according to the impact value. As the grade improves from C16/20 to C30/35, the strength of oblique sections raises more intensively.

With the upgrade of the concrete, from C30/35 to C40/50, the bearing capacity of the support zones changes slightly. The similar pattern is observed with respect of the transverse reinforcement coefficient ρ_{sw} when it changes from 0.0016 to 0.0044. Low-cycle loading and increase of the levels from 0.5 to 0.8 of destructive load produces a negative effect on the test element bearing capacity.



Conditional data designations:
 - - - - Before destroying the experimental beams of the series 1;
 - . - . - Before destroying experimental elements of the series 3;
 ——— Before the destruction of reinforced carbon fiber reinforced concrete beams series 5.

Figure 2. Destructive transverse force V_u or transverse loading (F_u) of the tested sample beams prior to their failure vs the value of the relative shear span a/h_0 (a), concrete grade C (b), quantity of the transverse reinforcement ρ_{sw} (c) and level of the low-cycle repeated loading η (d).

Analysis of mathematical models (1)...(3a) shows that they are of the same type by quality, and the impact of the design factors and external factors are similar by quality. The differences are in the quantitative indicators only.

Thus, the strength of the oblique sections of the tested sample beams of the first, third and fifth series, that was reduced to working area of the transverse section, increases relatively to their reduced average values 5.60; 5.14 and 8.74, accordingly:

- with reduction of the relative shear span a/h_0 from 3 to 1 in the indicated series by 84, 80 and 90%, accordingly;

- with the change of the concrete grade from C16/20 to C40/50 25, 22 and 16%, accordingly;

- with the increase of the quantity of transverse reinforcement ρ_{sw} from 0.0016 to 0.0044 by 12,16 and 5%, accordingly;

- with reduction of the non-reversal loading η from 0...0.8 to 0...0.5 in the third series; at single-time reduction of the relative shear span a/h_0 and increase of the concrete grade within the above indicated limits by 7% in the first, 9% in the third and 5% in the fifth series;

- with a single-time reduction of the relative shear span a/h_0 and a level of the non-reversal low-cycle loading in the third series.

It is evident that the main cause of the bearing capacity reduction in low-cycle non-reversal loading lies in the structural disturbance of concrete, particularly in the support zones, its decompaction and partial loss of cohesion with the reinforcement.

The maximum growth of the residual deformations in concrete and transverse reinforcement of the tested beams of the first and third series was recorded during the first 2-3 cycles and, as a rule, they were stabilized before the fifth-sixth cycles at the loading levels $\eta=0...0.50 - 0...0.65$. In some samples made of the lowest concrete grade and the minimum transverse reinforcement at loading $\eta=0...0.8$ these deformations were not stabilized and the samples failed in 6...9 cycles because of reaching the structural fatigue or due to possible reduction of their strength characteristics caused by a statistical error when determining the destructive high-level loads.

The tested sample beams of the fifth series that were strengthened with external composite reinforcement were deformed almost elastically until reaching the limit state in the compressed concrete or in the tensioned metal or composite reinforcement.

Not overreinforced ($\rho_{sw} \leq 0.003$ (Bpl); $\rho_f \leq 0.018$ (A500C)) tested sample beams subjected to a single-time static stage-wise increase (first series) and low-cycle non-reversal (third series) loading failed, as a rule, according to B/M pattern, i.e., in oblique sections and the prevailing action of the bending moment as a result of the yield of the longitudinal working reinforcement in the unsafe diagonal crack mouth and the transverse reinforcement that crosses such crack [8]. As the quantity of the transverse reinforcement increases $\rho_{sw} \geq 0.0044$, the similar test elements having medium ($a/h_0=2$) and large ($a/h_0=3$) shear spans failed according to C/V pattern, i.e., in the diagonal crack under the prevailing action of the transverse force due to yield of the transverse reinforcement and shear or bearing of the compressed zone of concrete above the top of unsafe diagonal crack; with the small shear spans ($a/h_0 \leq 1$) the similar test samples failed sometimes according to Δ/cm pattern beyond the oblique compressed strip located between two diagonal cracks as a result of crush of this strip concrete that follows the trajectory of the main compressing stresses.

Destruction of the normal sections of the test beam was strengthened in the fifth series by CFRP and was accompanied, as a rule, by yield of the metal and composite

structure, possible detachment of the protective concrete layer and breaking CFRP external reinforcement [9].

Destruction of the support zones of the fifth series beams that have small shear span also began from excessive deformation and detachment of the external composite reinforcement along with the protective concrete layer and crushing of concrete beyond the oblique compressed strip.

Basic parameters of test elements crack resistance

During testing sample beams for short-term single-time and low-cycle load we monitored creation, development and opening width of the cracks on their surface. The width of normal crack opening was determined at the level of tensioned working reinforcement, and that of the diagonal cracks – in the mid-height of the beam in those places where visually was the greatest [10].

The normal cracks appeared the first within the pure bend zone and under the focused forces at the loading levels $\eta=0.15...0.25$ of the breaking level. As loading was being increased these cracks developed towards the compressed zone, their opening width was being increasing as well and new cracks were formed in the zone of joint action of the bending moment and the transverse force and they gradually were becoming more inclined towards the point where the concentrated load was applied.

First diagonal crack appeared at loading $\eta=0.4...0.6$ of the breaking load in the middle height of the beams having small or medium shear spans, or they developed out of normal cracks in the samples having large shear spans, maximum quantity of the transverse and minimum quantity of the longitudinal working reinforcement.

The process of the normal and diagonal cracks in the beams of the first and third series developed as forecast: in parallel with the internal stress growth new cracks were formed, lengths and opening width of the existing cracks increased and subsequent development of these cracks depended on intensity of the transverse reinforcement in the shear spans. If its quantity was sufficient, the tested samples failed in the normal sections, the working reinforcement yield [11], and if the reinforcement quantity was insufficient – the earlier formed diagonal cracks merged together to form one major or several almost parallel cracks to form a strip; failure began beyond the cracks associated with a possible yield of the transverse and longitudinal rods and subsequent shear or crushing of the concrete compressed zone.

With the fifth series beams strengthened with external composite reinforcement we noted further development of the earlier formed cracks and appearance of new cracks, so-called secondary normal cracks, in middle part of the beams, and in the support areas wrapped in CFRP the diagonal crack appeared.

The mathematical models of the normal crack opening in the pure bend zone in the middle part of the beams at the level of the tensioned reinforcement are as follows:

- in common beams subjected to stage-wise static increasing loading (series 3) of the corresponding levels.

$$\hat{Y}\left(W_{cr,\perp,1,2,3}^{\eta F_{r,1}}\right) = 0.14 - 0.02x_1 + 0.03x_2 + 0.01x_3 + 0.05x_4 + 0.01x_1^2 - 0.03x_2^2 + 0.02x_4^2 + 0.01x_1x_3 + 0.01x_1x_4 + 0.02x_2x_4 + 0.01x_3x_4, mm$$

$$\text{Variability coefficient } \bar{U} = 6.2\%; \quad (4)$$

- in damaged and brought to the limit state beams of the 1st group in series 3 of the tested samples – the beams strengthened with CFRP sheets (series 5) subjected to, accordingly, low-cycle loading $\eta 1F_{u,1}$ and prior to their failure at $0.95F_{u,f}$:

$$\hat{Y}(W_{cr,\perp,f}^{\eta F_{u,1}}) = 0.31 + 0.18x_1 + 0.02x_2 + 0.03x_3 + 0.09x_4 + 0.02x_1x_3 + 0.06x_1x_4, mm$$

Variability coefficient $\mathcal{U} = 10.5\%$; (5)

$$\hat{Y}(W_{cr,\perp,f}^{0.95F_{u,f}}) = 0.46 + 0.28x_1 + 0.03x_2 + 0.03x_3 + 0.05x_4 + 0.03x_1x_3 + 0.03x_1x_4, mm$$

Variability coefficient $\mathcal{U} = 10.4\%$; (6)

Geometrical interpretation of the above mathematical models is shown in Fig. 3.

The conducted research proved that the opening width of normal cracks in the middle part of the damaged beams at the loading levels preset by the test schedule was, on the average, 2.2 times greater than that one in the continuous beams of the first and third series.

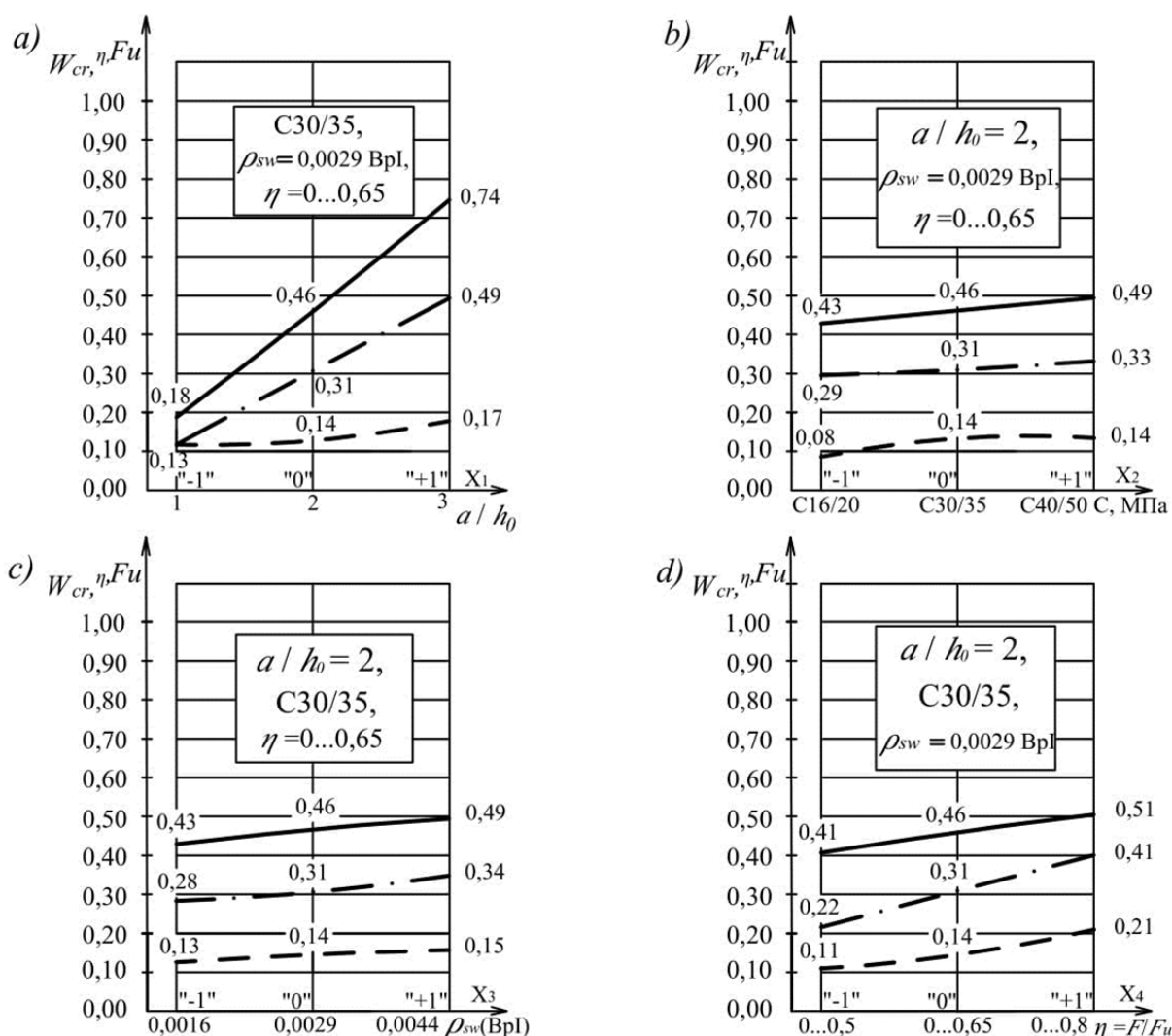
The analysis indicates that the maximum opening width of the normal cracks in the pure bend zone of the indicated series is increasing as compared with the average values of 0.14, 0.31 and 0.46 mm at the average values of the studied factors:

- with increase of the relative shear span a/h_0 from 1 to 3 b 29, 116 and 122%;
- with the change of the concrete grade from C16/20 to C 40/50 (actually to C 30/35) by 43, 13%;
- with the increase of the quantity of transverse reinforcement ρ_{sw} from 0.0016 to 0.0044 by 14, 19 and 13%;
- with the increase of loading η from 0.5 to $0.8F_u$ by 71 and 58%, and on achievement of $\eta = 0.95 F_{u,f}$ – by 22%;
- at single-time increase of:
- the relative shear span value and quantity of the transverse reinforcement within the indicated limits by 7, 13 and 13%, accordingly;
- the relative shear span value and the loading by 7%;
- the concrete grade due to the increase of the bearing capacity and loading level by 14 and 13% in the fifth series;
- quantity of the transverse reinforcement by the same reason and the loading level increase by 7% in the first series.

Main parameters of material deformability and the test beam samples

When performing experimental studies direct measurements of deformations in the extreme, most compressed concrete fibres in this cycle and, accordingly, the tensioned working reinforcement in the span middle (in the pure bend zone) were made, as well as the averaged evaluation of the deformation of the support zone transverse reinforcement in the tested beam samples.

Diagrams illustrating experimental and analytical relative deformations were constructed for each tested r.c. elements after each cycle of the corresponding levels repeated loading, including the stage immediately preceding the failure [12].



Conditional data designations:

- — — For the effects of a step-by-step static (series 1) and low-cycle sign-constant load (series3) at given levels;
- . - . - For the action of a small cycle load $\eta Fu,1$;
- For the action of a small-cycle load before their destruction $0,95Fu,f$.

Figure 3. Impact of the relative shear span value a/h_0 (a), concrete grade C (b), quantity of transverse reinforcement ρ_{sw} (c) and level of low-cycle repeated loading η (d), on the opening width of normal cracks in the “pure bend” zone in the middle of the beams at the level of tensioned reinforcement.

It was experimentally established that the values of relative deformation of the materials after each repeated loading cycle considerably increase upon reaching a certain level and residual deformation accumulate until their stabilization which, as a rule, takes place after 4...8 loading cycles and reaches 60...80% of the total residual deformation of the compressed concrete zone. Generally, in the second and third loading cycles occur 15...25% more, and in the 4...8 cycles – only 5...10% of these deformations. At that, the low-cycle loading action considerably impacts the stress-strain state of the tested beams. In particular, the stress diagram of the compressed zone changes gradually due to concrete compaction and re-distribution of inner stresses takes place between the compacted concrete and tensioned reinforcement wherein the corresponding deformations change. In some tested samples that had large shear spans and were subjected to high levels of

repeated loading ($\eta=0,8$) there occurred no stabilization of the residual deformations of the concrete or reinforcement, sometimes both of the concrete or reinforcement, and their failure, as non-overreinforced elements, took place in the normal sections as a result of the yield of the longitudinal working reinforcement or both due to the reinforcement yield and crushing the compressed zone concrete.

Similarly to the compressed concrete under repeated loading, deformation of the tensioned longitudinal working reinforcement takes place [13]. The tests proved that the residual deformations in such reinforcement reach $(20...50) \cdot 10^{-5}$ and are stabilized to 4...8 cycles when the beams were unloaded to zero in the first cycles.

Residual deformations in the transverse reinforcement and the concrete in oblique sections comprised 25...60% of the total deformations [14]. Their greatest increment was recorded in the first cycle ($\approx 20...50\%$) and at additional loading in the last cycle. Due to reduction of plastic deformations the accumulation process of residual deformations in the support zone at stable level of low-cycle transverse loading fades gradually. Deformations in the transverse reinforcement and in the support zone concrete stabilize, as a rule, before the 4...8 cycle of such loading.

Relative deformations of the compressed concrete in the pure bend zone of the tested beams

Mathematical models of the relative deformations of the compressed concrete in the tested samples of common beams and strengthened beams of 1, 3 and 5 series in accordance with the loading levels $\eta_1 F_{u,1}$ preset by the schedule are as follows:

$$\hat{Y}(\varepsilon_{c,1}^{\eta F_{u,1}}) = (84 + 17x_1 + 10x_2 + 7x_3 + 21x_4 + 4x_1x_3 + 5x_1x_4) \cdot 10^{-5},$$

$$\text{Variability coefficient } \bar{U} = 5.1\%;(7)$$

$$\hat{Y}(\varepsilon_{c,3}^{\eta F_{u,1}}) = (92 + 17x_1 + 10x_2 + 7x_3 + 21x_4 + 4x_1x_3 + 5x_1x_4) \cdot 10^{-5},$$

$$\text{Variability coefficient } \bar{U} = 6.7\%; \quad (8)$$

$$\hat{Y}(\varepsilon_{c,f}^{\eta F_{u,1}}) = (91 + 21x_1 + 5x_2 + 14x_3 + 21x_4 - 4x_1^2 - 2x_3^2 - 12x_1x_2 + 8x_1x_3 + 11x_1x_4 - 7x_2x_3 + 4x_3x_4) \times 10^{-5},$$

$$\text{Variability coefficient } \bar{U} = 9.6\%;(9)$$

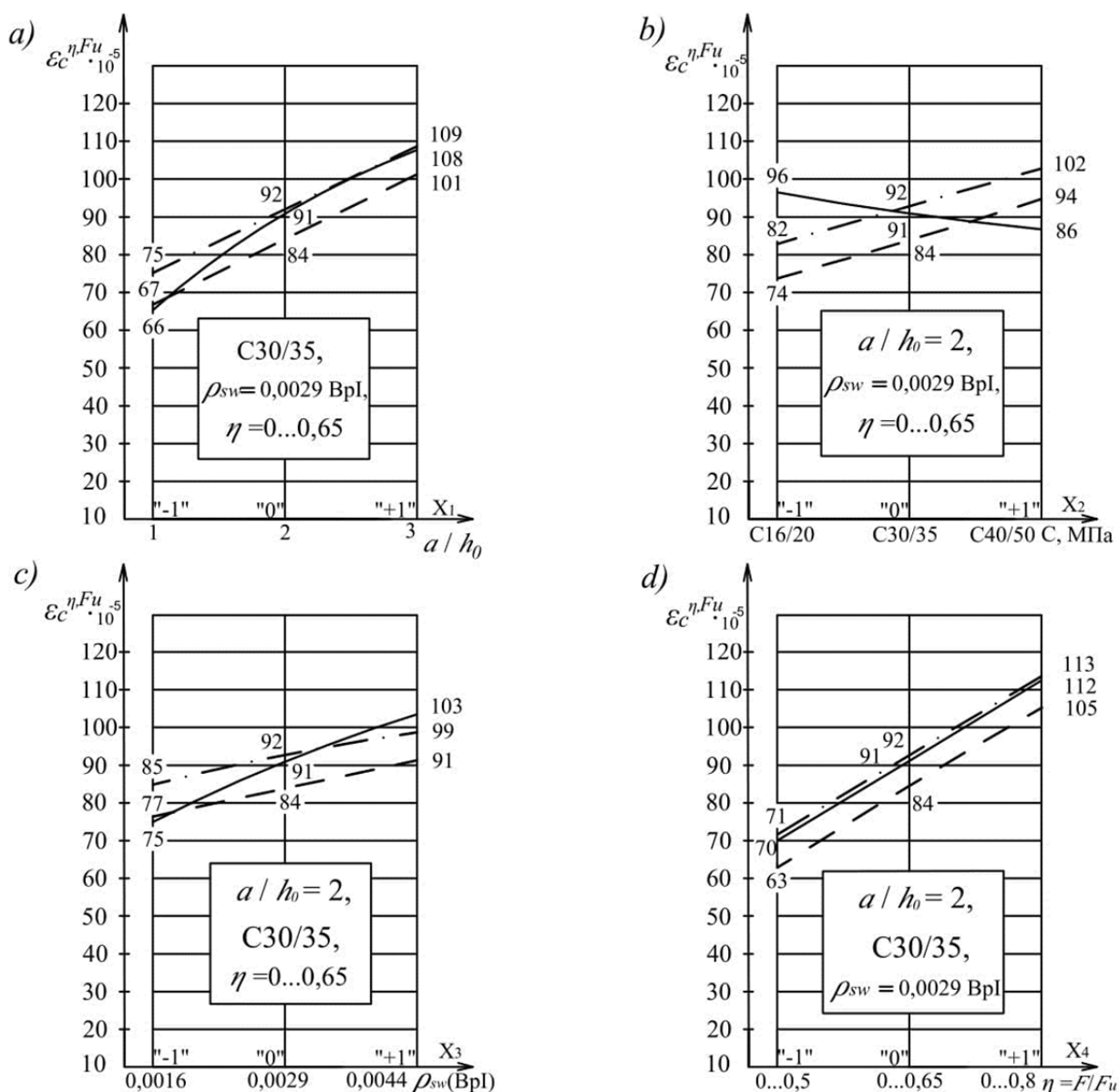
Their geometrical interpretation is shown in Figure 4.

The processing of experimental data on the deformation of the compressed zone concrete in the center of the spans of the research elements after their stabilization at the appropriate level of low-cycle load, as well as before the destruction of the beams at $\eta = 0.95F_u$ allowed to derive the following mathematical models:

$$\hat{Y}(\varepsilon_{c,1}^{0,95F_{u,1}}) = (129 + 30X_1 + 15X_2 + 11X_3 + 6X_1X_3) \cdot 10^{-5}$$

$$\text{Variability coefficient } \bar{U} = 6.5\%; \quad (10)$$

$$\hat{Y}(\varepsilon_{c,3}^{0,95F_{u,3}}) = (149 + 30X_1 + 11X_2 + 11X_3 - 4X_1^2 - 2X_2^2 + 6X_1X_3) \cdot 10^{-5}$$



Conditional data designations:

- Under the action of a one-time load (series 1) at given levels;
- · - · - For the action of a small cycle load (series 3) to a given level η ;
- For the action of the low-cycle load of reinforced beams (series 5) at the established levels.

Figure 4. Relative deformations of the compressed concrete in the tested beam samples vs the value of the relative shear span, a/h_0 (a), concrete grade C (b), quantity of the transverse reinforcement ρ_{sw} (c) and level of the low-cycle repeated loading η (d).

Variability coefficient $\bar{v} = 6.1\%$; (11)

$$\hat{Y}(\varepsilon_{c,f}^{0,95 F_{u,f}}) = (264 + 94X_1 - 25X_2 + 7X_4 - 4X_1^2 - 23X_1X_2) \cdot 10^{-5}$$

Variability coefficient $\bar{v} = 5.1\%$; (12)

Their geometrical interpretation is shown in Figure 5.

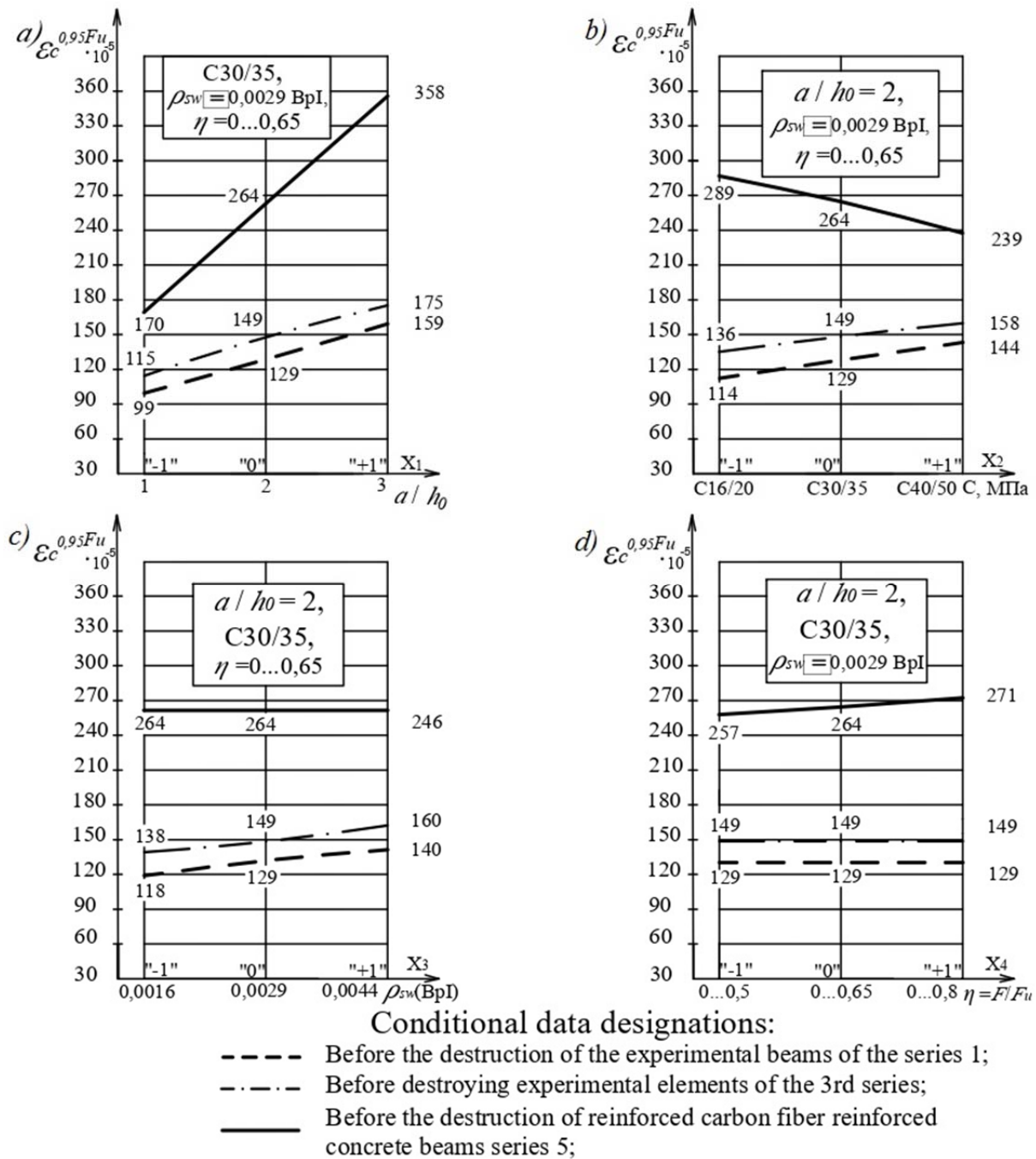


Figure 5. Dependence of relative deformations of compressed concrete test specimens-beams on the magnitude of the relative passage of the slice, a/h_0 (a), the class of concrete C (b), the number of transverse reinforcement ρ_{sw} (c), the level of low-cycle reloading (d).

Average relative deformation values of the compressed concrete in the middle part of beams after their stabilization under low-cycle static loading.

Relative deformations of the compressed concrete in r.c. beams of 1, 3 and 5 series prior to failure increase upwards as compared with the average values:

- relative shear span a/h_0 from 1 to 3 - by 47%, 40% and 71%, accordingly;
- concrete grade from C16/20 to C40/50 - by 23%, 15% and 19%;
- quantity of transverse reinforcement ρ_{sw} from 0.0016 to 0.0044 - by 17 and 15%;
- level of transverse loading η from 0.5 to 0.8 - by 15% and 5%.

Conclusions

1. Peculiarities of the stress-strain state of the tested beam samples are presented. Dependence of the nature and kind of their failure on the relevant ratio of the design factors and factors of external impacts, particularly presented and kind of external strengthening with composite materials was established for the first time.

2. Due to the adopted methodology new experimental data was obtained in order to essentially specify physical models reflecting behaviour of oblique sections of the span r.c. structures subjected to high-level low-cycle repeated loading which resulted in description for the first time of the system impact of the shear span a/h_0 , concrete grade C, transverse reinforcement coefficient ρ_{sw} and level of repeated loading η on crack resistance, deformability and strength of the tested beam samples.

3. Application of the mathematical theory of planning, adopted plan and levels of changing design factors and external impact factors make it possible to apply a system approach to analyse the events and compare the obtained data.

4. Presence of the external carbon fibre-reinforced polymer strengthening in the lower tensioned zone of the beams in the 5th series and on their support zones makes it possible to enhance bearing capacity of the beams as compared with similar beams of the 3rd series, subjected to similar low-cycle loading, by 1.7 times on the average, and partially change the nature of their failure. In doing so, the average value of the normal crack opening width in the "pure bend" zone is increased from 0.31 to 0.46 mm; the average relative deformations and tensioned steel reinforcement of A500C class increase from $258 \cdot 10^{-5}$ to $546 \cdot 10^{-5}$.

5. Increase of the shear span a/h_0 from 1 to 3 not only reduces by 2 and 2.5 times the destructive transverse low-cycle loading, accordingly, in common (series 3) and CFRP reinforced (series 5) r.c. beams but also defines the nature of such failure. With a small shear span ($a/h_0 = 1$) a" tested beam samples failed in the support zones because of oblique cracks or strips accompanied with detachment of the carbon fibre sheet in the average and large shear spans ($a/h_0 = 2$ or 3); increase of the quantity of external composite reinforcement in these areas leads, as a rule, to destruction of the tested elements in the normal sections within the "pure bend" zone, which is accompanied by yield of the tensioned metal and composite reinforcement, and the concrete of the compressed zone is subjected to critical deformations. The maximum opening width of the normal cracks increased by 0.49 mm in the common beams of the third 3rd series to 0.74 mm in the carbon fibre reinforced elements.

6. The performed research proved that upgrading concrete from C16/20 to C40/50 results in higher bearing capacity of the common beams of the 3rd series by 22% only. In the carbon-reinforced beams – only by 15%, because the tensile strength increase of the concrete and "lags behind" the compression strength growth of the concrete when the concrete grade is upgraded. The maximum opening width of the normal cracks accompanied with a change of the concrete grade within the indicated limits and at average values of other design factors increases from 0.33 mm in common beams to 0.49 mm in reinforced elements with upgraded concrete grade within the indicated limits. Similarly to bearing capacity of the tested beam, deformations of steel and composite reinforcement also increase.

7. Along with a greater quantity of transverse steel reinforcement - from $\rho_{sw} = 0.0016$ to $\rho_{sw} = 0.0044$, the bearing capacity of common beams (series 3) is increasing in a non-

linear way, the same as the carbon-fibre strengthened elements (series 5), on the average by 15%. With a change of this factor within the preset limits the opening width of normal cracks is also increasing by 15% and reaches the maximum value of 0.49 mm in the strengthened beams while the average values of other design factors are preserved. With the common beams the increase of the transverse reinforcement increases deformations in steel reinforcement by 18%, however, with the strengthened beams the deformations of steel and composite reinforcement remain stable and sufficiently high until failure.

8. A change in the low-cycle transverse loading levels η from 0...0.5 to 0...0.8 with the common beams (series 3) results in reduction of their bearing capacity by up to 10% while with the strengthened beams (series 5) their strength remains stable. Higher level of said loading within the indicated limits increases the opening width of normal cracks in common beams by 60%, and in the strengthened beams – by 22% while average values of the design factors remain the same. Deformations of the steel and external composite reinforcement increase in all series by 10% on the average when the levels of such loading change within the indicated limits. While the present factor did not influence the deformations in the compressed concrete of common beams, such impact in the strengthened elements comprised by 6% only.

References

1. Posobie no proektirovaniyu betonnyh i zhelezobetonnyh konstrukcij iz tyazhelogo betona bez predvaritel'nogo napryazheniya armatury (k SP 52-101-2003). Moskva, 2005, pp. 36-38.
2. Babich E. M., Pogorelyak A. P. Prochnost' betona posle dejstviya malociklovoj szhimayushchej. *Izv. vuzov. Ser. Stroitel'stvo i arhitektura*, 1976, №4, pp. 33-36.
3. Babich E. M., Kuhnyuk O. M. Deformacijni karakteristiki betonu pri os'ovomu malociklovomu stisku. *Visnik Rivnenskogo derzhavnogo tekhnichnogo universitetu: zbirnik naukovih prac'.* – Rivne: Vid-vo RDTU, 1999. – Vipusk 2. – Chastina 3, pp. 21-25.
4. Babich E. M., Krus' YU. A., Panchuk YU. N. Rabota melkozernistogo betona v usloviyah malociklovogo staticheskogo nagruzheniya. *Izv. vuzov. Ser. Stroitel'stvo*, 1995, №9, pp. 26-32.
5. Vegera, P., Blikharsky, Z. «Planning Experiment for Researching Reinforced Concrete Beams with Damages», *Lecture Notes in Civil Engineering Volume 47*, 2020, pp. 243-250.
6. Standart organizacii. Usilenie zhelezobetonnyh konstrukcij kompozitnymi materialami SikaR. STO 13613997-001-2011. Moskva: OAO «CNII Promzdaniy», OOO «Zika», 2011, pp. 61.
7. Karpiuk V., Kostyuk A., Maistrenko O., Somina Yu. Influence of intermittent cyclic loading on reinforced concrete resistance model. *Electronic journal of the faculty of civil engineering of Osijek, Croatia*. 2017, number 15, pp. 59-74.
8. Iakovenko I. A., Kolchunov V. I. "The development of fracture mechanics hypotheses applicable to the calculation of reinforced concrete structures for the second group of limit states," *J. Appl. Eng. Sci.*, vol. 15, no. 3, 2017, pp. 371–380.
9. Blikharsky Z., Brózda K., Selejdak J. "Effectiveness of Strengthening Loaded RC Beams with FRCM System," *Arch. Civ. Eng.*, vol. 64, no. 3, 2018, pp. 3–13.
10. Baoguo Han, Xun Yu, Jinping Ou, Self-Sensing Concrete in Smart Structures, 2014, pp. 115-254.
11. Dem'Yanov A. I., Yakovenko I. A., Kolchunov V. I. "The development of universal short dual-console element for resistance of reinforced concrete structures under the action torsion with bending," *Izvestiya Vysshikh Uchebnykh Zavedenii, Seriya Tekhnologiya Tekstil'noi Promyshlennosti*, vol. 370, no. 4, 2017, pp. 246–251.
12. Karpyuk V. M., Somina YU. A., Kostyuk A. I., Majstrenko O. F. «Osoblivosti napruzhenno-deformovanogo stanu i rozrahunku zalizobetonnih konstrukcij za dii ciklichnogo navantazhennya visokih rivniv». Odesa, 2018, pp. 65-68.
13. Banthia N. *Fiber Reinforced Polymers in Concrete Construction and Advanced Repair Technologies*. Department of Civil Engineering University of British Columbia, 2013, pp. 37.
14. Klaus Friedrich, Ulf Breuer, *Multifunctionality of Polymer Composites*, 2015, pp 56-103.

DOI: 10.5281/zenodo.3713368
CZU 66.047.75



DRYING INSTALLATION FOR GRANULAR PRODUCTS IN THE SUSPENSION LAYER

Mihail Balan*, ORCID ID: 0000-0002-7788-345X,
Mircea Bernic, ORCID ID: 0000-0001-6166-6947,
Natalia Țislinscaia, ORCID ID: 0000-0003-3126-5792

Technical University of Moldova, 168, Stefan cel Mare bd., Chișinău, Republic of Moldova

*Corresponding author: Mihail Balan, mihail.balan@pmi.utm.md

Received: 01. 09. 2020

Accepted: 03. 18. 2020

Abstract. One of the main problems of wet plant products drying processes is the long duration of thermal tartarization, which consequently leads to the diminution of the quality indices. This problem is exacerbated in the case of oil products drying, high in fatty acids receptive to oxidation processes. For such products, especially granulation, as grape seeds are, drying in a suspended layer with microwave application is beneficial. This method allows automatic selection of already dried particles from the seed table and removing them from the heating zone, thus ensuring a maximum reduction of heat treatment time, so also favorable conditions for oxidation of fatty acids. The paper presents the construction of a laboratory installation for the study of the kinetics of drying processes in suspended layer with microwave application. The installation allows the online recording of the temperature, speed and humidity of the air in oilseeds and out and periodic recording of the mass decrease of the product.

Introduction

Taking into account that grapes contain up to 7% seeds, after their processing, in the Republic of Moldova annually approx. 18-20 thousand tons of grape seeds are obtained. The industrial processing of grape seeds reflects a number of specific technological operations including drying [4, 6, 16].

At the moment there are many researches in the field of drying process optimization of plant seeds, including grapes, through various methods of energy input: convection, in the microwave field, with the application of ultrasound, infrared rays, etc. Convection drying is one of the simplest and most commonly used methods, but which is accompanied by a long duration of the process, and as a consequence, diminished quality of the finished product (appearance of microflora, creation of oxidation conditions, etc.) [6, 13, 14].

Application of electromagnetic fields of different wavelengths (microwave, infrared, etc.) essentially intensifies the process, ensuring a much higher quality of dry seeds. Particular effects in order to obtain an optimal correlation between quality and energy consumption are observed when applying convection in combination with the energy of the electromagnetic fields [9, 10]. The application of ultrasound is an efficient source of

intensification of the drying process of the plants of porous capillary structure highlighted but weaker to the seeds, however this method ensures a certain degree of sterilization "in the cold" [11, 15, 18].

Discussions, often contradictory, also take place in view of the state of the product layer upon drying (fixed bed, sliding bed, vibrating bed, fluidized bed, etc.) [12]. Although drying in mobile bed (fluidizing, vibrating or suspended) creates a better contact of the seed surface with the air and reduces the influence of the border layer, thus ensuring an intensification of the mass exchange between the product and the environment, however, most authors are skeptical about this method because of the risk of crack formation in the seed bark, caused by the mechanical impact between them or between the seeds and the walls of the drying chamber. However, we believe that the mobile bed can be successfully used in drying processes, but for this it is necessary that the velocity of the air flow is also determined due to the fact that the kinetic energy transmitted to the seeds is insufficient for the creation of cracks at collision.

In this case, one of the methods of the grape seeds drying process intensification can be considered to dry in a suspended layer with internal heat sources application - microwaves. This method increases the quality of the dry product and reduces the energy consumption due to the selective application of drying time for each particle, so that, once humidity is reached to the final value, the particle is eliminated from the heat treatment area. In order to research the above mentioned drying process, a laboratory installation has been developed which is described in the present article.

I. Materials and methods

Air flow and speed in the experimental drying plant have been determined based on the mass balance equation. The intensity of electromagnetic field required for the product lifting has been determined on the basis of heat balance equation, the constructive elements of the installation were selected through calculation of resistance. All these calculations were performed taking into account *MathCad 15* software.

The *3D SolidWord* 3D design software was used to design the installation.

The simulation of the kinematics and dynamics of the mixture of air (drying agent) and grape seeds was performed using the *ANSYS software*, applying the laws of numerical methods.

As the internal heating source was accepted *2450 MHz* frequency microwaves generated by a magnetron *2M210-M1 Panasonic* type rated power of *900 W*.

II. Results and Discussion

In order to obtain a stable seed bed, an air velocity corresponding to that of the floating particles it is required in our case *8.5 m/s*, which cannot be modified. Thus, the variation of the productivity of the drying plant can be achieved only by changing the diameter of the aerodynamic tube in which this suspended bed is created, so the air flow is directly proportional to the productivity, and constitutes for grape seeds *430 m³/(h·kg)*. Obviously, with an increased air flow and taking into account that not all the heat will be transmitted from the air to the product, the convection heating of the seeds in a suspended bed becomes unprofitable, it is accompanied by essential heat losses with the air used. In order to reduce the heat loss, the thermal energy released in the product (seeds) was accepted as a result of the electromagnetic fields - microwaves acting. Microwaves only possible to heat the product, excluding heat losses removed from the workroom with drying

agent (air) and reducing them to the minimum from walls environment. At the same time, the given method of applying the heat energy allows the localization of the heating (drying) process only in the area of formation of the electromagnetic field, which coincides with the one of suspension (floating) of the wet granules, thus ensuring a good self-selection of the dry particles.

The drying system consists of the carcass 1 (figure 1) on which the construction elements are mounted, namely: the power supply unit consisting of the lock 5 driven by the electric motor 12; the drying system (air) supply system, consisting of the fan 4 operated by the electric motor 13 and the air filter 11; the aerodynamic tube 6 with a conical shaped section on which the drying chamber 8 is fitted, equipped with the magnetron 7; the exhaust system consisting of the exhaust pipe 9 and the cyclone 10.

The system is equipped with temperature sensors and humidity of the air mounted at the inlet and outlet of the aerodynamic tube 6. The air speed is controlled within the limits $0...20\text{ m/s}$ by changing the fan speed 13 using the frequency converter 2, which allows us to ensure the suspended bed not only for grape seeds with other granular products that have a much higher floating speed. The temperature of the product in the microwave heating zone is measured with the *EC060V* type thermoset., measurement error $\pm 0,99^{\circ}\text{C}$. The mass decrease of the product is determined by the periodic extraction of samples from the drying area and their subsequent weighing on the electronic scale type *JJ2000B*, measurement error $\pm 0,01\text{g}$.

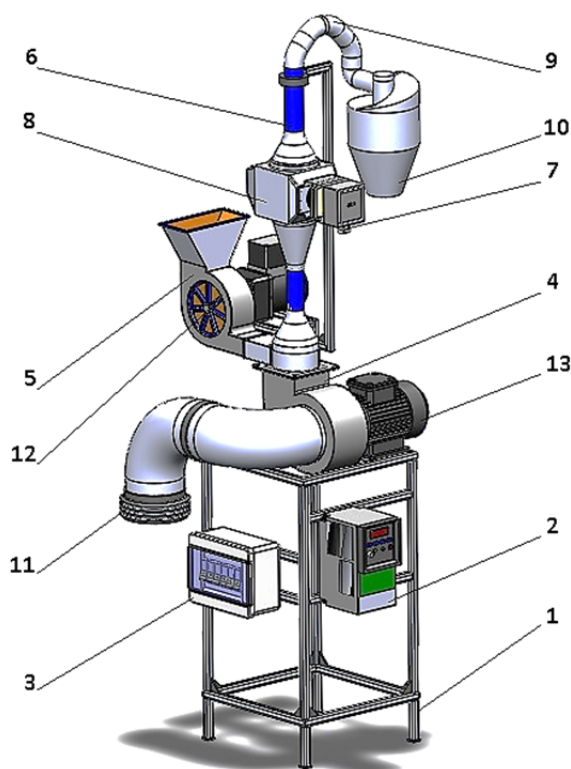


Figure 1. General view of the drying plant in suspended layer: 1 - carcass; 2 – frequency converter; 3 – control panel; 4 - fan; 5 - sluice; 6 – aerodynamic tube; 7 – magnetron; 8 – drying room; 9 – outlet pipe; 10 - cyclone; 11 - filter; 12 – electric motor; 13 – electric motor.

As mentioned above, the stability of the bed suspended by the seeds was ensured by the air speed being consistent with the speed of the floating seeds., but at the same time

this is due to the specific shape tability of aerodynamic tube 6, which shows two truncated cones (a speaker and a biasing) overlay. The area of formation of the bed is in the place of overlap of these two geometric figures, in which the air velocity is maintained, corresponding to the speed of seed drift.

The geometrical shape of the aerodynamic tube 6 was developed using the computer simulation of the kinetics and dynamics of the air-seed mixture flow through it from the considerations of obtaining in the drying area a stable seed bed in suspended state (figure 2). Thus, the areas A and C is the maximum speed of the mixture (*aprox. 15 m/s*), so the particles travel through them without being noticed, and in zone B (consisting of a diffuser and overlapping confuser), due to the slow enlargement of the diffuser's diameter, the air velocity decreases to the value of the flowing of the wet seeds. (*8,5 m/s*) [3, 4]. Due to the inertia forces, the area in which the air velocity is set equal to that of the wet seed float was obtained in the second half of the confounder. This is where the product is heated in the microwave field. With the drying (mass reduction) of the particles, the floating speed also decreases, so that the already dried particles are driven by the flow of air and moved from the heating zone. Due to the further narrowing of the conical area, the air velocity increases, which ensures a better entrainment of the dry granules, which is further eliminated from the aerodynamic tube due to the increased mixing speed in zone A [5].

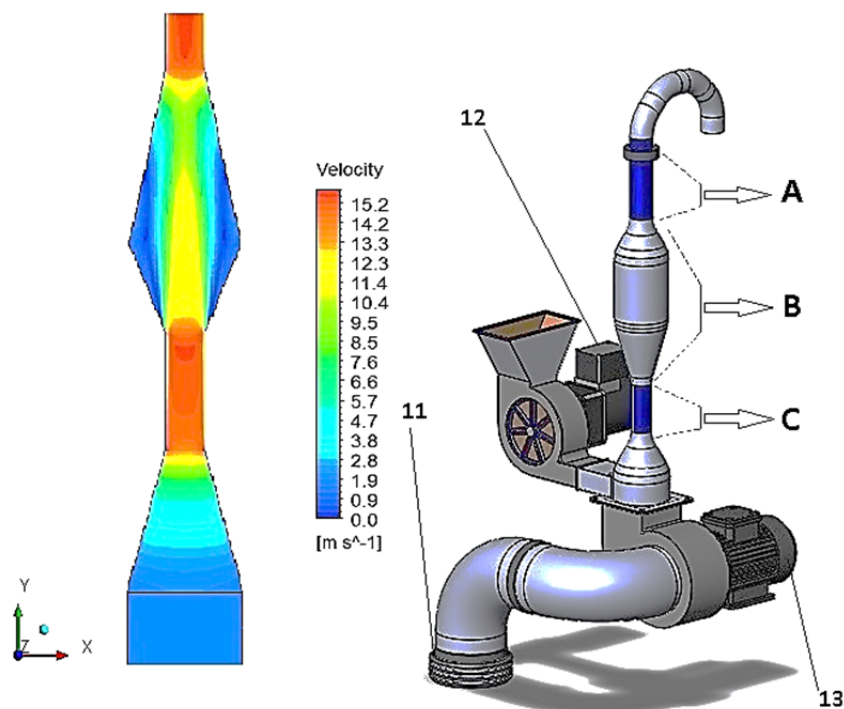


Figure 2. Variation of linear speed over the entire section of the tube with three zones.

Drying plant operates in the following way. The wet granules are charged through the lock 5 in the lower area of the aerodynamic tube, where they are taken by the air flow carried by the fan 4. In zone B (in the middle of the confounder) the wet granules stop and go into a state of suspension, being in a Brownian state of motion. In the present area an electromagnetic field is formed, which subjects to volume heating air blown granules, drying them. The dry granules, losing weight, rise in the upper area of the confuser where they are driven by the air flow with increasing speed and through tube A they are conveyed in cyclone 10 where the separation of the dry product takes place.

Conclusion

The proposed laboratory installation for kinetics research of wet granular products drying process in a suspended layer and subjected to heat treatment with microwave application allows to obtain a stable suspended bed. The air speed can be adjusted within the range 0 - 20 m/s, which allows the installation to be used for a wide range of granular products, the floating speed within the given range. The possibility of regulating the temperature of the product within the limits of 20 – 100 °C is sufficient to research drying processes of wet granular products of plant origin. The installation allows online recording of temperature, speed and humidity of the air in and out and periodic recording of product mass decrease.

References

1. Ghid pentru producătorii de struguri pentru masă / elab. : *Gheorghe Nicolaescu, Panfil Apruda* - Ch.: "Iunie Prim" SRL, 2007.-128 p.
2. Gracielle Johann, Maraisa Lopesde Menezes. Comparing models to Neumann and Dirichlet conditions in grape seed drying // *Applied Thermal Engineering*, Volume 93, 25 January 2016, Pages 865-871.
3. Moşneguţu Emilian. Contribuţii privind sortarea aerodinamică a produselor agricole, Universitatea Tehnică „Gh. Asachi” Iaşi, 2006, Facultatea de Inginerie Mecanică, Catedra Maşini Agricole.
4. Moşneguţu Emilian, Panainte Mirela, Savin Carmen. Separarea amestecurilor de particule solide în curenţi de aer verticali, Ed. Alma Mater Bacău, 2007.
5. Hong-Weili Tingwang, Changchang Binsun Wen-Penghong, Yun-Long Zhou. Multi-scale nonlinear analysis of drying dynamics in the mixed pulsed drying fluidized beds. // *Powder Technology*, Volume 339, November 2018, pp. 958-969.
6. Roberts J.S., Kidd D.R., Padilla-Zakour O. Drying kinetics of grape seeds. *Journal of Food Engineering*, Vol. 89, Issur 4, 2008, pp. 460-465.
7. Burdo O.G., Bandura V.N., Levtrinskaya Yu. O. Electrotechnologies of targeted energy delivery in the processing of food raw materials. / *Journal Surface Engineering and Applied Electrochemistry*. Vol. 2, Issur 2, 2018, pp. 210-218.
8. Clemente G., Sanjuán N., Cárcel J.A., Mulet A. Influence of temperature, air velocity, and ultrasound application on drying kinetics of grape seeds. *Drying Technology* 2014, 32 (1), 68 – 76.
9. Rute Quelvia De Faria, Amanda Rithieli Pereira Dos Santos, Yvan Gariepy, Edvaldo Aparecido Amaral Da Silva, Maria Márcia Pereira Sartori, Vijaya Raghavan. Optimization of the process of drying of corn seeds with the use of microwaves. *Drying Technology* 2019, pp.37 (14), p.1745 – 1756.;
10. Bernic Mircea. Uscarea produselor oleaginoase in camp UHF cu aport de energie prin impuls. Ch.: 2011, 271 p.
11. Gabriela Clemente, Neus Sanjuan, Juan Andres Carcel, Antonio Mulet. Influence of Temperature, Air Velocity, and Ultrasound Application on Drying Kinetics of Grape Seeds. *Drying Technology* 2014, 32 (1), pp. 68 – 76.
12. M. A. S. Barrozo A. Mujumdar & J. T. Freire. Air-Drying of Seeds: A Review. *Drying Technology* 2014, 32 (10), pp. 1127 – 1141.
13. John S. Roberts, Olga Padilla-Zakour, David R. Kidd. Drying kinetics of grape seeds. *Journal of Food Engineering* 2008, 89 (4), pp. 460-465.
14. S. Azzouz I. Hermassi R. Chouikh A. Guizani, A. Belghith. The convective drying of grape seeds: Effect of shrinkage on heat and mass transfer. *Food Process Engineering* 2017, 41 (1).
15. Magdalena Sledz, Artur Wiktor, Malgorzata Nowacka, Dorota Witrowa-Rajchert. Drying Kinetics, Microstructure and Antioxidant Properties of Basil Treated by Ultrasound. *Food Process Engineering* 2017, 40 (1).
16. Jun Wang, Arun S. Mujumdar, Weisong Mu, Jianying Feng, Xiaoshuan Zhang, Qian Zhang, Xiao-Ming Fang, Zhen-Jiang Gao And Hong-Wei Xiao. Grape Drying: Current Status and Future Trends. *Grape and Wine. Biotechnology. Capter 7* Editors Antonio Morata, Iris Loira, 2016 pp. 145-167.
17. G. Clemente, N. Sanjuan J. Bon, R. Peña J.V. Garcia-Perez. Grape Seeds Dehydration under Forced Convection Conditions. *Defect and Diffusion Forum* (Volumes 283-286), 2009, pp. 610-615.
18. Visanu Vitali. Peaches convective drying. DOI: 10.5281/ZENODO.2557337. CZU 664.854:634.25. 2018.

DOI: 10.5281/zenodo.3713370
CZU 664.3



PECULIARITIES OF WALNUT OIL STATE IN SOME FOOD EMULSIONS

Oxana Radu*, 0000-0001-9260-6314

Technical University of Moldova, 168, Stefan cel Mare bd., Chisinau, Republic of Moldova
*oxana.radu@sa.utm.md

Received: 12. 22. 2019

Accepted: 02. 24. 2020

Abstract. The replacing of traditional lipids with more health-promoting oils containing polyunsaturated fatty acids (PUFA) is a modern trend in food industry. The principles of emulsions formation containing walnut oil (up to 90% PUFA) were studied in order to accumulate information that would help to design new functional products. The phase diagrams of the state of three-component systems – *Walnut oil / Water / Ethanol* and *Walnut oil / Polyphenol extract / Water* were investigated. It was shown that walnut oil was more prone to form W/O emulsions than O/W ones, that can possibly be explained by the presence of natural surfactants in it. This property of walnut oil was used within the functional spread obtaining. It has been established that the elaborated product represents an emulsion, in which water micelles and air inclusions are dispersed in continuous lipid phase, consisting of solid lipids. Withal, the structure stability of spread rich in PUFA from walnut oil was ascertained being almost analogous to milk-based butter, retaining its functionality and high biological value within a month at the temperature regime up to 5°C.

Keywords: *polyunsaturated fatty acids, microstructure, phase diagrams, spread, aggregative stability.*

Introduction

There has been an increasing tendency within food industry toward relating physicochemical, organoleptic, and nutritional properties of food emulsions to the type, concentration, structure, and interactions of their constituent components [1].

A wide variety of different types of oils has been used in food emulsions, including soybean, corn, canola, olive, safflower, and sunflower oils. The trend has been to replace traditional oils with more health-promoting oils containing polyunsaturated lipids. Walnut oil is one of these beneficial oils, which further study can provide good perspectives for food industry developing [2]. Walnuts are valuable sources of polyunsaturated fatty acids (PUFA; up to 90% of the oil), predominantly linoleic (47.4%) and α -linolenic (15.8%) acids [3]. The walnut oil consumption reduces serum cholesterol levels in humans, decreasing the total triacylglycerol levels and the risk of cardiovascular diseases [4, 5]. However, these fatty acids limit the shelf life of walnuts and walnut-containing products due to their high susceptibility to oxidation. The lipid oxidation of walnut-containing products during storage affects their quality parameters by decreasing their nutritional, sensory, and chemical properties, in addition to their economic value [6, 7]. The susceptibility of lipids to

oxidation is a major cause of quality deterioration in food emulsions. The reaction mechanism and factors that influence oxidation are appreciably different for emulsified lipids than for continuous lipid phase [8]. The physical state of the droplets in an emulsion can influence a number of its most important physicochemical, organoleptic, and biochemical properties, including appearance, rheology, stability, and gastrointestinal transformations. The production of margarine, butter, whipped cream, and ice cream depends on a controlled destabilization of an O/W emulsion containing partly crystalline droplets [1]. The improved principles understanding of emulsions formation to contain walnut oil will aid to design a range of new functional products.

The aggregative stability of emulsions containing walnut oil

Walnut oil obtained through cold pressing represents a complex composition that includes, besides various fatty acids, phospholipids (16.5 g/kg) [9]. These substances contain hydrophilic groups and therefore have a surface activity [10]. Thus, cold-pressed walnut oil, unlike refined oils, should have its own surface activity [11]. From this point of view, it was proposed to investigate the aggregative stability of emulsions with walnut oil.

Systems containing nonpolar phase – cold-pressed walnut oil, and polar phase – water and ethanol obtained by rectification have were investigated. Walnut oil was obtained from freshly picked and manually peeled nuts, aged for 24 h over anhydrous sodium sulfate to uniquely remove the aqueous phase with its attendant substances.

“Three-component” emulsions were obtained, and diagrams of the type “*property = f (composition)*” in the form of Gibbs-Roseboom Triangle were developed. The phase stability of the system was investigated by the microscopic analysis of the physical state of samples prepared according to the 10 reference points (Figure 1 and Figure 2).

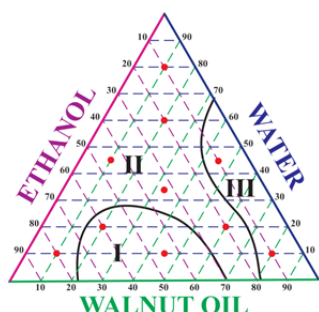


Figure 1. Different types of emulsions in Walnut oil/ Water / Ethanol System.

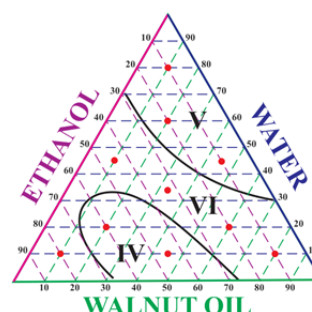


Figure 2. Phases with different aggregative stability in Walnut oil/ Water / Ethanol System.

According to the Figure 1, three different types of emulsions were formed: W/O emulsions (region I with 25...65% walnut oil), O/W emulsions (region II with 0...30% walnut oil) and O/W/O three-phase emulsions (region III with 40...100% walnut oil). The formation of W/O emulsions on the left side of the region was quite unexpected, because the apolar phase (in other words, dispersion medium for W/O emulsions) was less than 50%. While investigating the aggregative stability of obtained emulsions (Figure 2), it was found out that two types of samples – antipodes by water content (0...30% water in region IV and 30...100% water in region V) had a low stability, approximately 2 minutes. On the contrary, samples obtained according to the equation of straight, *Water = Ethanol* (region VI with 0...100% walnut oil), showed a high stability, which reached up to 5...10 minutes.

Thus, it was revealed, that walnut oil was more prone to form W/O emulsions than O/W ones. Perhaps, this fact is due to the presence of phospholipids in it, which have surfactants properties [12]. That is why it has been proposed to realize the additional study of the aggregative stability of systems, which nonpolar phase contained, besides walnut oil, a lipid extract from green tea leaves with a high content of phospholipids [13, 14]. Water was used to form the polar phase of samples. Due to the fact that obtained emulsions included two nonpolar components, the reference points for their formation were moved to the polar corner of the triangle (to water content increasing), releasing the apolar part of the diagram, located along the Water axis = 0% (Figure 3 and Figure 4).

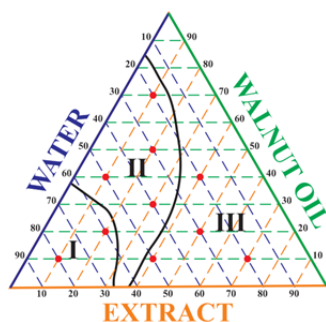


Figure 3. Different types of emulsions in Walnut oil / Polyphenol extract / Water system.

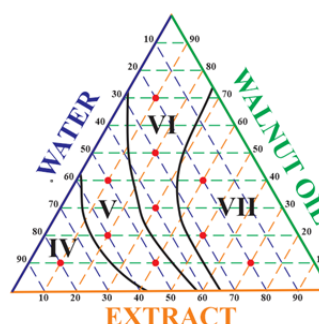


Figure 4. Phases with different aggregative stability in Walnut oil / Polyphenol extract / Water system.

The formation of Walnut oil / Polyphenol extract / Water system also revealed three regions with different phase status (Figure 3). O/W emulsions were established in samples with the highest water content (region I with 0...30% extract, 0...35% walnut oil, 60...100% water). O/W/O three-phase emulsions were formed in samples with 35...85% walnut oil, 15...65% water and in samples with 30...40% extract, 60...70% water (region II). Thus, the tendency to form three-phase emulsions was manifested more in compositions with walnut oil, than in those with green tea extract. W/O emulsions (region III) were formed in the wide range of extract concentrations, 40...100%. In contrast, the respective range is much narrower for walnut oil, 85...100%. Thus, the diagram analysis showed that the lipid extract of green tea stabilized W/O emulsions. The aggregative state evaluation of Walnut oil / Polyphenol extract / Water system defined four regions, showing the stability increasing “from water to oil” (Figure 4): region IV (< 1 min), region V (2...5 min), region VI (5...7 min), and region VII (> 7 min). Therefore, the lipid extract of green tea demonstrated the pronounced effect of W/O emulsions stabilization, the most stable samples having aqueous phase content up to 30%.

The influence of walnut oil on the structure of spread type emulsions

Due to the presence of animal and vegetable components, the chemical and structural composition of spread containing walnut oil is more complicated than in milk-based butter. Spreadable products, both spreads and butter without vegetable components, represent polydisperse, multi-phase and multicomponent systems with variable composition. The polydispersity of spreads is due to the presence of solid lipid phase, aqueous phase and gaseous phase in the form of fragmented particles, whose dimensions vary: 0.01-2 μm milk fat crystals, 1...30 μm water droplets and up to 20 μm air bubbles [15].

Taking into account temperature and rate of acylglycerols cooling, different crystalline polymorphic structures are formed during the crystallization process of food emulsions [16]. Because of the large difference between the melting temperatures of dairy and vegetable fats, the lipid phase of spread containing walnut oil may be represented as either a continuous phase of solid lipid crystals, or liquid oil micelles dispersed evenly with those of aqueous between solid lipid crystals, or liquid oil incorporated and stabilized within the solid crystal network [17]. The last proposed structure, in our opinion, is the least likely from the thermodynamic point of view. In order to establish the peculiarities of walnut oil state in spread type emulsions, the microscopic analysis of spread containing sweet cream and 20% walnut oil was made [18]. It was necessary to specify in what way the presence and way of walnut oil lipids incorporation contributed to the formation of product structure and stability. With an eye to highlight spread phases, water-soluble or/and liposoluble dyes (methylene blue, sudan III) were added while samples obtaining (Figure 5).

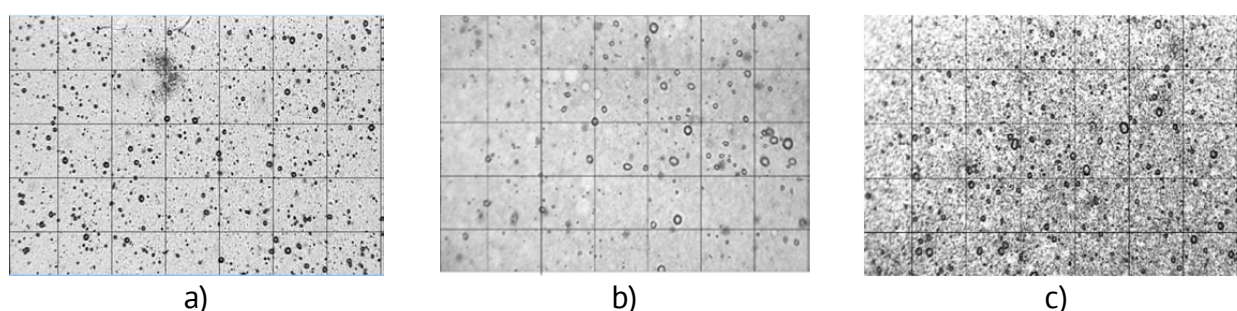


Figure 5. Spread images obtained by microscope analysis with 100x100 μm cells, where different dyes were applied:
a) sudan III, b) methylene blue, c) sudan III and methylene blue.

The microscope images of spread (Figure 5) showed that the obtained product represented an emulsion, where water micelles and air inclusions were dispersed in a continuous lipid phase, which, in its turn, was formed from solid lipid crystals (Figure 6).

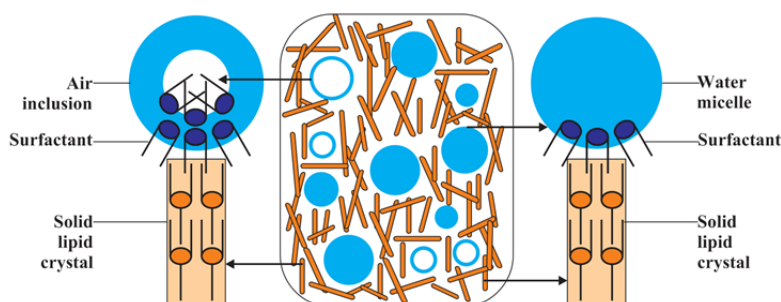


Figure 6. The schematic representation of spread microstructure:
polar (●) and non-polar (—) parts.

The structural stability of spreads containing walnut oil

Factors that affect the oxidative stability of food emulsions are the chemical structure of lipids, interfacial characteristics, droplets characteristics (concentration, dimensions) and the interaction with aqueous phase components (salt, sugars, proteins) [19, 20]. The instability phenomenon and the initial state conversion of spread can be established by evaluating the changes of the size and number of particles that form the system. That's why the aggregative stability of the microstructure of spread containing sweet cream and 20% walnut oil [18] was investigated (Figure 7). The obtained samples,

with 10 - 40 g weight in each, were packaged in aluminum foil and stored at two temperature regimes: $t = (3 \pm 2)^\circ\text{C}$ and $t = - (6 \pm 3)^\circ\text{C}$. The lipid phase creaming, accompanied with coalescence and aqueous phase elimination, manifested over 30 days of keeping the spread at $t = (3 \pm 2)^\circ\text{C}$ and over 37 days at $t = - (6 \pm 3)^\circ\text{C}$. The changes of spread sensory properties, established by product consistency softening, were detected along with the appearance of the first signs of water micelles coalescence.

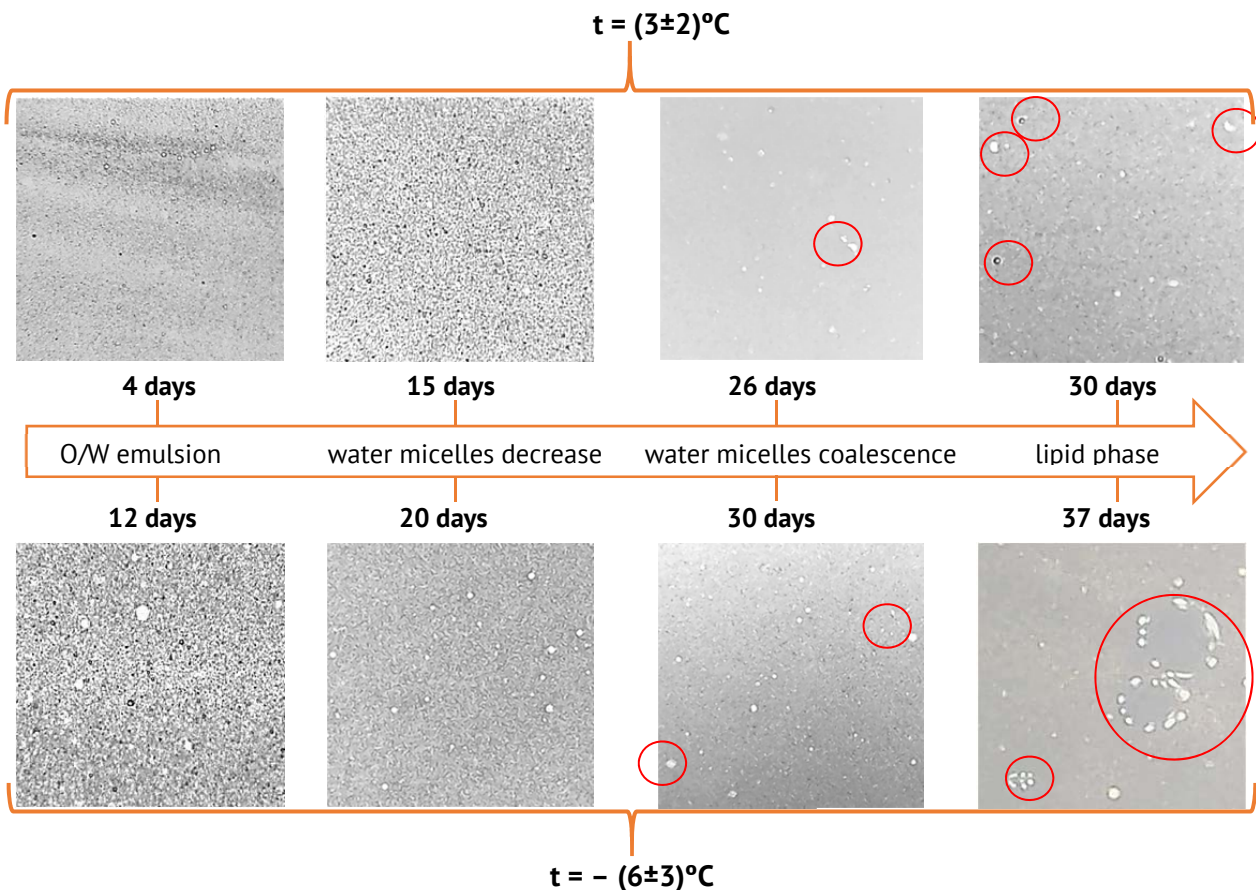


Figure 7. The aggregative stability of the microstructure of spread containing walnut oil.

Conclusions

The physical state of droplets in emulsions containing walnut oil depends on its composition (PUFA and phospholipids content) and influence on most important product physicochemical, organoleptic, and biochemical properties, including appearance, rheology, stability, and gastrointestinal transformations. Thus, it was demonstrated, that walnut oil is more prone to form W/O emulsions than O/W ones. We explain this fact by the presence of phospholipids in its composition, which have surfactants properties. It was confirmed through the analysis of emulsions with an increased phospholipids concentration – *Walnut oil / Green tea extract / Water* system, that showed the pronounced effect of W/O emulsions stabilization, the most stable samples having aqueous phase content up to 30%.

The microstructure of spread containing sweet cream and 20% walnut oil represents an emulsion, where water micelles and air inclusions are dispersed in a continuous lipid phase, which, in its turn, is made of solid lipid crystals. This contributes to the fact that spread containing walnut oil possesses the rate of structural degradation analogous to milk-based butter and retains its functionality and high biological value within a month at the temperature regime up to 5°C .

Acknowledgments. Gratitude and great appreciation are expressed to the National Scholarship Programme of the World Federation of Scientists for the support in a scientific activity.

References

1. McClements D.J. *Food emulsions. Principles, practices, and techniques*. In: CRC Press, 2016. ISBN-13: 978-1-4987-2669-6.
2. Nikovska K. Oxidative stability and rheological properties of oil-in-water emulsions with walnut oil. *J. Advance Journal of Food Science and Technology* 2(3), 2010. – pp. 172-177. ISSN: 2042-4876.
3. Slatnar A., et al. Identification and quantification of phenolic compounds in kernels, oil and bagasse pellets of common walnut (*Juglans regia* L.). In: *Food Research International*, 67, 2015. – pp. 255-263. DOI:10.1016/j.foodres.2014.11.016.
4. Patel G. Essential fats in walnuts are good for the heart and diabetes. In: *J. Am. Diet. Assoc.*, 105(7), 2005. – pp.1096-1097. DOI:10.1016/j.jada.2005.05.193.
5. Estruch R., et al. Primary prevention of cardiovascular disease with a Mediterranean diet. In: *The New England Journal of Medicine*, 368, 2013. – pp. 1279-1290. DOI:10.1056/NEJMoa1200303.
6. Grosso A.L., Asensio C.M., Nepote V., Grosso N.R. Antioxidant activity displayed by phenolic compounds obtained from walnut oil cake used for walnut oil preservation. In: *J. Am. Oil Chem. Soc.* (95), 2018. – pp.1409-1419. DOI:10.1002/aocs.12145.
7. Crowe T., White P.J. Oxidation, flavor and texture of walnuts reduced in fat content by supercritical carbon dioxide. In: *J.American Oil Chemists' Society*, Vol.80 (6), 2003.– pp.569-574. DOI:10.1007/s11746-003-0739-4.
8. McClements D.J., Decker, E.A. Lipid oxidation in oil-in-water emulsions: impact of molecular environment on chemical reactions in heterogeneous food systems. In: *Journal of Food Science* 65 (8), 2000. – pp.1270-1282. DOI:10.1111/j.1365-2621.2000.tb10596.x.
9. Fregapane G., Ojeda-Amador R.M., Salvador M.D. Virgin walnut (*Juglans regia* L.) oil. In: *Fruit Oils: Chemistry and Functionality*, 2019. – pp. 133-147. DOI:10.1007/978-3-030-12473-1_5.
10. Birdi K.S. *Handbook of Surface and Colloid Chemistry*. Taylor & Francis Group, 2016. ISBN-13: 978-1-4665-9668-9.
11. Baerle A., Popovici C., Radu O., Tatarov P. *Effect of Synthetic Antioxidants on the Oxidative Stability of Cold Pressed Walnut Oil*. *Journal of Food and Packaging Science, Technique and Technologies*, 2016, №9. – pp. 19-24.
12. Radu O., Baerle A., Tatarov P., Popovici C. *Aggregative stability of model emulsions containing walnut oil (*Juglans regia* L.)*. Conference of Modern Technologies in the Food Industry, October 18-20, Chisinau, 2018. pp.230-231. ISBN 978-9975-87-428-1.
13. Bidlack W.R., Rodriguez R.L. *Nutritional Genomics: The Impact of Dietary Regulation of Gene Function on Human Disease*. In: CRC Press, 2012. ISBN-13: 978-1-4398-4453-3.
14. Afzal M., Safer A. M., Menon M. Green tea polyphenols and their potential role in health and disease. In: *Inflammopharmacology*, Vol. 23 (4), 2015. – pp. 151. DOI:10.1007/s10787-015-0236-1.
15. Vyshemirskij F.A. Fizicheskaya struktura i konsistenciya slivochnogo masla. [Physical structure and consistency of butter]. M: ANO "Molochnaya promyshlennost", 2013. – pp. 53-56. – in Russian.
16. Tatarov P. *Chimia produselor alimentare. [Food chemistry]* Chisinau: MS Logo, 2017. – in Romanian.
17. Arellano M., Norton I.T. Smith P. Specialty oils and fats in margarines and low-fat spreads. In: *Woodhead Publishing Series in Food Science, Technology and Nutrition*, 2015. – pp. 241-270. DOI:10.1016/B978-1-78242-376-8.00010-7.
18. Technical University of Moldova, MD. *Procedeu de obținere a amestecului de grăsimi tartinabile pe bază de smântână dulce*. [Process of the preparation of a spreadable fats mixture based on sweet cream]. Patent no. 1281. Inventors: Radu O., Popescu L., Tatarov P., Baerle A. Publ.: BOPI, 2018-09-30.
19. Kiokias S., Dimakou C., Oreopoulou V. Effect of heat treatment and droplet size on the oxidative stability of whey protein emulsions. In: *Food Chemistry* 105, 2007. – pp. 94-100. DOI:10.1016/j.foodchem.2007.03.053.
20. Griffiths A.D, Tawfik D.S. Miniaturising the laboratory in emulsion droplets. In: *Trends Biotechnol.* 30(10), 2006. – pp.1-8. DOI: 10.1016/j.tibtech.2006.06.009.

DOI: 10.5281/zenodo.3713372

CZU 551.464.7:664



MICROALGAE – NON-TRADITIONAL SOURCES OF NUTRIENTS AND PIGMENTS FOR FUNCTIONAL FOODS

Angela Gurev*, ORCID ID: 0000-0001-8493-5257,
Veronica Dragancea, ORCID ID: 0000-0002-5938-0410,
Svetlana Haritonov, ORCID ID: 0000-0002-9244-8982

Technical University of Moldova, 168, Stefancel Mare bd., Chisinau, Republic of Moldova

*Corresponding author: Angela Gurev, angela.gurev@chim.utm.md

Received: 12.18.2019

Accepted: 02.28.2020

Abstract. The aim of this review is to draw the attention of researchers and technological engineers from the Moldovan food industry towards the potential of microalgae as a non-traditional source of nutrients and biological active substances, such as proteins, essential amino acids, carotenoids, vitamins, polyunsaturated fatty acids ω_3 , phytosterols, polysaccharides, phenolic acids, microelements, etc., which can be used to increase the nutritional and functional value of conventional foods. The study synthesizes information regarding the profile of biologically active substances obtained from various microalgae species, analyses the nutritional value of microalgae biomass and their field of application. This review focuses on pigments contained in microalgae (carotenoids, chlorophylls and phycobiliproteins), deals with their biological activity and health benefits. It draws attention to the results of the recent research, which proves that microalgae pigments exhibit pronounced antioxidant properties, protect cells from the radiation, capture free radicals and reduce the oxidative stress in the body, prevent cancer, inflammation and cardiovascular diseases, modulate the immune system, prevent the macular degeneration, etc. Review describes in more detail the carotenoids class and elucidates the qualitative and quantitative content of carotenoids in some microalgae. It discusses the areas of use of the pigments accumulated in microalgae and their further application as natural food additives and dyes.

Keywords: *bioactive compounds, carotenoids, chlorophylls, health benefits, food additives, phycobiliproteins, phytonutrients, xanthophylls.*

Introduction

One of the food industry objectives is elaboration and implementation in production of functional foods, which could bring health benefits to population. Functional foods are obtained by adding lacking functional ingredients or phytonutrients to conventional products, consumed on a daily basis.

Functional ingredients, which are not synthesized by the human body, are essential and must be supplied with food.

Besides the traditional sources of phytonutrients, (vegetables, fruits, berries, plants, etc.), microalgae are in the spotlight due to their high nutritional value and the ability to synthesize biologically active substances with a varied structure: carotenoids, proteins, essential amino acids, vitamins, polyunsaturated fatty acids ω_3 , polyphenols, phytosterols, polysaccharides, sulfur compounds, microelements, etc. [1 - 8]. Research has proven the health benefits of microalgal metabolites, for example the pigments from microalgae – carotenoids, chlorophylls and phycobiliproteins exhibit pronounced antioxidant properties, protect cells from the ultraviolet radiation, capture free radicals and reduce the oxidative stress in the body, prevent cancer, inflammation and cardiovascular diseases, modulate the immune system, prevent the macular degeneration and are widely applied in the food, cosmetic and pharmaceutical industries, etc. [9 - 13]. Carotenoids with a varied structure, in much higher concentrations compared to traditional sources, can be obtained from microalgae [3]. Most of the carotenoids suggested by the pharmaceutical industry are chemically synthesized, but due to the side-effects associated with medicine administration, public interest in recent times has focused on natural products with health-promoting effects as alternatives to conventional drugs [12]. Furthermore, pigments from microalgae are natural colorants, vitamin precursors, harmless to the human body and can substitute adverse, synthetic additives and noxious dyes used by the food industry [1, 4, 11].

Nevertheless, despite being one of the richest sources in phytonutrients, with a high nutritional value and health benefits, the microalgae's potential is not fully explored. Consequently, the modern food industry's current objectives are to use the microalgae as a renewable source of bioactive substances and natural colorants, obtain and establish the chemical structure of the new compounds, study the biological activity and the technological requirements regarding the optimization and implementation of phytonutrients in the production of functional foods.

Microalgae – organisms with a promising potential

The term "Microalgae" includes cyanobacteria and eukaryotic microorganisms, which are microscopic aquatic organisms, and similar to terrestrial plants, use the solar energy and carbon dioxide for photosynthesis and produce a wide variety of complex substances and biologically active compounds. There are microalgae that have their habitat in the soil. Of the 200.000 estimated species for microalgae, up to 50.000 have been described so far [1 - 4].

The aquatic microalgae, some of the oldest terrestrial organisms, are adapted to survive in adverse environmental conditions – wastewater, waters with varied salinity, high or low temperatures, UV radiation, environments with varied nutrients' availability, etc., producing chemicals of various structures [3 - 6]. They are characterized by the ability to grow and multiply rapidly, within a short life cycle, also being easy to manipulate. Microalgae's efficiency in fixing the carbon dioxide (CO_2) in the atmosphere is 10 to 50 times higher than that of terrestrial plants [14]. Microalgae are also responsible for the circuit in nature of elements such as sulfur, phosphorus, carbon, nitrogen and microelements. They consume nutrients from wastewater, including chemicals and heavy metals. Over 99,9% of algal biomass is mainly made from: C, N, S, P, O, and H, sodium (Na), potassium (K), calcium (Ca), magnesium (Mg), iron (Fe), chlorine (Cl), silicon (Si), and other traces of elements. Thus, the cultivation of microalgae reduces the level of pollutants in the air and in the aquatic environment [15].

Being one of the most important trophic links in the aquatic ecosystems, microalgae are a renewable, valuable source of biologically active substances, highly cultivated in recent years and used in the food, pharmaceutical, cosmetic, medical, agricultural, zootechnical, poultry, fish industries, etc., for their high content of lipids, fatty acids, essential acids, steroids, carotenoids, pigments, polyphenols, vitamins, oligosaccharides, polysaccharides, amino acids, proteins, halogenated compounds, sulfur compounds, microelements, etc. [1 - 11]. Most microalgae accumulate metabolites in biomass; some, known for their high lipid content, are being researched as an ecological, renewable source of fuel – biodiesel [5 - 6].

Microalgae – a source of functional ingredients

Nowadays, there is a growing demand for functional foods, beneficial for the human body. The functional foods are obtained by adding the functional ingredients or micronutrients lacking in the daily consumed conventional food [16]. Functional ingredients such as essential fatty acids (ω -3, ω -6), phytosterols, prebiotics and probiotics, carotenoids, polyphenols, vitamins, etc., are not synthesized in the human body, being essential, they must be supplied with food.

A healthy lifestyle implies a balanced diet that includes phytonutrients delivered both from traditional sources (vegetables, fruits, berries, plants, etc.) as well as from non-traditional sources such as microalgae. The Chinese have been consuming the *Nostoc* microalgae species for more than 2000 years [3], lately; species such as *Spirulina* and *Chlorella* have been introduced as functional foods in Japan, Taiwan and Mexico [6 - 10]. Currently, the most consumed microalgae belong to the species *Spirulina sp.*, *Chlorella sp.*, *Dunaliella terticola*, *D. salina*, *Odontella aurita* and *Aphanizomenon flos-aquae*, due to their high nutritional value and high protein content [17].

Microalgae biomass is regarded as a superior source of phytonutrients and antioxidants, not only because of the greater productivity of microalgae, compared to conventional terrestrial sources but also because of the content of bioactive substances in the cell, estimated as follows: 8–14% pigments, 12–30% carbohydrates, 4–20% lipids, 40–70% proteins and significant amounts of vitamins A, C, B₁, B₂, B₁₂, E, K, and D [7].

Table 1 lists the biologically active substances that are obtained today from microalgae [6-9, 17-19].

Table 1

Major bioactive compounds extracted from microalgae

Microalgae	Bioactive compounds
<i>Botryococcus braunii</i>	Linear alkadienes (C ₂₅ , C ₂₇ , C ₂₉ and C ₃₁), alkatrienes (C ₂₉)
<i>Chlorella ellipsoidea</i>	Zeaxanthin, violaxanthin
<i>Chlorella minutissima</i> , <i>Nanochloropsis</i> , <i>Nitzschia</i> , <i>Phaeodactylum</i> and <i>Odontella aurita</i>	Eicosapentaenoic acid (EPA)
<i>Chlorella protothecoides</i>	Lutein, zeaxanthin, canthaxanthin
<i>Chlorella pyrenoidosa</i>	Lutein, sulfated polysaccharides
<i>Chlorella sp.</i>	Carotenoids, sulfated polysaccharides, sterols, polyunsaturated fatty acids (PUFAs)
<i>Chlorella vulgaris</i>	Astaxanthin, canthaxanthin, peptide, oleic acid

Continuation Table 1

<i>Chlorella zofingiensis</i>	Astaxanthin
<i>Cryptothecodinium cohnii</i> , <i>Schizochytrium spp.</i>	Docosahexaenoic acid (DHA)
<i>Dunaliella salina</i>	Trans- β -carotene, cis- β -carotene, β -carotene, oleic acid, linoleic acid, palmitic acid
<i>Dunaliella spp.</i>	Diacylglycerols
<i>Haematococcus pluvialis</i>	Astaxanthin, lutein, zeaxanthin, canthaxanthin, β -carotene, oleic acid
<i>Isochrysis galbana</i> , <i>Phaedactylum tricomutum</i>	Lipids, fatty acids
<i>Nostoc linckia</i> , <i>Nostoc spongiaeforme</i>	Borophycin
<i>Nostoc sp.</i>	Cryptophycin
<i>Porphyridium sp.</i>	Phycobiliproteins
<i>Spirulina fusiformis</i>	Diacylglycerols
<i>Spirulina platensis</i>	Phycocyanin, C-phycocyanin, phenolic acids, tocopherols, vitamin E, neophytadiene, phytol, PUFAs, oleic acid, linolenic acid, palmitoleic acid
<i>Spirulina sp.</i> and <i>Porphyridium cruentum</i>	Polysaccharides

Microalgae are used in the food industry for the high protein content, similar to that from traditional sources, but having a higher quality than the proteins from oat, rice, soy and legumes, thus lower compared to meat, milk and fish proteins [6].

According to bibliographic sources, microalgae produce 4-15 tons of protein per hectare annually, whereas legumes yield 1-2 tons/ha per year, and soy – 0.6-1.2 tons/ha per year [9]. Moreover, microalgae are an excellent source of ω_3 polyunsaturated fatty acids in their most active form – α -linolenic essential acids (ALA), eicosapentaenoic (EPA) and docosahexaenoic (DHA) [10, 19], minerals and vitamins [2, 13, 20].

Algae dried biomass is easily digested by the human body. In vitro investigations through the enzymatic method with application of pepsin and pancreatin, have shown that *Arthrospira platensis* (*spirulina*), *Chlorella sorokiniana* IAM-C212 and *Chlorella vulgaris* had the highest digestibility, while *Tetraselmis suecica*, *Phaedactylum tricornutum*, and *Porphyridium purpureum* were the least digestible, likely because of the presence of robust cell walls or of exopolysaccharides that might have limited the action of digestive enzymes [3].

Nowadays, *Chlorella* and *Spirulina* species are consumed as functional foods in dry form, tablets or encapsulated, etc. *Spirulina* has been called a “superfood” due to the high content of nutrients, of which up to 70% of the dry mass being protein [20 - 23].

Spirulina is also used for its antioxidant, immunostimulatory and cholesterol-lowering properties; while the sulfated polysaccharides contained in biomass act as antiviral agents.

Spirulina has been shown to contain 6.7 times more protein than tofu, 1.8 times more calcium than milk, 51 times more iron than spinach and 31 times more carotenoids than carrot [20, 21].

Table 2 shows the mass parts of proteins, lipids and carbohydrates in some of the cultivated microalgae species [9, 22, 23].

Table 2

Composition of microalgae species in percentage of dry biomass matter

Microalgae sp.	Composition, % of dry matter		
	Protein	Lipids	Carbohydrates
<i>Chlorella vulgaris</i>	51-58	14-22	12-17
<i>Chlorella pyrenoidosa</i>	57	2	26
<i>Chlamydomonas reinhardtii</i>	48	21	17
<i>Dunaliella salina</i>	57	6	32
<i>Dunaliella bioculata</i>	49	8	4
<i>Haematococcus pluvialis</i>	48	15	27
<i>Isochrysis galbana</i>	50-56	12-14	10-17
<i>Euglena gracilis</i>	39-61	22-38	14-18
<i>Pophyridium cruentum</i>	28-39	9-14	40-57
<i>Prymnesium parvum</i>	28-45	22-38	25-33
<i>Spirulina maxima</i>	60-71	6-7	13-16
<i>Spirulina platensis</i>	46-63	4-9	8-14
<i>Scenedesmus obliquus</i>	50-56	12-14	10-17
<i>Synechococcus spp.</i>	63	11	15
<i>Tetraselmis maculata</i>	52	3	15

Chlorella, in addition to valuable nutrients, contains β -1,3-glucans, which stimulate the immunity, decrease the blood triglyceride concentration, capture free radicals and eliminate the toxins [23].

The concentration of provitamin A, vitamins E, B₁ and folic acid in microalgae is higher compared to the traditional sources: *Dunaliella tertiolecta* synthesizes vitamins B₁₂ (cobalamin), B₂ (riboflavin), vitamin E (tocopherol) and provitamin A (β -carotene). *Tetraselmis suecica* is an excellent source of vitamins B₁ (thiamin), B₃ (nicotinic acid), B₅ (pantothenic acid), B₆ (pyridoxine) and vitamin C (ascorbic acid) [24].

Scientific research confirms that *Chlorella* species contain vitamins B₇ (biotin) and B₁₂ in high concentrations [16]. Table 3 analyses the vitamins profile of *Spirulina* and *Chlorella* algae species [25].

Table 3

Vitamin profile of two species of microalgae: *Spirulina* and *Chlorella*(in mg kg⁻¹ unless otherwise stated)

Vitamins	<i>Spirulina</i>	<i>Chlorella</i>	Vitamins	<i>Spirulina</i>	<i>Chlorella</i>
Provitamin A	2330000 IU kg ⁻¹	55500 IU kg ⁻¹	Vitamin B ₆	8	17
β -carotene	1400	1808	Vitamin B ₁₂	3.2	1259
Vitamin E	100	<10 IU kg ⁻¹	Inositol	640	1650
Thiamin B ₁	35	15	Folic acid	0.1	296
Riboflavin B ₂	40	48	Biotin	0.05	1916
Niacin B ₃	140	238	Pantothenic acid	1	13

According to the 1997 Regulation, the EU included some microalgae in the list of foods authorized in the EU market. The list included *Aphanizomenon flos-aquae* from

Klamath Lake, *Arthrospira platensis*, *Chlorella luteoviridis*, *C. pyrenoidosa*, and *C. vulgaris*. *Odontella aurita*, *Tetraselmis chuii* and astaxanthin from *Haematococcus pluvialis* were successively approved as food or food ingredients [26].

In order to increase the nutritional and functional value of the conventional foods, microalgae and microalgae phytonutrients are used to enrich pasta, bakery products, snack foods, confectionery, sweets, beverages, dairy products, etc. For example, the dry biomass of *A. platensis* (*Spirulina*) can be incorporated in pasta flour up to 20% and up to 8.36% in biscuits; dry biomass of *Dunaliella* (without β -carotene and glycerol) up to 10% in bread flour; astaxanthin can be incorporated in cake flour up to 15%; *Chlorella sp.* Dry biomass can be added to yogurt in a proportion of up to 10% [9]. Microalgae are also an excellent source of nutrition for fish and aquatic organisms, for animals, cattle, swine, poultry, etc. [8, 10].

Pigments from microalgae

As mentioned above, microalgae are an excellent source of ecological and renewable pigments. They determine the microalgae's specific colour: e.g. the green colour is due to chlorophyll, the red and blue colours are due to phycobiliproteins, the yellow, orange and red colours – carotenoids synthesized by microalgae.

Microalgae are also classified by colour, e. g. *Chlorophyceae* (green color), *Rhodophyceae* (red color), *Cyanophyceae* (blue green), and *Pheophyceae* (brown). In most algae the predominant pigments are: chlorophyll *a*, *b* and *c*, β -carotene, xanthophylls, phycocyanin and phycoerythrin. Currently, pigments with predominant content are obtained from certain microalgae species, for example β -carotene is obtained from *Dunaliella salina* [27 - 29], astaxanthin is obtained from *Hematococcus pluvialis* and *Chlorella* species [30]; fucoxanthin is obtained from *Muriellopsis* and *Isochrysis aff. Galbana* [31], zeaxanthin from *Dunaliella salina* [28], phycobiliproteins- phycoerythrin and phycocyanin from *Porphyridium* and *Anabaena* species [32 - 34].

Pigments from microalgae - carotenoids, chlorophylls and phycobiliproteins are biologically active compounds, vitamin precursors in human diet and animal feed, and can be also used as additives and natural dyes in the food, cosmetic and pharmaceutical industries, etc. [35].

Different methods of obtaining pigments from microalgae biomass have been developed. As mentioned above, pigments in the plant cells are found not only in the form of free but also glycosylated, esterified with fatty acids or as protein complexes.

For a better extraction it is necessary to lyse the microalgae cell walls and to release the contained bioactive substances. Cell lysis and pigment extraction can be accomplished by several methods, which can be further combined: a) mechanical grinding; b) milling; c) freeze-thaw; d) ultrasonic assisted extraction; e) microwave extraction; f) supercritical fluids extraction; g) pulse electric field extraction; h) enzyme assisted extraction; i) organic solvent extraction.

These methods have advantages and disadvantages, described in the bibliographical sources [36].

Supercritical fluids extraction (CO_2 and ethanol) and the use of non-toxic and non-flammable, recyclable solvents are increasingly applied for the full use of the microalgae biomass, which, besides the pigments, contains various valuable biologically active compounds.

Carotenoids, structure and classification

Carotenoids, also called tetraterpenoids, are the most widespread class of photosynthetic pigments synthesized by plants, algae, fungi and cyanobacteria. Some fungi and insects (aphids, mites) generate carotenoids through other mechanisms [37, 38]. Animals do not synthesize carotenoids in their bodies; they are delivered with food and stored in the adipose tissues. It is well known the vital importance of carotenoids obtained from food for the development and normal functioning of the human body.

Up to 1100 carotenoid pigments are known today; they are responsible for the yellow, orange and red colors in plants, flowers, algae, fruits, vegetables, berries, etc., [36-38]. The carotenoids contained in the body tissues can be in the form of free, glycosylated, esterified with fatty acids or as protein complexes [36].

Most carotenoids are tetraterpenoids composed of 8 molecules of isoprene (2-methyl-but-1,3-diene), $(C_5H_8)_8$ and contain 40 carbon atoms in the molecule. The simplest carotene is lycopene with a hydrocarbon chain (consisting only of a carbon and a hydrogen), which contains double conjugates bonds Figure 1.

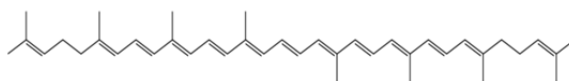


Figure 1. Lycopene.

At the ends of the hydrocarbon chain, acyclic or cyclic groups can be formed: γ -carotene, β -carotene, etc., Figure 2.

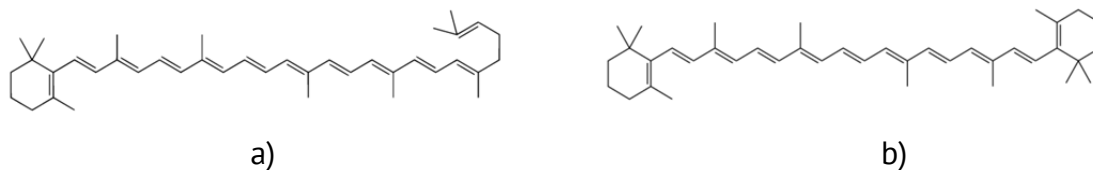


Figure 2. a) γ -carotene; b) β -carotene.

At the double bonds between the polyene carbon atoms, in the chain, the configuration is trans (*E*) and must be indicated in the name, e. g.: (*all-E*)-lycopene. Based on the chemical structure, carotenoids are divided into two major classes:

- 1) **carotenes** – are the carotenoids composed only from atoms of carbon and hydrogen: α -carotene, β -carotene, γ -carotene and lycopene;
- 2) **xanthophylls** – oxygenated carotenoids: lutein, contains hydroxyl groups (alcoholic); canthaxanthin, with carbonyl groups (ketone); astaxanthin contains both functional groups (alcoholic and ketone); fucoxanthin with esteric groups, Figure 3.

Apart from these two major classes, carotenoids with less than 40 carbon atoms in the molecule are also known: apocarotenoids, which are formed by oxidative cleavage, as would be the abscisic acid (plant hormone), retinol (vitamin A_1), retinoic acid, etc. [5]. C_{50} Carotenoids, with more than 50 carbon atoms in the molecule, have a complex structure, often being glycosylated. For example, soil bacteria (*Corynebacterium glutamicum*) are unique in the production of the C_{50} decaprenoxanthin carotenoid and its glycosylated forms [36, 37], Figure 3.

Carotenoids are also classified into **provitamins A**, which can be converted in the body into retinol, such as α -carotene, β -carotene, γ -carotene and β -cryptoxanthin and **non-provitamins A**, such as lutein, zeaxanthin and lycopene [36].

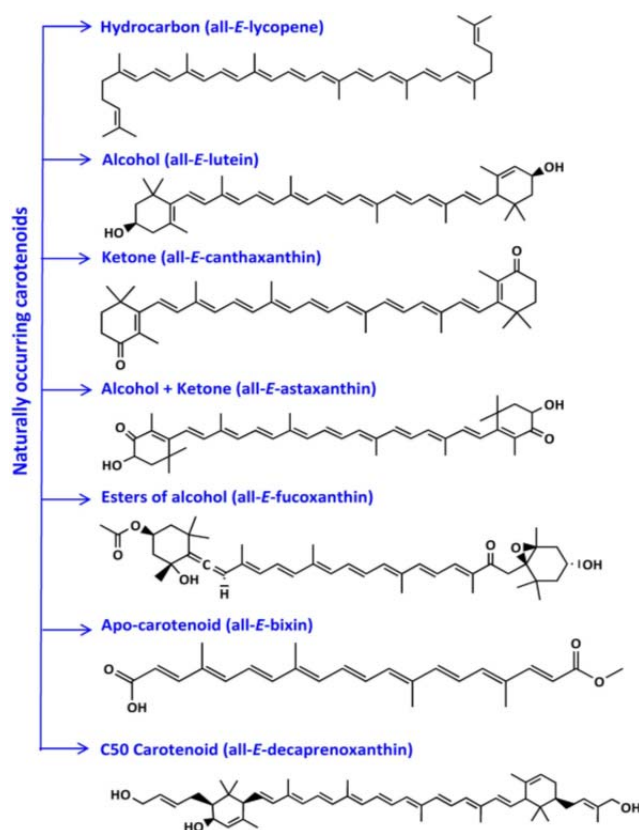


Figure 3. Carotenoids widespread in nature [36].

The biological activity of the carotenoids

Carotenoids are lipophilic pigments, soluble in lipids and non-polar organic solvents, with a high antioxidant activity, playing a key role in plant photosynthesis. The structure of carbon chains with conjugated double bonds determines the biological role of the carotenoids, which consists in sending the energy from the absorbed light straight to the chlorophyll molecules or in transporting the energy from one chlorophyll molecule to another, moreover, carotenoids protect plant cells from the effects of excess light exposure by scavenging reactive oxygen species (*ROS*), such as singlet oxygen molecules and free radicals in the process of photosynthesis [37, 39, 40].

Carotenoids from plants are important biologically active phytonutrients for the animal organisms, having multiple effects, including provitamin A activity. In the human body, β -carotene is converted into two molecules of vitamin A, while α -, γ -carotene and β -cryptoxanthin in one molecule of vitamin A [40, 41]. In the human body, the carotenoids supplied from food have pronounced antioxidant activity and reduce the oxidative stress by capturing free radicals [42]. It is well known that *ROS*, formed under stress conditions, damage tissues, causing so inflammation, attack the neutrophils and form superoxide radicals that lead to lipid peroxidation and cell membrane lysis [43 - 45]. Carotenoids inhibit free radicals by electron transfer (which occurs due to the conjugated double bonds), by assignment of hydrogen atoms to free radicals or by binding the free radicals. Scientific research has proved that carotenoids can interact directly with some types of free radicals, eliminate the *ROS* from the environment, at the same time preventing their further formation [43, 46, 47].

The therapeutic value of carotenoid has been elucidated [47], and it includes the prevention and treatment of the chronic inflammatory diseases [43, 47], cancer, cardiovascular [48], renal, pulmonary, liver, intestinal diseases, the treatment of metabolic disorders, autoimmune diseases, HIV, sepsis, multiple sclerosis, atherosclerosis, etc. [49 - 55]. It was established that in the treatment of cancer, cardiovascular diseases and eye disorders, the administration of β -carotene, lycopene, lutein and zeaxanthin is extremely important [56]. However, it has also been established that administering synthetic β -carotene to smokers stimulates the lung cancer [57].

Carotenoids contained in the eye retina – lutein and zeaxanthin, prevent retinal damage and protect it against light and ultraviolet radiation [55, 56]. The same photoprotective effect slows down the aging process of the body and skin and prevents photodermatitis and skin cancer [58]. Due to the antioxidant, photoprotective properties, carotenoids are widely used in the cosmetic industry [1, 4, 5].

Carotenoids from microalgae

Characterized by diversity, some structures not being found in the traditional sources, Tables 4, 5. Microalgae synthesize both carotenoids and xanthophylls found in terrestrial sources (β -carotene, lutein, zeaxanthin, antheraxanthin) as well as microalgae specific pigments (e.g., astaxanthin, fucoxanthin, diatoxanthin, diadinoxanthin) [4, 11].

Microalgae carotenoids can be classified into two categories. Primary carotenoids, which are the components of the photosynthetic apparatus, essential for survival and secondary carotenoids, which are produced under specific environmental conditions (high light intensity, UV radiation, nutrient variation, salinity, etc.), for cell protection. Lycopene, α -carotene and β -carotene are primary carotenoids. Secondary carotenoids are synthesized from primary carotenoids under specific conditions of cultivation or under the action of abiotic factors. When triggering the photoprotective mechanism, called the xanthophyll cycle, lutein, zeaxanthin, astaxanthin, canthaxanthin, antheraxanthin, violaxanthin, neoxanthin, fucoxanthin, diadinoxanthin, diatoxanthin, etc. are formed [59].

In comparison with traditional sources, microalgae have the ability to synthesize carotenoids with a varied structure in much higher concentrations Table 4. In the *Phormidium autumnale* microalgae were identified 24 types of carotenoids, of which β -carotene, lutein and zeaxanthin with major content, reaching a concentration of 225.44 $\mu\text{g}\cdot\text{g}^{-1}$, 117.56 $\mu\text{g}\cdot\text{g}^{-1}$ and 88.46 $\mu\text{g}\cdot\text{g}^{-1}$ of biomass, respectively [60]. A single species of microalgae is able of producing several active components; for example, *Chlorella Sorokiniana* produces carotenoids with the mass of 0.59% from the dry matter, and α -tocopherol, β -carotene and lutein content of 112, 600 and 4300 $\mu\text{g}\cdot\text{g}^{-1}$ of dry matter, respectively [61].

The market demand for carotenoids obtained from natural sources is constantly increasing, especially for β -carotene, lutein, astaxanthin, zeaxanthin and fucoxanthin [3,9]. Currently, the largest microalgae producing companies are widely cultivating the *Spirulina*, *Chlorella*, *Dunaliella*, *Haematococcus*, *Aphanizomenon flos-aquae* species and the red microalgae of the *Porphyridium* genus [11] both for their high nutritional value, as well as for the increased content of pigments and other biologically active substances.

The commercial source of lutein is the petals of Marigold flowers (the genus *Calendula*), although the research has shown that microalgae have 3 - 6 times more lutein per unit mass [62]. The green species of *Chlorella* produce lutein, violaxanthin and

zeaxanthin [63]; the green algae *Dunaliella salina* produce a large quantity of carotenoids that can be converted to pro-vitamin A in the human body [27 - 29]. Usually, most microalgae synthesize β -carotene and other types of carotenoids, some are major components in the biomass extracts [12], Table 4.

Table 4

Carotenoids produced by microalgae

Microalgae Species	Major Carotenoid	Other Carotenoids	Concentration % (TC/DW)
<i>Chlorella sp.</i>	Lutein	Astaxanthin	0.23
<i>Chlorella ellipsoidea</i>	Violaxanthin	Antheraxanthin, zeaxanthin	-
<i>Chlorella Sorokiniana</i>	β -carotene	Lutein	0.59
<i>Chlorella pyrenoidosa</i>	Lutein	Violaxanthin, Loroaxanthin, β -carotene, α -carotene	0.2-0.4
<i>Chlorella vulgaris</i>	Canthaxanthin, lutein	Astaxanthin, violaxanthin	-
<i>Chlorella zofingiensis</i>	β -carotene	Canthaxanthin, astaxanthin	3.7
<i>Chlorococcum humicola</i>	Violaxanthin	Astaxanthin, lutein, zeaxanthin, β -carotene, α -carotene	-
<i>Coelastrella striolata var. Multistriata</i>	Canthaxanthin	Astaxanthin, β -carotene	4.75
<i>Dunaliella salina</i>	β -carotene	Zeaxanthin, lutein, α -carotene	10-13
<i>Haematococcus pluvialis</i>	Astaxanthin	β -carotene, lutein, canthaxanthin, neoxanthin, violaxanthin, zeaxanthin, echinenone	6.0
<i>Isochrysis aff. galbana</i>	Fucoxanthin		1.8
<i>Odontella aurita</i>	Fucoxanthin	Diadinoxanthin, β -carotene	2.2
<i>Phaeodactylum tricornutum</i>	Fucoxanthin	Diadinoxanthin, zeaxanthin, neoxanthin, violaxanthin, β -carotene	1.65
<i>Porphyridium cruentum</i>	Zeaxanthin	β -carotene	Zeax. 97.4 from TC
<i>Scenedesmus sp.</i>	Lutein	Astaxanthin	0.18
<i>Spirulina maxima</i>	β -carotene	Astaxanthin, lutein, β -cryptoxanthin, zeaxanthin, echinenone, oscillaxanthin, myxoxanthophyll	<0.8
<i>Spirulina pacifica</i>	β -carotene	Cryptoxanthin, zeaxanthin	-

Note: TC—Total carotenoids; DW—Dry weight of microalgae

 β -carotene

It is the orange-red colour pigment, soluble in non-polar solvent (carbon disulfide, benzene, hexane, chloroform). Currently it is obtained from *Dunaliella salina* and *D. bardawil*

microalgae, where it is contained in a larger quantity (3-5% of the dry mass), compared to other sources [65 - 67]. Recent studies show that the β -carotene quantity produced by microalgae can be increased by modifying the cultivation conditions – high salinity, high light intensity, UV radiation, extreme temperatures and varying the nutrient content of the environment [28, 66, 67]. Researchers have determined that with modifying the cultivation conditions, *Dunaliella salina* can accumulate up to 10 - 14% of β -carotene in dry mass [27]. Both *cis*- and *trans*- forms of β -carotene, with a high bioavailability and bio efficiency [68] as well as oxygenated carotenoids (xanthophylls) [28] are contained in the *Dunaliella* species. *Spirulina* species accumulate 0.8–1.0% of β -carotene dry mass and *Rhodophyta* accumulate α and β -carotene and their hydroxylated derivatives [65].

The health benefits of the β -carotene derived from microalgae have been proved [41]. The natural form of β -carotene obtained from microalgae is easily assimilated by the body, has higher bio efficiency and has no adverse effects as compared to a synthetic form [69, 70]. Some researchers claim that the natural sources contain only one or two types of carotenoids in low concentrations and that they do not meet all the requirements [12]. Nevertheless, microalgae contain different carotenoids in high concentrations with a broad applicability. The purified β -carotene extract of *D. salina*, for example, is accompanied by other carotenoids with pronounced beneficial effects, in particular: lutein, neoxanthin, zeaxanthin, violaxanthin, cryptoxanthin and α -carotene Table 4. Research has shown the adverse effects of synthetically obtained β -carotene, which administered in high pharmacologic doses (30mg) for a long period of time, increase the probability of lung cancer in smokers. The reason might be β -carotene's tendency to form apocarotenal by oxidative cleavage, suspected of causing cancer [71].

Research has shown that the administration of β -carotene from *Dunaliella* microalgae inhibits the oxidation of low-density lipoprotein (*LDL*) and influences plasma triglycerides, cholesterol and high-density lipoprotein (*HDL*) levels [16, 17, 72], prevents atherosclerosis, protects the cells from oxidative stress [73], boosts the immunity [74], prevents cancer, macular degeneration, asthma and other degenerative diseases [6, 19, 75]. β -carotene and other carotenoids, such as phytoene and phytofluene, from *Dunaliella*, provide health benefits through antioxidant effects, photoprotection against the UV radiation, prevention of premature aging and other disorders [27, 29]. It was proved that the oral intake of β -carotene from *Dunaliella spp.* can prevent UV-induced erythema in humans [76].

The fields of application of carotenoids derived from microalgae are diverse, β -carotene being one of the most important carotenoids, which besides the pronounced antioxidant properties, when in the human body, converts into two molecules of vitamin A [41]. It is included in multi-vitamin complexes and other supplements. Oily, purified extracts of carotenoids from microalgae are sold in containers or in capsules [64]. Due to its antioxidant and photoprotective properties, along the suppressing of the aging effect the UV radiation has on the skin, microalgae derived β -carotene is largely used in the cosmetic industry, in creams, skin care lotions, hair care and as a natural dye [77]. Dry microalgae biomass and β -carotene enriched extracts are used to feed animals, cattle, poultry, fish, shellfish, etc. Microalgae is behind the color of the aquatic organisms (salmon, shellfish) and the egg yolk [5, 8, 12].

Nowadays, the commercialized β -carotene, used in pharmaceutical and food industries is chemically synthesized. β -carotene is the most common colorant and natural

food additive, with E number *E160a*, used to increase the appeal of foods, beverages, dairy, bakery, confectionery, spices, etc. [3, 9, 16].

Astaxanthin

Keto-carotenoid, a red-orange pigment, lipid-soluble, with a major content in the freshwater microalgae *Haematococcus pluvialis*, with a 4-6% of its dry matter [78,79]. This keto-carotenoid has a higher degree of stability. Astaxanthin is largely contained in the thick-walled *Haematococcus* alanospore cells and to make it bioavailable, the cell wall has to be destroyed [35, 36].

Cultivating *H. pluvialis* species outdoors may lead to water contamination with other microorganisms; therefore, researchers prefer to use photobioreactors [17]. *Chlorella zofingiensis* microalgae, under stress conditions (light, radiation, nitrogen limitation) synthesize astaxanthin, but to a lesser extent than *Haematococcus* [80].

Astaxanthin, promoted as a multi-benefit dietary supplement, has a 100-fold higher antioxidant activity compared to α -tocopherol, regarding the protective effects against lipid peroxidation [77, 78, 81] and a 10-fold higher compared to β -carotene as a scavenger of various reactive species, being considered the super vitamin *E* [82]. Astaxanthin is not converted to vitamin *A* in the human body so it is completely nontoxic if given orally. Besides, when antioxidant activity of various microalgae extracts was tested in Human Umbilical Vein Endothelial Cells cells, the antioxidative cell protection was almost 90 times higher with the natural astaxanthin containing esters than with the synthetic xanthophyll [83]. Astaxanthin is also an antiglycant and is able to protect proteins from glycation [84].

Research has shown that astaxanthin reduces the carcinogenic effect of aflatoxins [85], protects cells from radiation [75], prevents atherosclerosis and cardiovascular diseases [78, 81, 86]. A study carried out on humans in an age group of 25–60 years showed that 12 weeks of astaxanthin administration significantly decreased serum triglyceride levels, while significantly increasing *HDL*-cholesterol levels. However, *LDL*-cholesterol levels remained unchanged [87]. Several studies have shown the chemo preventive effect of astaxanthin and its role in fighting chronic inflammation, metabolic disorders and eye diseases [88]. Some researchers have reported that *Helicobacter pylori*-infected mice fed with astaxanthin extracted from the microalga *H. pluvialis*, showed reduced levels of gastric inflammation [89]. It has been proved that astaxanthin has an immunomodulatory effect, suppresses the development of carcinogenic cells, boosts the production of immunoglobulin and antibodies in the body [74, 82]. Several studies have reported that astaxanthin has significant anti-cancer effects on certain cancer types such as prostatic hyperplasia and prostatic cancers. Astaxanthin mainly inhibits the enzyme 5- α -reductase, which is involved in abnormal prostate growth [78]. An investigation on the differential effects of algal extracts (containing 14% astaxanthin) and synthetic astaxanthin on cancer cells in culture showed that treatment with both, algal extracts and synthetic astaxanthin, can protect cells against UVA-induced *DNA* damage [90]. In another study, the occurrence of colon cancer induced by azoxymethane in *F344* rats was significantly lower in rats fed with 500 ppm astaxanthin or canthaxanthin for 34 weeks [91]. It was also reported that both topical and oral use of astaxanthin can suppress skin hyper-pigmentation, inhibit synthesis of melanin, and improve the condition of all skin layers [92].

Astaxanthin can be used in diabetes treatment, research reports the anti-hyperglycemic effects of astaxanthin [93, 94]. Other researchers suggest that astaxanthin

may be applied in the prevention of neuronal disorders associated with age-related macular degeneration, in the prevention of diseases such as Alzheimer, Parkinson and other disorders of the nervous system [88]. Furthermore, the oxidative protection of the brain and the neuroprotective effect of astaxanthin may also be due to the fact that this carotenoid can cross the blood-brain barrier as it has been observed in rats' brain tissue and in other experimental animals [95].

Nowadays, astaxanthin is used in various fields: in aquaculture as a pigmentation source, as well as in nutraceuticals, food and animal feed industries. In the fish industry, astaxanthin is used as food for salmon, shellfish and is considered an essential vitamin for the development of the fish brood. Microalgae extracts enriched with astaxanthin are a natural source of pigments, which increase the immunity of the aquatic organisms and improve their color [96]. Using astaxanthin enriched extracts in poultry feed leads to skin and egg yolk pigmentation.

Currently, astaxanthin for aquatic organisms and animal feed is synthetically produced. The European Commission considers it food dye and it is given the E number *E161j*. The distinction between natural and synthetic astaxanthin is a matter of stereoisomerism. *H. pluvialis* produces only the (3*S*, 3'*S*) stereoisomer, while in a synthetic form, (3*R*, 3'*R*) stereoisomers are also present. Natural compounds differ from the synthetic ones in bioavailability and bio efficiency [97].

Astaxanthin is a nutraceutical with therapeutic effect. Astaxanthin represents 75% from the total extracts of carotenoids from *Haematococcus pluvialis*, sold as capsules [64]. Astaxanthin extracts are used as a natural dye in the cosmetic industry and ingredients for moisturizers, skin and hair lotions and serums due to their photoprotective properties and for slowing down the aging processes [78].

Canthaxanthin

It is the reddish-orange pigment, a lipid-soluble keto-carotenoid (also called Lucantin red). Large amounts of canthaxanthin are produced by *Coelastrella striolata* and *Chlorella zofingiensis* microalgae under salt stress and nitrogen-deprivation conditions [98, 99]. It is also contained in *Dunaliella salina* [100], *Chlorella vulgaris* and *Scenedesmus komareckii* [101] microalgae. Small quantities of canthaxanthin are also produced by *Haematococcus pluvialis* and *Botryococcus braunii* [102].

Research has shown that canthaxanthin has antioxidant, anti-inflammatory and neuroprotective properties [103]. It can be found in the egg yolk and it has the role of protecting the embryo from oxidative stress [104]. It was also reported the anti-cancer activity of canthaxanthin, this inhibiting significantly the growth of melanoma and fibrosarcoma tumor cells at a concentration of 100 mM [105]. Treatment with canthaxanthin also induced apoptosis in human colon adenocarcinoma and melanoma cells lines in a dose- and time-dependent manner [106]. The effects of canthaxanthin on chemically induced mammary carcinogenesis in mice showed that dietary intake of canthaxanthin for three weeks prior to the induction of cancer with dimethylbenzanthracene could reduce the occurrence of cancer by 65% [107].

Canthaxanthin is associated with E number *E161g* and is approved for use as a food coloring agent in different countries, is primarily obtained through synthetic methods; it is stable at pH 2-8 and as the majority of carotenoids, it is light sensitive and oxidizes in the presence of oxygen. It is used as a feed for poultry, to render a golden color to the birds'

skin and egg yolk as well as feed for some salmon and fish species. It is also used as food dye in bakery, confectionery, beverages and meat products [3, 9].

Ingestion of canthaxanthin stimulates tanning, leaving the skin with a golden shade. If consumed in large quantities, it crystallizes in the retina and causes canthaxanthin retinopathy, the process is reversible, however [108].

Cathaxanthin was not obtained from microalgae for practical application, due to its reduced content, it is found in the form of a mixture with other carotenoids – purified carotenoid extract.

Lutein

The lipid-soluble pigment, it appears yellow at low concentrations and orange-red at high concentrations, is one of the most important carotenoids for the human being. Lutein is isomeric with zeaxanthin, differing only in the placement of one double bond Table 5. A greater quantity of lutein is synthesized under conditions of temperature variation in the *Scenedesmus almeriensis* and *Muriellopsis* species of microalgae [109, 110]. An accumulation of 0.55% of lutein in the dry biomass of *Scenedesmus almeriensis* when varying the light intensity, temperature and nutrient concentration, has been identified in some research [110]. The production rate of lutein in *Chlamydomonas zofingiensis*, *Chlorella protothecoides* and *D. salina* varies with the environment's pH [1, 5, 63].

Being one of them most important carotenoids found, lutein is essential to the macula lutea (or yellow spot) in the retina and lens of the eye, several reports indicate that dietary supplementation with lutein alone or lutein together with other nutrients can improve visual function in patients suffering from atrophic age-related macular degeneration [111].

Research has shown the therapeutical effect of lutein in treating cancer, cardiovascular diseases, in preventing the retinal degeneration, cataract and in protecting the eye against light and ultraviolet radiation [1, 5, 6].

As a food additive, lutein has the E number *E161b*, is used in the pharmaceutical industry and in producing vision supplements; as a dye in the cosmetic industry and an ingredient in moisturizers and tanning lotions. In the food industry, lutein is used both as an additive and a colorant. It is also used as a supplement in poultry feed for egg yolk coloring; also used in the fish industry and in animal feed [3, 5, 6]. Currently, lutein is obtained from the flower petals of Marigold (the genus *Calendula*), although microalgae contain 3-6 times more lutein per unit of mass [62].

Zeaxanthin

An isomer of lutein has the same colour, similar properties and manifests health benefits. It is the photoprotective pigment in plants and it is accumulated in the mutated *D. salina* microalgae [28]. *Spirulina* microalgae also accumulate zeaxanthin, but it is rapidly converted into astaxanthin [11]. In *Porphyridium cruentum*, zeaxanthin accounts for 97.4% of the total of carotenoids [12]; the unicellular *Nannochloropsis* microalgae produce fatty acids and a significant quantity of zeaxanthin, astaxanthin and canthaxanthin [112].

Zeaxanthin exhibits a pronounced antioxidant activity, and similar to lutein, protects the retina, the eye from light and UV radiation and improves the vision. In vivo studies have shown that administration of lutein-zeaxanthin for 8 weeks increases the amount of macular pigment in humans [113]. Zeaxanthin reduces the oxidative stress in the body, prevents cardiovascular diseases, cancer and has an anti-inflammatory effect [114]. Lutein,

in association with zeaxanthin (considering a daily intake of 6 mg in humans), protects tissues from free radicals and can prevent atherosclerosis, cataract, diabetic retinopathy and age-related retinal degeneration [114].

As a food additive, zeaxanthin has the E number *E161h*. It is used in the pharmaceutical industry, as a food additive, dye (yellow-red pigment). The use of zeaxanthin producing microalgae in the food of shellfish, salmon and poultry increases the quality and color of the product [5].

Fucoxanthin

It is the pigment found in diatomic microalgae and chloroplasts of brown algae. It gives the microalgae a brown or olive-green color. It was isolated for the first time from *Fucus*, *Dictyota* and *Laminaria* marine algae [115]. It accumulates in the *Phaeodactylum tricornutum* microalgae species [116]. Due to its unique structure Table 5, it exhibits pronounced antioxidant, anti-inflammatory, antidiabetic, antiphotaging and neuroprotective properties [115, 116]. Research has shown that fucoxanthin reduces the body weight and lipid levels in blood [117]. The study reports that fucoxanthin significantly decreases the serum glucose and plasma insulin levels in diabetic/obese mice and reduces hyperglycemia [118]. Moreover, it was also proved to have an anticancer effect in different types of cancer, including colon cancer and leukemia in animals [119]. As a result of the study of the effect of fucoxanthin (at 5 and 10mM concentration) on the viability of 6 types of cancerous cells, it was proved that incubation for 72 hours reduces the viability of 5 lines of cancerous cells [120]. The anti-cancer effect of fucoxanthin was much stronger compared to that of lycopene, at the same concentration. Also, after incubating the prostate cancer cell lines with fucoxanthin at a concentration of 20mM for 48 hours, the percent of apoptotic cells exceeded 30% [121]. A study to compare the effects of carotenoids such as β -carotene and astaxanthin, with those fucoxanthin on human colon cancer cells has showed that the xanthophyll carotenoid, fucoxanthin, has higher anti-cancer activity than the other carotenoids. Taken together, the study clearly showed that the fucoxanthin metabolites (halocynthiaxanthin and fucoxanthinol) have greater anti-cancer activities than fucoxanthin [119].

Another study showed that administering fucoxanthin supplements can prevent osteoporosis and rheumatoid arthritis [123].

The biological activity, the health effects and the bioavailability of fucoxanthin have only begun to be investigated. The *P. tricornutum* carotenoid extract is the main supplement with a major content of fucoxanthin, sold at the moment.

Diadinoxanthin, diatoxanthin, violaxanthin, neoxanthin, loroxanthin, etc

The listed xanthophylls, although not sufficiently studied, are of great interest to researchers. The content of xanthophylls in microalgae varies and is highly dependent on the cultivation conditions. As it was mentioned before, they are synthesized for protecting the cells from the oxidative stress and the influence of abiotic factors. Usually, microalgae accumulate several types of carotenoids, some of which are major components in biomass extracts, Table 4.

The study of the biological activity, elucidation of health benefits and practical implementation of the above mentioned xanthophylls are the main objective of research conducted in various fields.

Chlorophylls

Chlorophylls *a* and *b* are liposoluble, green pigments, present in almost all of the terrestrial and aquatic photosynthetic organisms. Chlorophyll *c* has a greenish-blue color and is more often found in seaweed while chlorophyll *d* is found in red algae and cyanobacteria. Microalgae are a rich source of chlorophyll, which is 0.5-1.5% from dry matter [124]. Several types of chlorophyll can be found in microalgae, for example *Phordium autumnale* contains both chlorophyll *a* ($2.7 \mu\text{g.g}^{-1}$) and *b* ($0.7 \mu\text{g.g}^{-1}$) [125].

Chlorophyll and its derivatives manifest beneficial health effects due to their antioxidant, anticarcinogenic, antigenotoxic and antimutagenic properties. Several studies have shown that chlorophyll is a detoxifying agent, stimulates bile secretion, improves the metabolism of proteins, carbohydrates and proteins [5, 9].

The potential of microalgae as a source of chlorophyll for food dye with a nutraceutical effect has not been fully studied, however, the semi-synthetic derivative of chlorophyll, chlorophyllin (additive *E141*), which contains copper instead of ions of magnesium (characteristic for the natural form) is used and can have adverse health effects for the human body.

Phycobiliproteins

Are hydrosoluble proteins in *Spirulina*, *Porphyridium*, *Rhodella*, *Galdieria* microalgae, in cryptophytes and glaucophyte [125 - 128]. It is a family of fluorescent proteins, highly soluble in water. From the point of view of the chemical structure, they are made of chromophores - bylines (linear tetrapyrrole prosthetic groups) covalently linked via thioether bonds to an apoprotein Table 5, capable of absorbing wavelengths between 470 and 660 nm. They have the mission to capture the light rays and pass them on to the chlorophyll during the photosynthesis process. Four groups of phycobiliproteins are known: phycoerythrin, phycoerythrocyanin, phycocyanin and allophycocyanin. The red phycobiliprotein - phycoerythrin and the blue phycobiliprotein- phycocyanin can serve as natural colorants in food, cosmetics and pharmaceuticals [127]. Currently, phycobiliproteins are used in health sectors as antioxidant, anticancer, antiviral, anti-inflammatory, anti-allergic, and neuro-protective material [5, 126, 127].

Phycoerythrin

The red *Porphyridium* microalgae are the main sources of the pinkish-red pigment - phycoerythrin [128]. These microalgae, grown in a usual aquatic environment, after three days accumulate 200mg of dye per liter of culture, with a concentration of phycoerythrin in the dye of 15%. Under optimal cultivation conditions, the phycoerythrin concentration may reach 30%. The color is stable at 60°C for 30 minutes and has a long shelf life at *pH* 6-7. It is very stable as an ingredient in dry food preparations, stored in low humidity conditions [127]. Phycoerythrin, besides the red color, has a yellow fluorescence.

This dye is not currently used as it has not been sufficiently tested, but it is known that rats fed with *Porphyridium* microalgae biomass, had a normal development, without any adverse effects.

Phycocyanin

It is one of the most accessible phycobiliprotein that has attracted most attention for its use in animal feed, foods, and health. Phycocyanin cannot be made synthetically but is synthesized in *Spirulina platensis* [126], *Porphyridium aeruginosum* and in the majority of

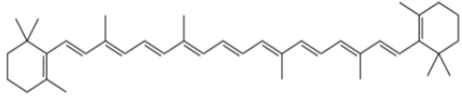
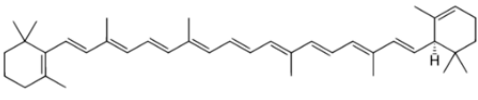
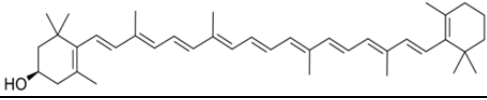
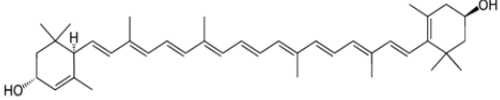
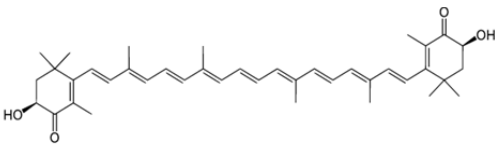
cyanobacteria. *P. aeruginosa* microalgae, for example, after 4 days of growth, accumulate 100mg of dye per liter of culture with a 60% content of phycocyanin. *P. aeruginosa* microalgae extract has a blue color and a red fluorescence [127, 128], which, with the change of the environment's pH, doesn't change and it is light-resistant but sensitive to the heat.

The phycocyanobilin groups are nutraceuticals which provide antioxidant and radical scavenging activity. Potential health effects related to phycocyanin include anti-inflammatory effects, anti-platelet aggregation, anti-carcinogenic effects, prevention of cholesterol-induced atherosclerosis, kainic acid-induced neural damage, kidney stone formation, thioacetamide-induced hepatic encephalopathy [126, 127].

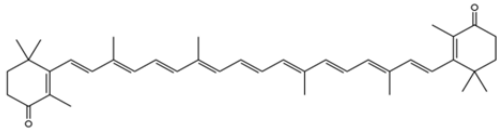
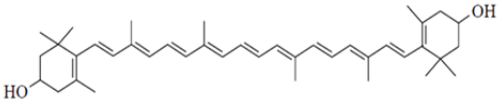
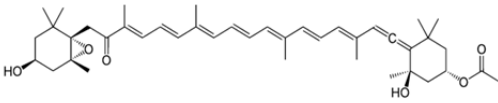
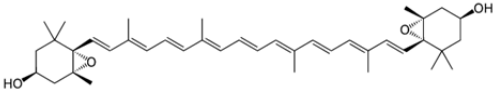
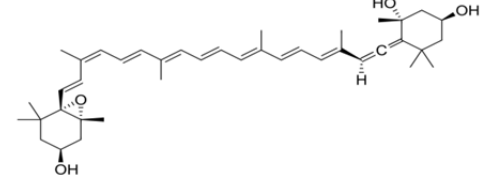
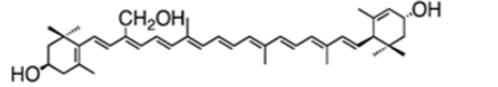
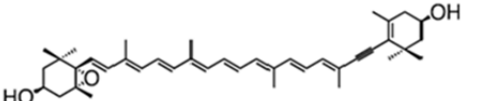
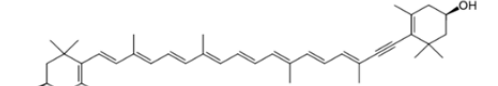
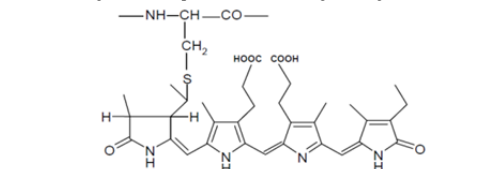
Nowadays, phycocyanin is obtained from *S. platensis* microalgae and is applied as food dye in the United States of America to confer color to sweets, desserts, beverages, fermented dairy products, etc. [64].

Within the European Union, the phycocyanin enriched *Spirulina platensis* extract is allowed to be used as a food dye.

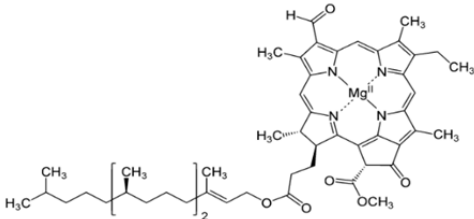
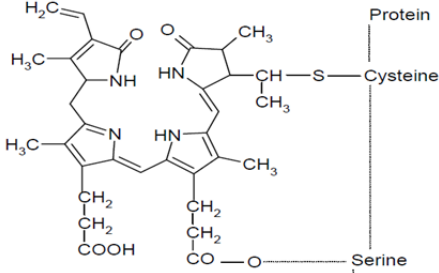
Table 5

Pigments from microalgae		
Carotenoids	Microalgae strains	References
<p><i>β-carotene</i></p> 	<p><i>Dunaliella sp.</i>: <i>D. salina</i>, <i>D. bardawil</i>, <i>D. tertiolecta</i>, <i>Haematococcus pluvialis</i>, <i>Scenedesmus almeriensis</i>, <i>Spirulina sp.</i>, <i>Chlorella sp.</i>, <i>Chlorococcum sp.</i>, <i>Chlamydocapsa sp.</i>, <i>Tetraselmis sp.</i></p>	<p>[11-13,18, 65-67]</p>
<p><i>α-carotene</i></p> 	<p><i>Chlorella sorokiniana</i>, <i>Chlorococcum humicola</i></p>	<p>[1,5,9,11,12]</p>
<p><i>β-cryptoxanthin</i></p> 	<p><i>Spirulina pacifica</i></p>	<p>[1,5,9,13,16]</p>
<p>Lutein</p> 	<p><i>Botryococcus braunii</i>, <i>Chlorococcum sp.</i>, <i>Chlamydocapsa sp.</i>, <i>Chlorella sp.</i>: <i>C. acidophila</i>, <i>C. fusa</i>, <i>C. protothecoides</i>, <i>C. pyrenoidosa</i>, <i>C. sorokiniana</i></p>	<p>[1,17,18,63, 109,110]</p>
<p>Astaxanthin</p> 	<p><i>Haematococcus sp.</i>, <i>Chlorella sp.</i>, <i>Coelastrella striolata</i>, <i>Monoraphidium sp.</i>, <i>Chlorococcum sp.</i>, <i>Chlamydocapsa sp.</i>, <i>Neosporangiococcum sp.</i></p>	<p>[12,78-80]</p>

Continuation Table 5

<p style="text-align: center;">Cantaxanthin</p> 	<p><i>Chlorella</i> spp., <i>Coelastrella striolata</i>, <i>Chlorococcum</i> sp., <i>Chlamydocapsa</i> sp., <i>Scenedesmus komareckii</i>, <i>Haematococcus lacustris</i>, <i>Neosporangiococcum</i> sp.</p>	<p>[2,3,98-102]</p>
<p style="text-align: center;">Zeaxanthin</p> 	<p><i>Scenedesmus almeriensis</i>, <i>Nannochloropsis oculata</i>, <i>Chlorella ellipsoidea</i>, <i>Chlorella nivalis</i>, <i>Dunaliella salina</i>, <i>Spirulina pacifica</i>.</p>	<p>[11,13,16,28, 65,112]</p>
<p style="text-align: center;">Fucoxanthin</p> 	<p><i>Phaeodactylum tricornutum</i>, <i>Chaetoceros gracilis</i> sp., <i>Odontella aurita</i>, <i>Cylindrotheca closterium</i>, <i>Nitzschia</i> sp., <i>Ochromonas</i> sp., <i>Sarcinochrysis marina</i>, <i>Isochrysis</i> sp., <i>Corallina officinalis</i>, <i>C. elongata</i></p>	<p>[12,17,18, 114,116]</p>
<p style="text-align: center;">Violaxanthin</p> 	<p><i>Chlorella ellipsoidea</i>, <i>Phaeophyceae</i>, <i>Chlorococcum humicola</i>, <i>Dunaliella salina</i>, <i>Oedogonium intermedium</i></p>	<p>[5,9,12-18]</p>
<p style="text-align: center;">Neoxanthin</p> 	<p><i>Dunaliella salina</i>, <i>Oedogonium intermedium</i>, <i>Chlamydomonadales</i> (Chlorophyta)</p>	<p>[11,13,65-67]</p>
<p style="text-align: center;">Loroxanthin</p> 	<p><i>Oedogonium intermedium</i>, <i>Euglenia sanguinea</i></p>	<p>[131,132]</p>
<p style="text-align: center;">Diadinoxanthin</p> 	<p><i>Euglenia sanguinea</i>, <i>Phaeodactylum tricornutum</i></p>	<p>[132,133]</p>
<p style="text-align: center;">Diatoxanthin</p> 	<p><i>Euglenia sanguinea</i>, <i>Phaeodactylum tricornutum</i></p>	<p>[132,133]</p>
<p style="text-align: center;">Phycobiliprotein-Phycocyanin</p> 	<p><i>Spirulina</i> sp., <i>Arthrospira platensis</i>, <i>Rhodella</i>, <i>Galdieria</i>, <i>cryptophyta</i> and <i>glaucoophyta</i></p>	<p>[5,63,126-128]</p>

Continuation Table 5

<p style="text-align: center;">Chlorophylls</p> 	<p style="text-align: center;">Formed by photosynthesis in most microalgae</p>	<p style="text-align: center;">[1,9,124,125]</p>
<p style="text-align: center;">Phycobiliprotein -Phycocerythrin</p> 	<p style="text-align: center;"><i>Porphyridium sp., Agardhiella subulata, Polysiphonia morrowii</i></p>	<p style="text-align: center;">[126-128]</p>

Taking into consideration the beneficial health effects of the natural phycobiliproteins pigments, or of the phycoerythrin or phycocyanin enriched microalgae extracts, studying the biological activity, elaborating methods of obtaining, solving the technological requirements and implementing these dyes in real life are the major objectives for researchers from various fields, among which, the food industry as well.

Conclusions

Microalgae are a promising source of bioactive ingredients for producing functional food, increasingly used for their content of proteins, essential amino acids, unsaturated fatty acids, pigments, vitamins, polysaccharides, minerals, etc. In the last decades, microalgae biomass and phytonutrients enriched extracts are used not only as pills, capsules or powders, but also used for enriching pasta, bakery, meat and confectionery products, sweets, beverages, dairy, protein drinks and baby food [26].

Microalgae are also an excellent source of food for fish and aquatic organisms, animals, cattle, swine, poultry, etc. Pigments accumulated in microalgae have beneficial health effects and they could replace the chemically synthesized food dyes.

The synthetic sources of food dyes are substances of petrochemical origin, organic acids and inorganic substances. Today, the majority of the food dyes are synthetically produced; their impact on the human health is often a negative one, with various side-effects [134]. The carotenoids obtained from microalgae are easily digested by the body, have a high bioavailability and no side-effects if compared to their synthetic alternatives [69 - 71, 97]. Taking all the things above into consideration, elaborating methods of obtaining pigments and other bioactive substances from nontraditional sources, such as microalgae, and improving the existing ones, obtaining and establishing the chemical structure of the new compounds, studying their biological activity, solving the technological requirements regarding the optimization and application of phytonutrients in food production, are objectives drawing more and more attention.

Moreover, microalgae as renewable sources of biologically active substances have not been fully explored, less than 40 strains being exploited today, thus the potential of thousands of species remaining undiscovered[11, 13, 17].

References

1. Sathasivam R., Radhakrishnan A. Hashem, E.F. ABD Allah. Microalgae metabolites: a rich source for food and medicine. In: *Saudi Journal of Biological Sciences*, 2019, 26, pp.709-722. <http://dx.doi.org/10.1016/j.sjbs>.
2. Morais M. G., Bruna S. V., E. G. Morais A. V. Costa. Biologically Active Metabolites Synthesized by Microalgae. In: *BioMed Research International*, 2015, Article ID 835761, pp.1-15.
3. Niccolai A., Chini Zittelli G., Rodolfi L., Biondi N., Tredici M. Microalgae of interest as food source: Biochemical composition and digestibility. In: *Algal Research*, 2019, 42, pp.1-9.
4. Saini D. K., Pabbi S., Shukla P. Cyanobacterial pigments: Perspectives and biotechnological approaches. In: *Food and Chemical Toxicology*, 2018, 120, pp. 616–624.
5. Spolaore P., Joannis-Cassan C., Duran E., Isambert A. Review: Commercial applications of microalgae. In: *Journal of Bioscience and Bioengineering*, 2006, 101, pp. 87–96.
6. Suganya T., Varman M., Masjuki H.H., Renganathan S. Macroalgae as a potential source for commercial applications along with biofuels production: A biorefinery approach. In: *Renewable and Sustainable Energy Reviews*, 2016, 55, pp. 909-941.
7. Becker E.W. Microalgae as a source of protein. In: *Biotechnology Advances*, 2007, 25 (2), pp. 207–210.
8. Becker W. Microalgae in human and animal nutrition. In: Richmond, A., ed. *Microalgal Culture*. Handbook, Blackwell, Oxford, 2004, 8, pp. 312–351.
9. Apurav K. K., Kit Wayne C., Krishnamoorthy R., Yang T., DINH-TOI C. E Pau-Loke, S., Microalgae: A potential alternative to health supplementation for humans. In: *Food Science and Human Wellness*. 2019, 8, pp. 16–24.
10. Liang S., Liu X., Chen F., Chen Z. Current microalgal health food R & D activities in China. In: Ang P.O., ed. *Asian Pacific Phycology*. 21st CenturyProspect. Challenges, Springer, Netherlands, Dordrecht, 2004, pp. 45–48.
11. Ambati, R. R., Gogisetty D., Aswathanarayana R.G., Ravi S., Bikkina P.N, BO, L., Yuepeng S. Industrial potential of carotenoid pigments from microalgae: Current trends and future prospects. *Critical Reviews*. In: *Food Science and Nutrition*, 2018, pp.1–22.
12. Raposo M.F.J De Morais A.M.M.B., De Morais R.M.S.C. Carotenoids from marine microalgae: A valuable natural source for the prevention of chronic diseases. In: *Marine Drugs*, 2015, 13, pp. 5128–5155.
13. Pulz O., Wolfgang G. Valuable products from biotechnology of microalgae. In: *Applied Microbiology and Biotechnology*, 2004, 65, pp. 635–648.
14. Wang B., Li Y., Wu N., Lan C.Q. CO₂ bio-mitigation using microalgae, *Applied Microbiology and Biotechnology*, 2008, 79, pp. 707–718. <http://dx.doi.org/10.1007/s00253-008-1518-y>.
15. Wehr J.D. Algae: anatomy, biochemistry, and biotechnology. In: *Journal of Phycology*, 2007, 43, pp. 412-414. <http://dx.doi.org/10.1111/j.1529-8817.2007.00335.x>.
16. Bech-Larsen T., Grunert K., The perceived healthiness of functional foods. A conjoint study of Danish, Finnish and American consumers perception of functional foods. In: *Appetite*, 2003, 40 (1), pp.9-14.
17. Varfolomeev S.D., Wasserman L.A. Microalgae as source of biofuel, food, fodder and medicine. *Applied Biochemistry and Microbiology*, 2011, 47, pp. 789-807.
18. Arad (Malis) S., & Yaron A. Natural pigments from red microalgae for use in foods and cosmetics. In: *Trends in Food Science and Technology*, 1992, 3, pp. 92–96.
19. Yukino T., Hayashi M., Inoue Y., Imamura J., Nagano N., Murata H. Preparation of docosahexaenoic acid fortified *Spirulina platensis* and its lipid and fatty acid compositions. In: *Nippon Suisan Gakkaishi*, 2005, 71, pp. 74–79.
20. Vismara R., Vestir S., Kusmic C., Barsanti L., Gualtieri P. Natural vitamin E enrichment of *Artemia salina* red freshwater and marine microalgae. In: *Journal of Applied Phycology*, 2003, 15, pp. 75–80.
21. Capelli B., Cysewski G.R. Potential health benefits of spirulina microalgae. In: *Nutrafoods*, 2010, 9, pp. 19–26. <http://dx.doi.org/10.1007/BF03223332>.
22. Christaki E., Florou-Paneri P., Bonos E. Microalgae: a novel ingredient in nutrition. In: *International Journal of Food Science and Nutrition*, 2011, 62, pp. 794–799. <http://dx.doi.org/10.3109/09637486.2011.582460>.
23. BLEAKLEY, S., HAYES, M. Algal proteins: extraction, application, and challenges concerning production. In: *Foods*, 2017, 6 (5), pp. 1–33. <http://dx.doi.org/10.3390/foods6050033>.
24. Fabregas J., Herrero C. Vitamin content of four marine microalgae. Potential use as source of vitamins in nutrition. In: *Journal of Industrial Microbiology*, 1990, 5, pp. 259–263. <http://dx.doi.org/10.1007/BF01569683>.
25. Borowitzka M.A. Algae as Food. In: Brian JB Wood, ed. *Microbiology of Fermented Foods*, 1998, New York, Springer Science.
26. EU *Novel food catalogue*. Disponibil: https://ec.europa.eu/food/safety/novel_food/catalogue/search/public/index.cfm
27. Xu Y., Ibrahim I.M., Wosu C.I., Ben-Amotz A., Harvey P.J. 2018. Potential of new isolates of *Dunaliella salina* for natural b-carotene production. In: *Biology*, 2018, 7(1), pp.1-14. <http://dx.doi.org/10.3390/biology7010014>.
28. Sathasivam R., Juntawong N., 2013. Modified medium for enhanced growth of *Dunaliella* strains. In: *International Journal of Current Science*, 2013, 5, pp. 67–73.
29. Ben-Amotz A., Mordhay A. Glycerol, β -carotene, and Dry Algae Meal Production by Commercial Cultivation of *Dunaliella*. In: Shelef G., Soeder C., ed. *Algae Biomass*, Oxford: Elsevier North-Holland Biomedical Press, 1980.

30. Liu Z. W., Zeng X.A., Cheng J.H., Liu D.B., Aadil R.M. The efficiency and comparison of novel techniques for cell wall disruption in astaxanthin extraction from *Haematococcus pluvialis*. In: *International Journal of Food Science & Technology*, 2018, 53, pp. 2012–2019. doi: 10.1111/ijfs.13810.
31. Kim S.M., Kang S.W., Kwon O.N., Chung D., Pan C.H. Fucoxanthin as a major carotenoid in *Isochrysis aff. galbana*: Characterization of extraction for commercial application. In: *Journal of Korean Society of Applied Biological Chemistry*, 2012, 55, pp. 477–483.
32. Thoisen C., Hansen B.W., Nielsen S.L. A simple and fast method for extraction and quantification of cryptophytes phycoerythrin. In: *MethodsX*, 2017, 4, pp. 209–13.
33. Chakdar H., Pabbi S. Extraction and purification of phycoerythrin from *Anabaena variabilis* (CCC421). In: *Phykos*, 2012, 42 (1), pp.25–31.
34. Sonani R.R., Rastogi R.P., Patel R., Madamwar D. Recent advances in production and application of pycobiliproteins. In: *World Journal of Biological Chemistry*, 2016, 7(1), pp.100-109.
35. Chew K.W., Yap J.Y., Show P.L., Suan N.H., Juan J.C., Ling T.C., Lee D.-J., Chang J.S. Microalgae biorefinery: high value products perspectives. In: *Bioresource Technology*, 2017, 229, pp. 53–62.
36. Saini R.K., Keum Y.S. Carotenoid extraction methods: A review of recent developments. In: *Food Chemistry*, 2018, 240, pp. 90-103.
37. Yabuzaki J. Carotenoids Database: structures, chemical fingerprints and distribution among organisms. Database, 2017, 1. Disponibil: <http://carotenoiddb.jp>, doi:10.1093/database/bax004.
38. Moran N. A., Jarvik T. Lateral transfer of genes from fungi underlies carotenoid production in aphids. In: *Science*, 2010, 328, (5978), pp. 624–627. <http://dx.doi.org/10.1126/science.1187113>.
39. Armstrong G.A., Hearst J.E. Genetics and molecular biology of carotenoid pigment biosynthesis. In: *FASEB Journal*, 1996, 10, pp. 228–237.
40. Eldahshan O.A., Singab A.N.B. Carotenoids. In: *Journal of Pharmacognosy and Phytochemistry*, 2013, 2, pp. 225–234.
41. Shete V., Quadro L. Mammalian metabolism of β -carotene: gaps in knowledge. In: *Nutrients*, 2013, 5, pp. 4849–4868. DOI: 10.3390/nu5124849.
42. Rao A.V., Agarwal S. Role of lycopene as antioxidant carotenoid in the prevention of chronic diseases: a review. In: *Nutrition Research*, 1999, 19, pp. 305–323.
43. Mittal M., Siddiqui M.R., Tran K., Reddy S.P., Malik A.B. Reactive oxygen species in inflammation and tissue injury. In: *Antioxidants & Redox Signaling*, 2014, 20, pp. 1126–1167. DOI: 10.1089/ars.2012.5149.
44. Pham-Huy L.A., He H., Pham-Huy C. Free radicals, antioxidants in disease and health. In: *International Journal of Biomedical Science*, 2008, 4, pp. 89–96.
45. Nimse S.B., Pal D. Free radicals, natural antioxidants, and their reaction mechanisms. In: *RSC Advances*, 2015, 5, 27986. DOI: 10.1039/c4ra13315c
46. Kopsell D.A., Kopsell D.E. Accumulation and bioavailability of dietary carotenoids in vegetable crops. In: *Trends in Plant Science*, 2006, 11, pp. 499–507.
47. YOUNG, I.S., WOODSIDE, J.V. Antioxidants in health and disease. In: *Journal of Clinical Pathology*, 2001, 54, pp. 176–186. DOI: 10.1136/jcp.54.3.176
48. Griffiths K., Aggarwal B., Singh R., Buttar H., Wilson D., De Meester F. Food antioxidants and their anti-inflammatory properties: A potential role in cardiovascular diseases and cancer prevention. Can In: *Disease*, 2016, 4, 28p. [CrossRef], doi: 10.3390/diseases4030028.
49. Gong X., Marisiddaiah R., Zaripheh S., Wiener D., Rubin L.P. Mitochondrial β -carotene 9',10' oxygenase modulates prostate cancer growth via NF- κ B inhibition: a lycopene independent function. In: *Molecular Cancer Research*, 2016, 14, pp. 966–975. DOI: 10.1158/1541-7786.MCR-16-0075
50. Huang X., Gao Y., Zhi X., Ta N., Jiang H., Zheng J. Association between vitamin A, retinol and carotenoid intake and pancreatic cancer risk: evidence from epidemiologic studies. In: *Scientific Reports*, 2016, 6. Published online 2016 Dec 12. doi: 10.1038/srep38936.
51. Von Lintig J. Provitamin A metabolism and functions in mammalian biology. In: *The American Journal of Clinical Nutrition*, 2012, 96, pp.1234–1244. DOI: 10.3945/ajcn.112.034629
52. Tso M., Lam T. Method of Retarding and Ameliorating Central Nervous System and Eye Damage. *USA Patent, No. 5527533*, 1996.
53. Castro-Puyana M. at all. Pressurized liquid extraction of *Neochloris oleoabundans* for the recovery of bioactive carotenoids with anti-proliferative activity against human colon cancer cells. In: *Food Research International*, 2017, 99 (3), pp. 1048-1055. Disponibil: <https://doi.org/10.1016/j.foodres.2016.05.021>.
54. Kim Y.S., Kim E., Park Y.J., Kim Y. Retinoic acid receptor β enhanced the anti-cancer stem cells effect of β -carotene by down-regulating expression of delta-like 1 homologue in human neuroblastoma cells. In: *Biochemical and Biophysical Research Communications*, 2016, 480, pp. 254–260. DOI: 10.1016/j.bbrc.2016.10.041.
55. Tapiero H., Townsend D.M., Tew K.D. The role of carotenoids in the prevention of human pathologies. In: *Biomedicine & Pharmacotherapy*, 2004, 58, pp.100–110.
56. Milani A., Basirnejad M., Shahbazi S., Bolhassani A. Carotenoids: biochemistry, pharmacology and treatment. In: *British Journal of Pharmacology*, 2016. Disponibil: <http://onlinelibrary.wiley.com/doi/10.1111/bph.v174.11/issuetoc>.
57. Touvier M., Kesse E., Clavel-Chapelon F., Boutron-Ruault M.C. Dual association of betacarotene with the risk of tobacco-related cancers in a cohort of French women. In: *Journal of the National Cancer Institut*, 2005, 97, pp. 1338–1344. DOI: 10.1093/jnci/dji276

58. Stahl W., Sies H. Carotenoids and flavonoids contribute to nutritional protection against skin damage from sunlight. *Molecular Biotechnology*, 2007, 37, pp. 26–30. DOI: 10.1007/s12033-007-0051-z.
59. Jahns P., Latowski D., Strzalka K. Mechanism and regulation of the violaxanthin cycle: The role of antenna proteins and membrane lipids. In: *Biochimica et Biophysica Acta-Bioenergetics*, 2009, 1787, pp. 3–14. [CrossRef] [PubMed].
60. Rodrigues D.B., Menezes C.R., Mercadante A.Z., Jacob-Lopes E., Zepka L.Q. Bioactive pigments from microalgae *Phormidium autumnale*. In: *Food Research International*, 2015, 77, pp. 273–279. <http://dx.doi.org/10.1016/j.foodres.2015.04.027>.
61. Matsukawa R., Hotta M., Masuda Y., Chihara M., Karube I. Antioxidants from carbon dioxide fixing *Chlorella sorokiniana*. In: *Journal of Applied Phycology*, 2000, 12, pp. 263–267.
62. Lin J.H., Lee D.J., Chang J.S. Lutein production from biomass: Marigold flowers versus microalgae. In: *Bioresources Technology*, 2015, 184, pp. 421–428. [CrossRef] [PubMed].
63. Del Campo J.A., Rodríguez H., Moreno J., Vargas M.A., RIVAS, J., GUERRERO, M.G. Accumulation of astaxanthin and lutein in *Chlorella zofingiensis* (Chlorophyta). In: *Applied Microbiology and Biotechnology*, 2004, 64, pp. 848–854.
64. Dufosse L., Galaupa P., Yaronb A., Malis Aradb S. et al. Microorganisms and microalgae as sources of pigments for food use: a scientific oddity or an industrial reality? / Trends 390. In: *Food Science & Technology*, 2005, 16, pp. 389–406.
65. Borowitzka L.J., Borowitzka M.A. β -Carotene (Provitamin A) production with algae. In: Erick J. Vandamme, ed. *Biotechnology of Vitamins, Pigments and Growth Factors*. London: Elsevier Applied Science, 1989.
66. Jahnke L. S. Massive carotenoid accumulation on *Dunaliella bardawil* induced by ultraviolet-A radiation. In: *Journal of Photochemistry and Photobiology, B: Biology*, 1999, 48, pp. 68–74.
67. Ben-Amotz A., Production of b-carotene and vitamin by the halotolerant algae *Dunaliella*. In: Ahaway, A., Zabrosky, O., ed. *Marine Biotechnology*. Plenum Press, New York, 1993, pp. 411–417.
68. Yeum K. J., Russel R. M. Carotenoids bioavailability and bioconversion. In: *Annual Review of Nutrition*, 2002, 22, pp. 483–504.
69. Olson J. A., & Krinsky N. I. Introduction. The colorful, fascinating world of the carotenoids: Important physiologic modulators. In: *FASEB Journal*, 1995, 9, pp. 1547–1550.
70. Ben-Amotz A., Levy Y. Bioavailability of natural isomers mixture compared with synthetic all-trans β -carotene in human serum. In: *American Journal of Clinical Nutrition*, 1996, 63, pp. 729–734.
71. Russel R.M. Beta-carotene and lung cancer". In: *Pure and Applied Chemistry*, 2002, 74 (8), pp. 1461–1467.
72. Burton G.W., Ingold, K.U. β -Carotene: An unusual type of lipid antioxidant. In: *Science*, 1984, 224, pp. 569–573.
73. Kikugawa K., Hiramoto K., Tomiyama S., Assano Y. β -Carotene effectively scavenges toxic nitrogen dioxide and peroxyntrous acid. In: *FEBS Letters*, 1997, 404, pp. 175–178.
74. Jyonouchi H., Hill R. J., Tomita Y., & Good R. A. Studies of immunomodulating actions of carotenoids. I. Effects of b-carotene and astaxanthin on murine lymphocyte functions and cell surface marker expression in in vitro culture system. In: *Nutrition and Cancer*, 1991, 19, pp. 93–105.
75. Savoure N., Briand G., Amory-Touz M. C., Combre A., Maudet M., & Nicol M. Vitamin A status and metabolism of cutaneous polyamines in the hairless mouse after UV irradiation: Action of b-carotene and astaxanthin. In: *International Journal for Vitamin and Nutrition Research*, 1995, 65, pp.79–86.
76. Heinrich U., Gartner C., Wiebusch M., Eichler O., Sies H., Tronnier H., Stahl W., Supplementation with beta-carotene or a similar amount of mixed carotenoids protects humans from UV-induced erythema. In: *Journal of Nutrition*, 2003, 133, pp. 98–101.
77. Stahl W., Sies H. Carotenoids and flavonoids contribute to nutritional protection against skin damage from sunlight. In: *Molecular Biotechnology*, 2007, 37, pp. 26–30. DOI: 10.1007/s12033.
78. Guerin M.E., Huntley M., Olaiola M. Haematococcus astaxanthin : applications for human health and nutrition. In: *Trends of Biotechnology*, 2003, 21, pp. 210–216. Disponibil: [http://dx.doi.org/10.1016/S0167-7799\(03\)00078-7](http://dx.doi.org/10.1016/S0167-7799(03)00078-7).
79. Lorenz R.T., Cysewski G.R. Commercial potential for Haematococcus microalgae as a natural source of astaxanthin. In: *Trends of Biotechnology*, 2000, 18, pp. 160–167.
80. Pelah D., Sintov A., Cohen E. The effect of salt stress on the production of canthaxanthin and astaxanthin by *Chlorella zofingiensis* grown under limited light intensity. In: *World Journal of Microbiology and Biotechnology*, 2004, 20, pp. 483–486.
81. Park J.S., Chyun J.H., Kim Y.K., Line L.L., Chew B.P. Astaxanthin decreased oxidative stress and inflammation and enhanced immune response in humans, In: *Nutrition & Metabolism*, 2010, 7 (18), pp. 1-10. Disponibil: <https://nutritionandmetabolism.biomedcentral.com/track/pdf/10.1186/1743-7075-7-18>.
82. Jyonouchi H., Sun S., Gross M. Effect of carotenoids on in vitro immunoglobulin production by human peripheral blood mononuclear cells: Astaxanthin, a carotenoid without vitamin a activity, enhances in vitro immunoglobulin production in response to a t-dependent stimulant and antigen. In: *Nutrition and Cancer*, 1994, 23(2), pp. 171–183.
83. Régnier P., Bastias J., Rodriguez-Ruiz V., Caballero-Casero N., Caballo C., Sicilia D., Fuentes A., Maire M., Crepin M., Letourneur D. Astaxanthin from *Haematococcus pluvialis* prevents oxidative stress on human endothelial cells without toxicity. In: *Marines Drugs*, 2015, 13(5), 2857–2874.

84. Sun Z., Liu J. Bl., Y.-H., Zhou Z.-G. Microalgae as the production platform for carotenoids. In *Recent Advances in Microalgal Biotechnology*; Liu, J., Sun, Z., Gerken, H., ed. *Omics Group eBooks*: Foster City, CA, USA, 2014, pp. 1–17.
85. Kobayashi M., Sakamoto Y. Singlet oxygen quenching ability of astaxanthin esters from the green alga *Haematococcus pluvialis*. In: *Biotechnology Letters*, 1999, 21, pp. 265–269.
86. Miki W. Biological functions and activities of animal carotenoids. In: *Pure and Applied Chemistry*, 1991, 63(1), pp. 141–146.
87. Yoshida H., Yanai H., Ito K., Tomono Y., Koikeda T., Tsukahara H., Tada N. Administration of natural astaxanthin increases serum HDL-cholesterol and adiponectin in subjects with mild hyperlipidemia. In: *Atherosclerosis*, 2010, 209, pp. 520–523.
88. Yuan J.P., Peng J., Yin K., Wang J.H. Potential health-promoting effects of astaxanthin: a high-value carotenoid mostly from microalgae. In: *Molecular Nutrition & Food Research*, 2011, 55, pp. 150–165.
89. Bennedsen M., Wang X., Willen R., Wadstrom T., Andersen L.P. Treatment of *H. pylori* infected mice with antioxidant astaxanthin reduces gastric inflammation, bacterial load and modulates cytokine release by splenocytes. In: *Immunology letters*, 1999, 70(3), pp. 185–189.
90. Lyons N.M., O'brien N.M. Modulatory effects of an algal extract containing astaxanthin on UVA-irradiated cells in culture. In: *Journal of Dermatological Science*, 2002, 30(1), pp. 73–84.
91. Tanaka T., Kawamori T., Ohnishi M., Makita H., Mori H., Satoh K., Hara A. Suppression of azoxymethane-induced rat colon carcinogenesis by dietary administration of naturally occurring xanthophylls astaxanthin and canthaxanthin during the postinitiation phase. In: *Carcinogenesis*, 1995, 16(12), pp. 2957–2963.
92. Tominaga K., Hongo N., Karato M., Yamashita E. Cosmetic benefits of astaxanthin on humans subjects. In: *Acta Biochimica Polonica*, 2012, 59 (1), pp. 43–47.
93. Xu L., Zhu J., Yin W., Ding X. Astaxanthin improves cognitive deficits from oxidative stress, nitric oxide synthase and inflammation through upregulation of PI3K/Akt in diabetes rat. In: *International journal of clinical and experimental pathology*, 2015, 8(6), pp. 6083–6094.
94. Sila A., Ghlissi Z., Kamoun Z., Makni M., Nasri M., Bougateg A., Sahnoun Z. Astaxanthin from shrimp by-products ameliorates nephropathy in diabetic rats. In: *European Journal of Nutrition*, 2015, 54, pp. 301–307.
95. Hussein G., Nakamura M., Zhao Q., Iguchi T., Goto H., Sankawa U., Watanabe H. Antihypertensive and neuroprotective effects of astaxanthin experimental animals. In: *Biological & pharmaceutical bulletin*, 2005, 28 (1), pp. 47–52.
96. Christiansen R., Lie O., Torrissen O. J. Growth and survival of Atlantic salmon, *Salmo salar* L, fed different dietary levels of astaxanthin. First-feeding fry. In: *Aquaculture Nutrition*, 1995, 1(3), pp. 189–198.
97. Grung M., D'souza F.M.L., Borowitzka M., Liaaen-Jensen S. Algal carotenoids 51. Secondary carotenoids 2. *Haematococcus pluvialis* aplanospores as a source of (3S,3'S)-astaxanthin esters. In: *Journal of Applied Phycology*, 1992, 4, pp. 165–171
98. Pelah D., Sintov A., Cohen E. The effect of salt stress on the production of canthaxanthin and astaxanthin by *Chlorella zofingiensis* grown under limited light intensity. In: *World Journal of Microbiology and Biotechnology*, 2004, 20, pp. 483–486.
99. Abe K., Hattori H., Hirano M. Accumulation and antioxidant activity of secondary carotenoids in the aerial microalga *Coelastrella striolata* var. microalga *Coelastrella striolata* var. multistriata. In: *Food Chemistry*, 2007, 100 (2), pp. 656–661.
100. Borowitzka M.A., Huisman J.M., The ecology of *Dunaliella salina* (Chlorophyceae, Volvocales)-effect of environmental conditions on aplanospore formation. In: *Botanica Marina*, 1993, 36, pp. 233–243.
101. Hanagata N. Secondary carotenoid accumulation in *Scenedemus komarekii* (Chlorophyceae, Chlorophyta, In: *Journal of Phycology*, 1999, 35(5), pp. 960 - 966.
102. Grung M., Metzger P., Liaaen-Jensen S. Algal carotenoids 53; secondary carotenoids of algae 4; secondary carotenoids in the green alga *Botryococcus braunii*, race L, new strain. In: *Biochemical Systematics and Ecology*, 1994, 22(1), pp. 25-29.
103. Chan K.C., Mong M.C., Yin M.C. Antioxidative and anti-inflammatory neuroprotective effects of astaxanthin and canthaxanthin in nerve growth factor differentiated PC12 cells. In: *Journal of Food Science*, 2009, 74(7), pp. 225–231.
104. SURAI, A.P., SURAI, P.F., STEINBERG, W., WAKEMAN, W.G., SPEAKE, B.K., SPARKS, N.H. Effect of canthaxanthin content of the maternal diet on the antioxidant system of the developing chick. In: *Journal British Poultry Science*, 2003, 44(4), pp. 612–619.
105. Huang D.S., Odeleye O.E., Watson R.R. Inhibitory effects of canthaxanthin on in vitro growth of murine tumor cells. In: *Cancer Letters*, 1992, 65(3), pp. 209–213.
106. Palozza P., Maggiano N., Calviello G., Lanza P., Piccioni E., Ranelletti F.O., Bartoli G.M. Canthaxanthin induces apoptosis in human cancer cell lines. In: *Carcinogenesis*, 1998, 19, pp. 373–376.
107. Grubbs C.J., Eto I., Juliana M.M., Whitaker L.M. Effect of canthaxanthin on chemically induced mammary carcinogenesis. In: *Oncology* 1991, 48, pp. 239–245.
108. Hueber A., Rosentreter A., Severin M. Canthaxanthin Retinopathy: Long-Term Observations. In: *Ophthalmic Research*, 2011, 46 (2), pp. 103–106.
109. Del Campo J.A., Moreno J., Rodríguez H., Vargas M.A., Rivas J., Guerrero M.G., Carotenoid content of chlorophycean microalgae: factors determining lutein accumulation in *Muriellopsis* sp. (Chlorophyta). In: *Journal of Biotechnology*, 2000, 76, pp. 51–59.

110. Sánchez J.F., Fernández-Sevilla J.M., Ación F.G., Cerón M.C., Pérez-Parra J., Molina-Grima E. Biomass and lutein productivity of *Scenedesmus almeriensis*: Influence of irradiance, dilution rate and temperature. In: *Applied Microbiology and Biotechnology*, 2008, 79(5), pp. 719–729.
111. Richer S., Stiles W., Statkute L., Pulido J., Frankowski J., Rudy D., Pei, K., Tsiplursky M., Nyland J. Double-masked, placebo-controlled, randomized trial of lutein and antioxidant supplementation in the intervention of atrophic age-related macular degeneration: The Veterans LAST study (Lutein Antioxidant Supplementation Trial). In: *Optometry*, 2004, 75(4), pp. 216–230.
112. Solovchenko A., Lukyanov A., Solovchenko O., Didi-Cohen S., Boussiba S., Khozin-Goldberg I. Interactive effects of salinity, high light, and nitrogen starvation on fatty acid and carotenoid profiles in *Nannochloropsis oceanica* CCLA 804. In: *European Journal of Lipid Science and Technology*, 2014, 116 (5), pp. 635–644.
113. Connolly E.E., Beatty S., Thurnham D.I., Loughman J., Howard A.N., Stack J., Nolan J.M. Augmentation of Macular Pigment Following Supplementation with All Three Macular Carotenoids: An Exploratory Study. In: *Current eye research*, 2010, 35(4), pp. 335–351.
114. Seddon J.M., Ajani U.A., Sperduto R.D., Hiller R., Blair N., Burton T.C., Farber M.D., Gragoudas E.S., Haller J., Miller D.T. Dietary carotenoids, vitamins A, C and E, and advanced age-related macular degeneration. In: *JAMA The Journal of the American Medical Association*, 1994, 272(18), pp. 1413–1420.
115. Peng J., Yuan J.P., Wu C.F., Wang J.H. Fucoxanthin, a marine carotenoid present in brown seaweeds and diatoms: metabolism and bioactivities relevant to human health. In: *Marine Drugs*, 2011, 9 (10), pp. 1806–28.
116. Kim S.M., Jung Y.J., Kwon O.N., Cha K.H., Um B.H., Chung D., Pan C.H. A potential commercial source of fucoxanthin extracted from the microalga *Phaeodactylum tricornutum*. In: *Applied biochemistry and biotechnology*, 2012, 166 (7), pp.1843–1855.
117. Hosokawa M., Miyashita T., Nishikawa S., Emi S., Tsukui T., Beppu F., Okada T., Miyashita K. Fucoxanthin regulates adipocytokine mRNA expression in white adipose tissue of diabetic/obese KK-Ay mice. In: *Archives of Biochemistry and Biophysics*, 2010, 504(1), pp. 17–25.
118. Nishikawa S., Hosokawa M., Miyashita K. Fucoxanthin promotes translocation and induction of glucose transporter 4 in skeletal muscles of diabetic/obese KK-Ay mice. In: *Phytomedicine*, 2012, 19, pp. 389–394.
119. Takahashi K., Hosokawa M., Kasajima H., Hatanaka K., Kudo K., Shimoyama N., Miyashita K. Anticancer effects of fucoxanthin and fucoxanthinol on colorectal cancer cell lines and colorectal cancer tissues. In: *Oncology letters*, 2015, 10(3), pp. 1463–1467.
120. Kotake-Nara E., Terasaki M., Nagao A. Characterization of apoptosis induced by fucoxanthin in human promyelocytic leukemia cells. In: *Bioscience Biotechnology and Biochemistry*, 2005, 69(1), pp. 224–227.
121. Maeda H., Hosokawa M., Sashima T., Takahashi N., Kawada T., Miyashita K. Fucoxanthin and its metabolite, fucoxanthinol, suppress adipocyte differentiation in 3T3-L1 cells. In: *International Journal of Molecular Medicine*, 2006, 18(1), pp. 147–152.
122. Kotake Nara E., Kushiro M., Zhang H., Sugawara T., Miyashita K., Nagao A. Carotenoids affect proliferation of human prostate cancer cells. In: *The Journal of Nutrition*, 2001, 131(12), pp. 3303–3306, Disponibil: <https://doi.org/10.1093/jn/131.12.3303>.
123. Das S.K., Ren R., Hashimoto T., Kanazawa K. Fucoxanthin induces apoptosis in osteoclast-like cells differentiated from RAW264.7 cells. In: *Journal of Agricultural and Food Chemistry*, 2010, 58, pp. 6090–6095.
124. Fan X., Bai L., Zhu L., Yang L., Zhang X. Marine algae-derived bioactive peptides for human nutrition and health. In: *Journal of Agricultural and Food Chemistry*, 2014, 62 (38), pp. 9211–9222.
125. Rodrigues D.B., Menezes C.R., Mercadante A.Z., Jacob-Lopes E., Zepka L.Q. Bioactive pigments from microalgae *Phormidium autumnale*. In: *Food Research International*, 2015, 77 (2), pp. 273–279.
126. Manirafasha E., Ndikubwimana T., Zeng X., Lu Y., Jing K. Phycobiliprotein: Potential microalgae derived pharmaceutical and biological reagent. In: *Biochemical Engineering Journal*, 2016, 109, pp. 282–296.
127. Arad (Malis), S., Yaron A. Natural pigments from red microalgae for use in foods and cosmetics. In: *Trends in Food Science and Technology*, 1992, 3, pp. 92–96.
128. Glazer A.N., Hixson C.S. Subunit structure and chromophore composition of rhodophyten phycoerythrins. Porphyrinidium cruentum B-phycoerythrin and B-phycoerythrin. In: *Journal of Biological Chemistry*, 1977, 252, pp. 32–42.
129. Bhattacharya S., Shivaprakash M.K. Evaluation of three *Spirulina* species grown under similar conditions for their growth and biochemicals. In: *Journal of the Science of Food and Agriculture*, 2005, 85, pp. 333–336.
130. Fernández-Rojas B., Hernández-Juárez J., Pedraza-Chaverri J. Nutraceutical properties of phycocyanin. *Journal of Functional Foods*, November 2014, 11, pp. 375–392.
131. Wang N., Manabe Y., Sugawara T., Paul N. A., Zhao J. Identification and biological activities of carotenoids from the freshwater alga *Oedogonium intermedium*. In: *Food Chemistry*, 2018, 242, pp. 247–255.
132. Merete G., Synn Göve L.J. Secondary carotenoids of algae; carotenoids in a natural bloom of *Euglena sanguine*. In: *Biochemical Systematics and Ecology*, 1993, Volume 21, 8, pp.757–763.
133. Hongli C., Haotian Ma Yulin C., Xiaoli Z., Song Q., Runzhi Li. C. Identification and functional characterization of two cytochrome P450 carotenoids hydroxylases from the diatom *Phaeodactylum tricornutum*. In: *Journal of Bioscience and Bioengineering*, 2019, 128 (6), pp. 755–765.
134. Parmar R.S., Singh C. A comprehensive study of eco-friendly natural pigment and its applications. In: *Biochemistry and Biophysics Reports*, 2018, 13, pp 22–26.

DOI: 10.5281/zenodo.3713374
CZU 663.2:66.063.4(478)



INFLUENCE OF MACERATION DURATION ON VIORICA WINES QUALITY

Natalia Vladei*, ORCID: 0000-0003-1094-6812

Technical University of Moldova, 168, bd. Stefan cel Mare, Chisinau, Republic of Moldova

**natalia.furtuna@adm.utm.md*

Received: 01. 15. 2020

Accepted: 03. 18. 2020

Abstract. The subject of the research refers to experimental wines obtained from local selection grape variety Viorica, which were macerated for 4, 8 or 12 hours at 10, 15 and 20 °C. The maceration duration had a positive influence on the general characteristics of the studied wines. The analysis of terpenic compounds by spectro-photometric method showed that increasing the contact time of the must with the solid phase from 4 to 8 hours increases by about 20 % the amount of free terpenes, while decreasing the amount of bound terpenes by 15 %. Once the duration is increased, the concentration of the non-reducing extract is also increased. Considering the increase in the intensity of the color and the REDOX potential with the duration of maceration, the macerated wines for 8 and 12 hours were defined as having oxidation notes with decrease of the sensory quality. Therefore, the maceration regimes for optimal extraction of terpenic compounds were concluded to be at the temperature of 15 °C for 4 hours, thereby increasing the aromatic potential of the local selection grape variety Viorica.

Keywords: *aroma, flavor, local selection variety, maceration, terpenes, wine.*

Introduction

The content of free and glycoside terpenes evidence obvious dynamic changes during the evolution of grapes berries. Knowledge about the bound and free volatile terpenes PVT/FVT ratio is very important for choosing the optimal regime for contact between the solid and liquid phases in order to improve the aromatic quality of wines [1].

High values of bound terpene content in juice and solid fraction are characteristic for several grape varieties, but, considering that they are hydrophilic, they do not essentially contribute to the aroma of the wine.

Therefore, the winemakers are interested in hydrolyzing these potential precursors for the release of volatile terpenes with floral aromas and enhancing the varietal aroma [2]. Depending on the content of free terpenes in the solid fraction, any extraction step during the winemaking process is beneficial in order to obtain a better quality of the wine's aroma.

Materials and methods

In order to carry out this study, the grapes of local selection grape variety *Viorica* were manually harvested from the plantations of the Scientific-Practical Institute of

Horticulture and Food Technologies from Chisinau and processed under micro-vinification conditions at the Technical University of Moldova.

In order to obtain information regarding the influence of the maceration duration and temperature on the content of terpenic compounds, the free and glycozidic monoterpenes were determined by the spectro-photometric method in nine experimental wine variants, by varying the maceration temperature and duration. All the variants were subject of sulfur dioxide addition in a concentration of 75-100 mg/dm³ applied on marc when macerating, gravitational racking and sulphitation after the completion of alcoholic fermentation. The principle of the spectro-photometric determination method consists in separating the aromas by water vapor (distillation) and colorimetric determination of free volatile terpenic aromas (FVT) in neutral medium and bound as precursors (PVT) in acidic environment by colour reaction with sulfuric vanillin [3].

Shortly before the analysis, the grape berries were crushed and homogenized in 200 cm³ phosphate buffer solution (pH 7,0) saturated with NaCl and stored at 4 °C. Subsequently the extracts were filtered and adjusted to pH 7,0 with 20% sodium hydroxide solution.

In order to determine the distribution of volatile monoterpenes in the solid and liquid fractions, the skin, pulp and seeds were manually removed. The pulp was homogenized and filtered to obtain the juice. The skins and the pulp residues were weighed and separately homogenized each in 200 cm³ saturated phosphate buffer solution (pH 7,0) and stored for 3 and 6 days at 4 °C. Subsequently the extracts were filtered and adjusted to pH 7,0 with 20% sodium hydroxide solution. In steam distillation flask there was added 50 cm³ of the sample, the pH of which was previously adjusted to 7,0 with 20% sodium hydroxide solution. The distillate was collected in a stoppered test tube, which was placed in an ice container. The distillation was stopped when collecting the volume 20 cm³ of distillate containing FVT. Without being stopped vapor flow, the test tube was replaced with another stoppered test tube of the same volume. In the distillation flask was added 2.5 cm³ of 20% orthophosphoric acid solution. The distillation was stopped upon accumulation of 20 cm³ of distillate, which contained PVT.

In two stoppered test tubes (10 cm³), there were taken 5 cm³ of the first and the second distillates. The absorbances of the samples were related to the calibration curve and were established the concentrations in terpenic aromas expressed in mg/cm³.

The content of FVT and PVT was calculated according to the Eq.(1):

$$\text{FVT or PVT} = a \times b/c \times d, (\text{mg/dm}^3) \quad (1)$$

where: a - the concentration of linalool read on the calibration curve, mg/dm³;

b - volume of distillate collected by distillation of samples, dm³;

c - volume of must used for distillation, dm³;

d - volume of aliquot used for spectro-photometric measurements, dm³.

The sensory analysis was carried out with the participation of seven tasters, which were offered for tasting the wines obtained from the grapes fermented with three local selection yeast strains. Sensory evaluation was performed according to a 100 points scale (ISO 4121:2003) and a specially designed form to highlight aromatic characteristics of wines [4]. Tasters rated the wines with points after what an average score was obtained for each sample, including flavor descriptors. Sensory quality assessment based on the calculation of weighted average scores was performed according to Eq.(2).

$$S_{wa} = S_{unwa} \times f_w \quad (2)$$

where: S_{unwa} – unweighted average scores (the arithmetic mean of the results);
 f_w – weighting factor.

The summation of the weighted average scores to obtain the total average score served to establish the organoleptic quality of the product [5].

Results and discussion

The content of free and bound monoterpenes reveals obvious dynamic changes during the evolution of grape berries. In the case of grape varieties for winemaking, the knowledge about the distribution in juice and skin, as well as the content of FVT and PVT, are very valuable for the application of contact treatments between the solid and liquid phase in order to optimize the aromatic quality of the wines [6].

Analyzing Figure 1, we see that the FVT and PVT contents in the Viorica variety averaged 0,02 and 0,37 mg/kg respectively. The distribution of FVT and PVT in juice, pulp and skin varies differently depending on the contact duration.

From Figure 1 we can observe important differences between the scores given for each characteristic, depending on the yeast strain used for fermentation.

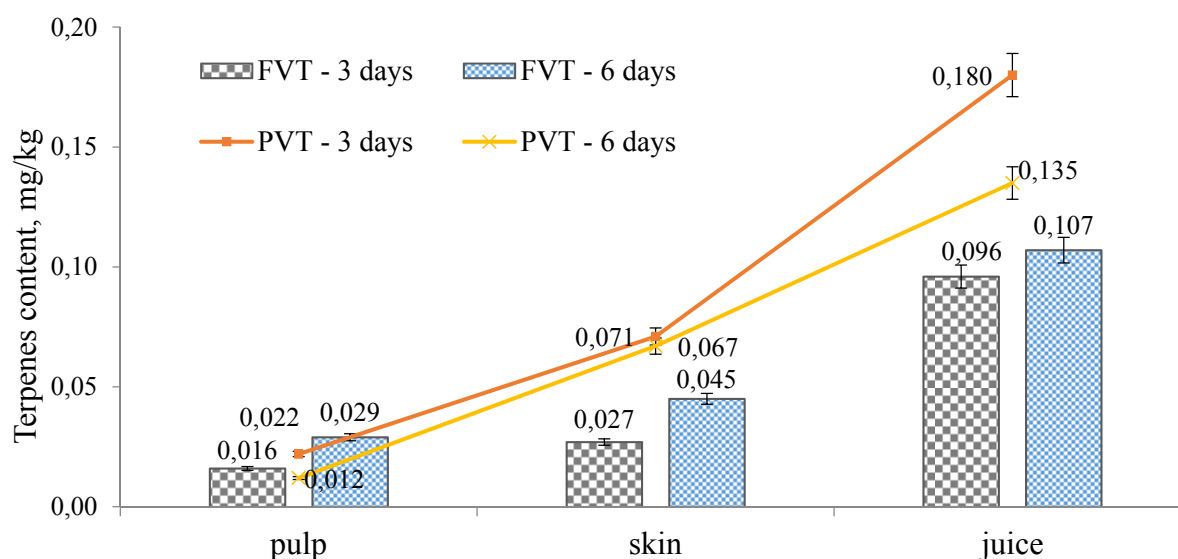


Figure 1. Distribution of FVT and PVT in different parts of Viorica variety grapes.

Also, from Figure 1, we observe a greater difference of the ratio PVT/FVT in the skin, both in the case of maintaining fractions for 3 days (2,63) and for 6 days (1,49), compared to the juice (1,88 – 3 days and 1,26 – 6 days) and pulp (1,07 – 3 days and 0,41 – 6 days). From the presented data, we observe that there is a general tendency of increasing the content of free terpenes with the increase of the contact time for all three fractions, which denotes an inevitable hydrolysis of the glycosidic precursors in the grapes. Thus, the hydrolysis of bound terpenes and the subsequent release of free terpenes allows improving the quality of the varietal aroma of wines from the local grape variety Viorica.

The results obtained from this initial assessment of the volatile and potentially volatile terpenes content, as well as their distribution between the component parts of the grape berries of a local selection variety develop a particular interest for varietal white wine production in Republic of Moldova.

Considering the significant influence of the raw material characteristics for the final product, it is very important to determine the effects of maceration on the general

characteristics of the wine, which is expressed by: improving the extraction of the aroma precursors and the composition of the wines. In order to study how different factors such as temperature and maceration time are reflected on the physico-chemical and sensory composition of wines, the most important physico-chemical parameters have been determined (Table 1).

Analyzing the data in Table 1, it can be observed that maceration duration and temperature significantly influence some characteristic parameters of wines. First of all, there is a tendency to increase the total acidity of samples during the maceration due to the migration of the organic acids from the solid parts of the berries in the liquid phase, with the concomitant decrease of the pH. Some researchers believe that this is due to the extraction and solubilisation of tartrates from the berry skin [7].

Regarding the content of volatile acidity, it can be mentioned that it increases insignificantly with the increase of the maceration time. At the same time, with the increase of the maceration duration and temperature is observed the increase of the non-reducing dry extract concentration with up to 0,8 g/dm³ compared to the initial version.

Table 1

Physico-chemical indices of *Viorica* variety dry white wines depending on the duration and temperature of maceration

Physico-chemical indices	V1	V2	V3	V4	V5	V6	V7	V8	V9
Alcohol, ± 0,1 % vol.	11,6	11,7	11,7	11,6	11,6	11,7	11,6	11,7	11,7
Titrateable acidity, ± 0,08 g/dm ³	6,84	6,84	7,05	6,65	6,72	6,94	6,52	6,75	6,75
Volatile acidity, ± 0,04 g/dm ³	0,26	0,33	0,33	0,26	0,33	0,33	0,40	0,40	0,40
Non-reducing dry extract, ± 0,5 g/dm ³	17,1	17,3	17,4	17,4	17,6	17,7	17,6	17,7	17,9
pH, ± 0,01 units	3,08	3,02	2,95	3,16	3,11	3,07	3,18	3,15	3,09
REDOX potential, ± 10 mV	224	228	235	239	241	246	248	257	264
Organoleptic score, ± 0,1 points (out of 100)	76	77	80	79	81	81	80	79	78

Legend: **V1** – t=10 °C and τ=4 h; **V2** – t=10 °C and τ=8 h; **V3** – t=10 °C and τ=12 h; **V4** – t=15 °C and τ=4 h; **V5** – t=15 °C and τ=8 h; **V6** – t=15 °C and τ=12 h; **V7** – t=20 °C and τ=4 h; **V8** – t=20 °C and τ=8 h; **V9** – t=20 °C and τ=12 h.

The REDOX potential has higher values (224–264 mV) as the contact time of the solid and liquid phase increases, but also in parallel with the increase of the maceration temperature. These results show that during the maceration takes place the extraction of polyphenolic compounds from the skin and pulp.

These results denote a larger polyphenol-oxidase enzymatic load of the *Viorica* variety, and the polyphenol compounds extracted during maceration show an increased

oxidation tendency. In this respect, researchers underline the action of polyphenol-oxidase on cinnamates (especially cinnamic tartrate), as the most important factor of browning [8].

These oscillations are due to the interaction of two interdependent phenomena: the extraction of polyphenols from the skin in the liquid phase (which leads to the tendency to browning) and the oxidation and polymerization reactions of these compounds (which, respectively, are manifested by their diminution). The preponderance of one mechanism or another depends largely on the concentration of oxygen dissolved in the must, the content of oxidase enzymes and temperature [9].

The influence of the maceration duration on the sensory analysis of the volatile aromatic complex of the studied wines is shown in Figure 2, from which we can observe greater values of the taste persistence, also of flavor and color intensity as the maceration duration increases. Thus, an increase of the taste persistence and color intensity is very important for all three maceration durations, which may be due to the increased accumulation of polyphenols and organic acids that takes place during this process.

Considering the increase of the color intensity and the REDOX potential with the maceration duration, the wines macerated for 8 and 12 hours were defined as having oxidation notes, the best results being obtained for 4 hours maceration.

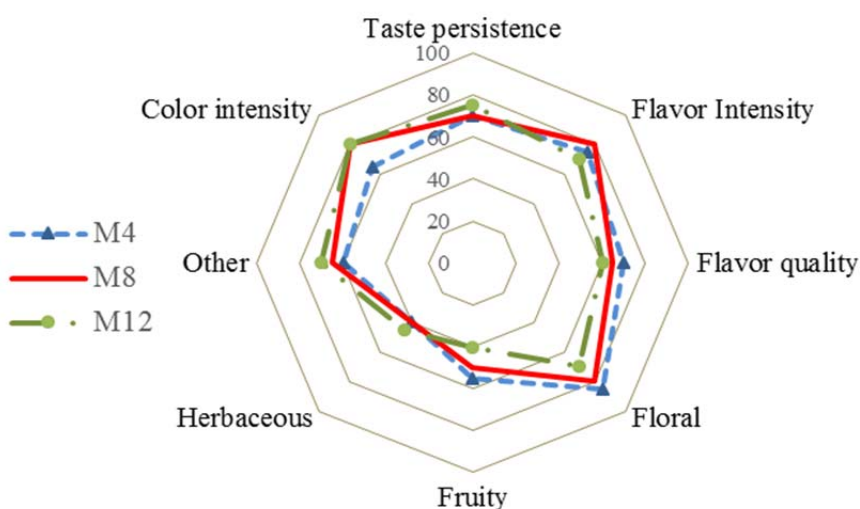


Figure 2. Sensory analysis of *Viorica* wines obtained through different maceration time (M4 – 4 hours; M8 – 8 hours; M12 – 12 hours) at the temperature of 15 °C.

Regarding the intensity and quality of the aroma, although there are clear differences in the aromas content depending on the maceration duration, the organoleptic assessment results showed significant differences, the 4 hours maceration reflecting higher values, also being characterized by notes of citrus, sage, basil, acacia and field flowers. In addition, the obtained wines are characterized by a balanced sensory profile with peaks oriented towards the class of floral aromas, which define the typicality of this variety [10].

The results obtained from the spectrophotometric analysis are indicated in Table 2, from which we can notice significant differences between the content of FVT and PVT depending on the maceration duration and temperature.

Table 2

Contents of free volatile terpene (FVT) and potentially volatile terpene (PVT) depending on the duration and temperature of maceration

Variants	FVT, $\mu\text{g}/\text{dm}^3$	PVT, $\mu\text{g}/\text{dm}^3$	FVT/PVT
V1	175,18	312,35	1,78
V2	191,62	310,42	1,62
V3	213,79	339,93	1,59
V4	203,45	346,68	1,15
V5	227,80	287,03	1,26
V6	209,58	346,85	1,66
V7	211,53	294,03	1,39
V8	294,28	338,42	1,24
V9	302,17	374,69	1,70

Legend: **V1** – $t=10\text{ }^\circ\text{C}$ and $\tau=4\text{ h}$; **V2** – $t=10\text{ }^\circ\text{C}$ and $\tau=8\text{ h}$; **V3** – $t=10\text{ }^\circ\text{C}$ and $\tau=12\text{ h}$;

V4 – $t=15\text{ }^\circ\text{C}$ and $\tau=4\text{ h}$; **V5** – $t=15\text{ }^\circ\text{C}$ and $\tau=8\text{ h}$; **V6** – $t=15\text{ }^\circ\text{C}$ and $\tau=12\text{ h}$;

V7 – $t=20\text{ }^\circ\text{C}$ and $\tau=4\text{ h}$; **V8** – $t=20\text{ }^\circ\text{C}$ and $\tau=8\text{ h}$; **V9** – $t=20\text{ }^\circ\text{C}$ and $\tau=12\text{ h}$.

This could be explained by the fact that the bound terpenes were hydrolyzed by the enzymes with β -glucosidase activity from the grapes and transformed into the free form.

From the results above we observe that increasing the contact time of must with the solid phase from 4 to 8 hours increases by about 20% the amount of free terpenes, while decreasing the amount of bound terpenes by 15%.

The lowest PVT/FVT ratio was recorded in the case of maceration at $15\text{ }^\circ\text{C}$ for 4 hours – V4 (1,15) compared to the sample macerated 4 hours at $10\text{ }^\circ\text{C}$ – V1 (1,78).

As well, we found that as the maceration temperature and duration increased, the amount of volatile terpenes increased and the content of precursors decreased.

However, in the case of maceration at $15\text{ }^\circ\text{C}$ for 8 hours a decrease of the PVT/FVT ratio is observed by 25 % compared to the maceration for 4 hours, and when maceration took 12 hours there is a 31 % increase compared to the sample macerated for 8 hours, meaning that the optimal extraction duration of volatile terpenic compounds is 8 hours.

Considering that terpenic glycosides are a non-volatile form of terpenes, which are considered to be the aromatic potential from which, by enzymatic or acidic hydrolysis, volatile terpenic fractions are released, increasing the precursors form of the terpenes content is very important [11].

This could explain the fact that the wines obtained by must maceration have an extended duration of preservation of the organoleptic quality, especially maintaining the specific varietal aroma.

The conditions for optimizing the production of wines with a high content in terpenic compounds were statistically processed by a factorial analysis using the response surface method. The results that were obtained and detailed above revealed that the most relevant variables with direct effect on the FVT and PVT content in the wines were the temperature (X_1) and the maceration duration (X_2).

In order to determine the coefficients of regression equation it was used the partial least squares method [12].

The equation Eq.(3) describes the polynomial square with two factors model:

$$Y = a + b \cdot X_1 + c \cdot X_2 + d \cdot X_{12} + e \cdot X_{22} + f \cdot X_1 \cdot X_2 \quad (3)$$

The response surface model was created with the MathCad program, which used the Central Composite Design type: 2 factors, 2 levels (+1, -1), 1 central point, 1 block (one experiment series).

The mathematical models correspond to a second degree polynomial equation.

The graphs of tridimensional response surface (Figure 3 a,b) are the graphic representation of the interaction between the two selected factors (temperature and duration) in order to determine the optimal concentration and further to reach the maximum concentration of free or bound volatile terpenic aromas for the local selection grape variety *Viorica*.

From Figure 3(a) we can note that the maximum of free terpenes extraction is at 15 °C in the interval of 8 – 12 hours.

The comparison between the experimental content of terpenes and the content predicted by the regression model imply that it can be used for future prediction of the Y response values (free and bound terpenes content) corresponding to particular values of regression variables.

Thus, the estimated mathematical model is relevant and the data are significant and reproducible.

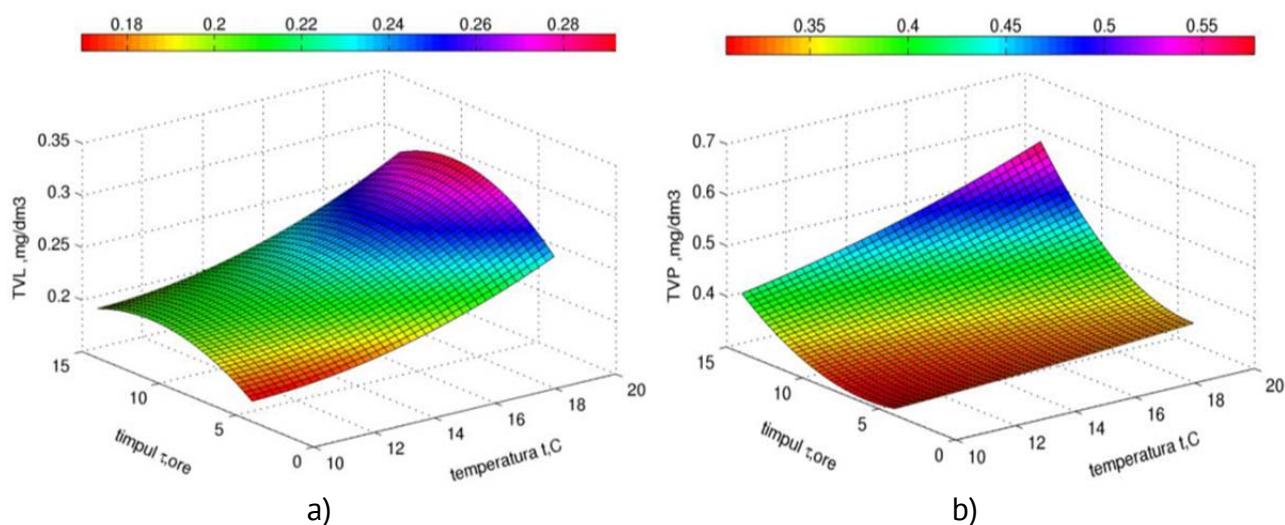


Figure 3. Response surface describing the variation of FVT (a) and PVT (b) content for the *Viorica* variety wines depending on temperature and duration.

Conclusions

Following the study, it can be mentioned that the maceration has a positive influence on the general characteristics of the wines obtained from local selection grapes *Viorica*.

According to these results, the maceration with extended duration does not lead to obvious improvements, observing a diminution of the sensory quality with the increase of the maceration duration (8 and 12 hours), being recommended a short maceration for 4 hours.

When the maceration temperature rises from 10 °C to 15 °C there is an essential leap in the content of volatile terpenes by 58 % and by 53 % for bound form. It was established that increasing the contact time of the must with the solid phase from 4 to 8 hours increases by about 20 % the amount of free terpenes, while decreasing the amount of bound terpenes by 15 %.

The maceration regimes for optimal extraction of terpenic compounds were concluded to be at the temperature of 15 °C for 4 hours, thereby increasing the aromatic potential of local selection variety *Viorica*.

References

1. Mateo JJ., Jimenez M. Monoterpenes in grape juice and wines. In: *Journal of Chromatography A*, 2000, 881, pp. 557–567.
2. Gonzalez-Barreiro C., Rial-Otero R., Cancho-Grande B., Simal-Gandara, J. Wine aroma compounds in grapes: A critical review. In: *Critical Reviews in Food Science and Nutrition*, 2013, 55(2), pp. 202-218.
3. Dimitriadis E., Williams P.J. The development and use of a rapid analytical technique for estimation of free and potentially volatile monoterpene flavorants of grapes. In: *American Journal of Enology and Viticulture*, 1984, 35, pp. 66–71.
4. Tzia C., Giannou V., Lignou S., Lebesi D. Sensory Evaluation of Foods. In: Varzakas T., Tzia C., ed *Handbook of Food Processing: Food Safety, Quality, and Manufacturing Processes*. CRC Press: Taylor & Francis Group, 2015, pp. 42-72.
5. Lawless H.T., Heymann H. *Sensory evaluation of food: principles and practice*, New York: Springer, 2010.
6. Maicas S., Mateo JJ. Hydrolysis of terpenyl glycosides in grape juice and other fruit juices: A review. *Applied Microbiology and Biotechnology*, 2005, 67, pp. 322-335.
7. Ribereau-Gayon P., Glories Y., Maujean A., Dubourdieu D. *Handbook of Enology Volume 2: The Chemistry of Wine and Stabilization and Treatments*. Chichester. John Wiley & Sons Ltd., 2006.
8. Darias JJ., Rodríguez O., Díaz E., Lamuela-Raventós R.M. Effect of skin contact on the antioxidant phenolics in white wine. In: *Food Chemistry*, 2004, 71, pp. 483-487.
9. Bayonove C., Baumes R., Crouzet J., Gunata Z. Arômes. In: *Oenologie-fondements scientifiques et technologiques*. Tec & Doc Lavoisier, Paris, 1998, pp. 163-235.
10. Furtuna N. Analysis of volatile compounds in three grape varieties of local selection from Republic of Moldova, In: *Research and Science Today*, 2014, 1(7), pp. 124-131.
11. Antoce O. A. *Oenologie, Chimie și analiză senzorială*. Editura Universitaria, Craiova, 2007.
12. Clocotici V. *Introducere în statistica multivariată*. Universitatea “Alexandru Ioan Cuza” Iași, 2007. [accesat 06.09.2019]. Disponibil: <http://www.scribd.com/doc/75749584/58/Analiza-dispersională-bifactorială>.

DOI: 10.5281/zenodo.3713376
CZU 577.164.2:664.8.036:634.21



STABILITY OF ASCORBIC ACID DURING THE TECHNOLOGICAL PROCESSES OF APRICOT COMPOTE FABRICATION

Antoanela Patras*, ORCID: 0000-0002-4054-4884,
Alina Loredana Baetu, Marius Baetu

"Ion Ionescu de la Brad" University of Agricultural Sciences and Veterinary Medicine, 3, Mihail Sadoveanu Alley, Iași,
700490, Romania

*Corresponding author: Antoanela Patras, apatras@uaiasi.ro

Received: 02. 18. 2020

Accepted: 03. 24. 2020

Abstract. Apricots are fruits with a short period of fresh-consumption and the compote fabrication is a usual method for their preservation. The present research is studying the changes in total vitamin C content, as well as the transformations between ascorbic acid and dehydroascorbic acid in four different phases of the technological flow of apricot compote fabrication. The ascorbate oxidase activity was also evaluated. The studied samples are represented by different stages of apricots during the technological flow of compote fabrication: raw material, washed fruits, after blanching (at 70 °C for 3 min), and finished product (after pasteurisation by maintaining at 95 °C the inside temperature of filled and closed jar for 15 min). Also, the ascorbic acid content after 3 months of compote preservation in the dark at 10 °C and respectively, 25 °C was measured. Three analytical methods were used: HPLC, reflectometry (using the Reflectoquant), and titrimetry (using 2, 6-dichlorophenol indophenol). The results proved that thermal processes seriously decreased the ascorbic acid content and increased the dehydroascorbic acid. The 3 months preservation at both temperatures has slight influence on the content of ascorbic acid, but at 25 °C the diminution of ascorbic acid and the increase of dehydroascorbic acid were more significant than at 10 °C.

Keywords: *ascorbate oxidase, blanching, dehydroascorbic acid, pasteurisation, preservation, technological flow, temperature, vitamin C.*

I. Introduction

Apricots are seasonal fruits preferred by consumers, being considered very tasty, with a specific and pleasant flavour [1]. Except the sensorial qualities, they are nutritious fruits, with an important content of carbohydrates, proteins, organic acids, minerals, but also antioxidants, such as ascorbic acid, carotene, phenolic compounds. According to previous studies, the apricots' content in vitamin C ranges between 7-10 mg/100 g [2].

During the storage period, in the vegetables and fruits harvested at maturity, there is a continuous decrease in the amount of ascorbic acid, the intensity of the decrease in the content of ascorbic acid being dependent on the species, variety, temperature [3]. By keeping vegetables and fruits for a few days at ambient temperature, a significant decrease of vitamin C content takes place [4]. Temperature has a great influence on the stability of

ascorbic acid in vegetables and fruits. For example, in green peas the decrease is 50% after 4 days of storage at ambient temperature and 10% at 0 °C; for green beans vitamin C decreases by 72% after 6 days at ambient temperature and by 12% by storage at 0 °C the same time period. According to Agar et al. [5], slices of kiwi stored 6 days at 0, 5 and 10 °C showed a decrease in ascorbic acid content and an increase in dehydroascorbic acid content compared to fresh slices, and with the increase of the temperature these modifications are more important. The structural features of each horticultural product influence the decrease of the ascorbic acid content. If the products have a relatively thick skin, this prevents the diffusion of oxygen inwards and the oxidation of ascorbic acid occurs slower [4]. Potatoes can contribute to human nutrition with a significant supply of vitamin C, but lose up to 50% of the ascorbic acid content after peeling and boiling in water; the loss is half by baking them in the oven, without peeling [6]. Ascorbic acid is thermally unstable, so it is important to know its content in products after thermic processing. During blanching, the level of ascorbic acid decrease depends on the type and duration of the treatment, and losses can be limited by the inactivation of oxidizing enzymes, as ascorbate oxidase. Smaller vitamin C diminutions are recorded in steam blanching (10-30 %) than in hot water blanching (10-50%) [7].

Ascorbic acid, AA, (vitamin C) is a water-soluble vitamin and a powerful antioxidant essential for a proper activity of the human body. It is involved in the immunity; intestinal iron absorption; biosynthesis of some neurotransmitters, of collagen and carnitine; decrease of lipid peroxidation; inhibition of carcinogenic nitrosamines production; reducing of the inflammatory response (anti-allergic action due to its anti-histaminic properties); diminution of the susceptibility to influenza virus, etc. The vitamin C does not accumulate as deposits in the body, so it needs to be constantly introduced from food. As previously stated, ascorbic acid is a reducing agent. It is oxidized to dehydroascorbic acid (DHA), with the loss of hydrogen (Figure 1). DHA is a soft oxidizing agent which can accept hydrogen to reform AA. In most biological systems, AA is present in much higher quantities than DHA, and is considered the active form of the vitamin C [8]. AA has a predominant role in ensuring immunity and participates in intestinal iron absorption processes [9, 10].

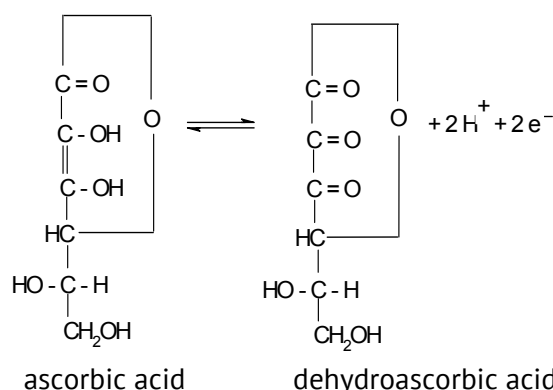


Figure 1. The interconversion ascorbic acid – dehydroascorbic acid.

II. Materials and methods

The studied material was represented by 4 stages of the technological flow of apricot compote fabrication: apricot raw material (A), washed fruits (W), after blanching with hot water at 70 °C for 3 min (B) and finished product after pasteurisation by maintaining at 95 °C the inside temperature of filled and closed jar for 15 min – apricot compote. From the compote were analysed the apricots (AC) and the syrup enveloping the fruits (SC). The finished product was also analysed, after a storage period of 3 months at 10 °C and 25 °C in order to research the stability of ascorbic acid. The samples were supplied by the company S.C. Contec Foods S.R.L. Tecuci in two consecutive years.

The extraction of ascorbic and dehydroascorbic acids for high-performance liquid chromatography (HPLC) used a solution of metaphosphoric acid stabilised with Na_3PO_3 (5%). The reduction of dehydroascorbic acid was performed by the reaction with dithiothreitol. The chromatographic conditions were: solution of sulphuric acid 0.0035 N as mobile phase, 0.60 mL/min flow rate, 30 °C temperature, UV detection. Two other methods were also used for the analysis of the total ascorbic acid content: the titrimetric method using 2, 6 dichlorophenol indophenol (2,6 DCFIF) [11, 12] and the reflectometric method using the Reflectoquant RQFlex, Merck [13]. The activity of ascorbat oxidase was assessed spectrophotometrically at 265 nm [14].

III. Results and discussions

The mean values obtained for the ascorbic acid content by the use of 2, 6 dichlorophenol indophenol and Reflectoquant were similar and during the second year were inferior compared to the first year (Figure 2). This difference can be explained by the initial parameters of the raw material (depending on the transportation/preservation conditions of apricots prior to industrialisation, but also to the geo-pedo-climatic conditions, variety, maturity stage and harvest period of the two studied years). But this research focused on the changes of the AA and DHA contents of the raw material due to the technological processes of compote fabrication, and to post-fabrication preservation conditions, unconcerned of the initial quality of the fruits.

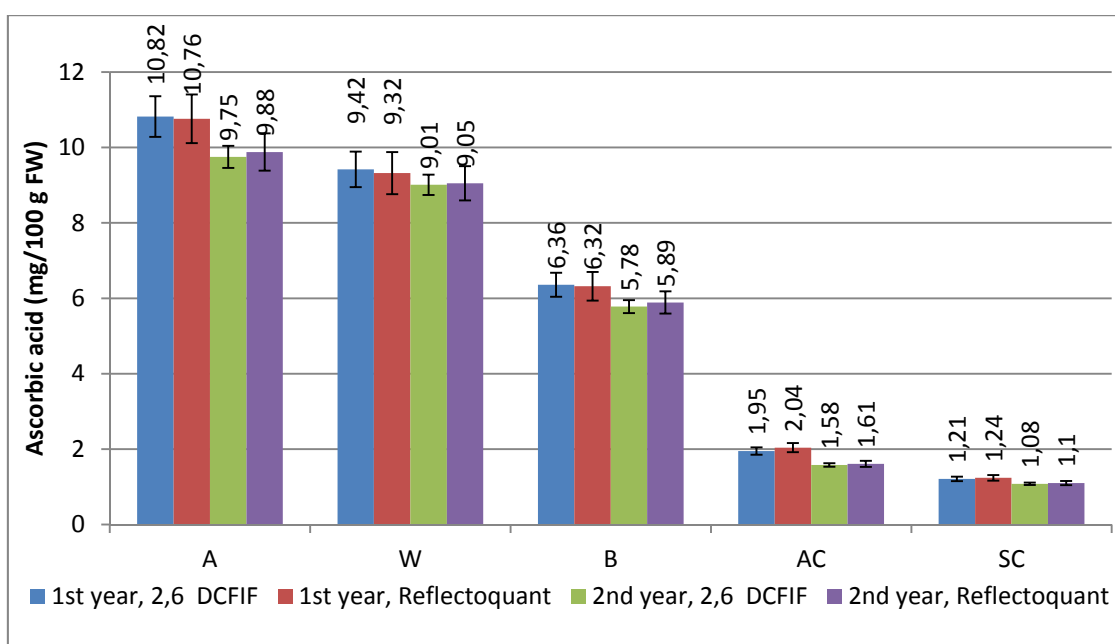


Figure 2. Dynamics of ascorbic acid content during the technological flow of apricot compote fabrication: apricot raw material (A), washed fruits (W), after blanching (B), apricots from compote (AC), and syrup from compote (SC), during two different years and employing 2,6 dichlorophenol indophenol and Reflectoquant methods.

Results are means of 3 determinations \pm standard deviation.

The washing process decreased the AA content by about 13%, while the blanching with hot water at 70 °C for 3 min, diminished it by about 41% compared to raw material. The last procedure, pasteurisation by maintaining at 95 °C the inside temperature of filled and closed jar for 15 min, strongly decreased the AA content of both apricots from compote (by 82%) and enveloping syrup (by 89%) compared to initial fruits. The difference between

the content of ascorbic acid in fruits and syrup of the final compote is light, proving the diffusion of AA outside from the fruits, which could also justify the strong decrease compared to raw material (Figure 2).

Concerning the preservation conditions (Figure 3), the studied period decreased the AA in fruits by 15% at 10 °C and by 46% at 25°C, and in the syrup by 8% at 10 °C and 21% at 25°C, respectively. The apricots in compote have more ascorbic acid than the enveloping syrup.

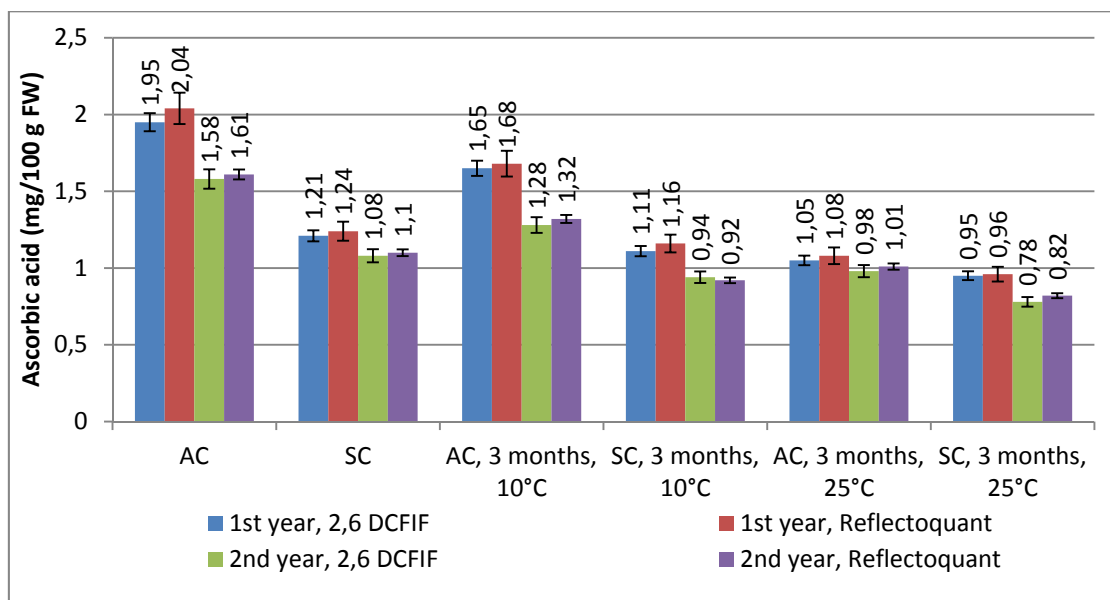


Figure 3. Ascorbic acid content after 3 months of preservation at 10 °C and 25 °C: apricots from compote (AC), syrup from compote (SC), during two different years and employing 2,6 dichlorophenol indophenol and Reflectoquant methods. Results are means of 3 determinations±standard deviation.

The HPLC analysis enables the determination of both AA and DHA and the results are shown in Figures 4 and 5. During the technological flow and preservation period, the decrease of ascorbic acid content is accompanied by the increase of the dehydroascorbic acid, which proves the oxidation of AA to DHA, according to the transformation presented in Figure 1. The general trend of the evolution of AA is similar to the one revealed by the other two employed methods (titrimetric and reflectometric). The HPLC determination brings a new result: the studied processes, most probably, determine the degradation of AA to other compounds, except the DHA. This is proved by the fact that the diminution of ascorbic acid is more important than the increase of dehydroascorbic acid. This fact is obvious for the pasteurisation (which is an aggressive thermal treatment): the diminution of ascorbic acid in AC and SC (with a mean of 8.6 mg/100 g FW and respectively, 9.2 mg/100 g FW) is accompanied by a lighter increase of dehydroascorbic acid (0.55 mg/100 g FW and respectively, 0.67 mg/100 g FW), compared to the raw material. The other thermal treatment, the blanching, determined a decrease of AA with a mean value of 2.8 mg/100 g FW and an increase of DHA with 0.37 mg/100 g FW. During the preservation, the degradation of ascorbic acid and the formation of dehydroascorbic acid are more equilibrated (Figures 4 and 5). As expected, at 10 °C, the degradation of ascorbic acid and the formation of dehydroascorbic acid are less important than at 25 °C. In the fruits from compote, the content of AA is bigger and the DHA is smaller than in the syrup, but differences are very light.

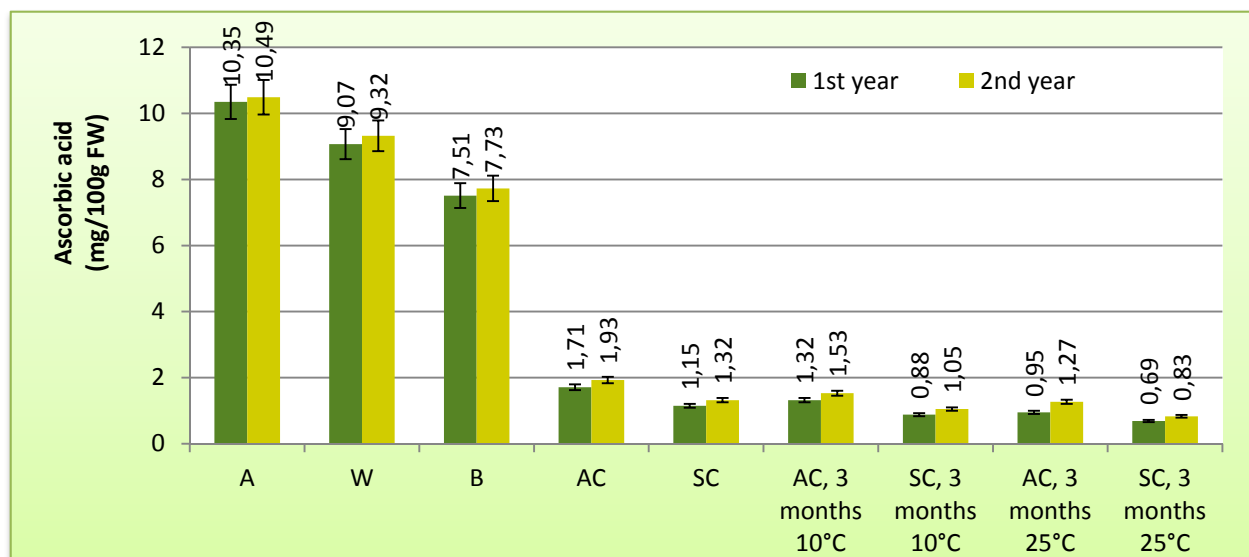


Figure 4. HPLC content of ascorbic acid during the technological flow of apricot compote fabrication and the 3 months preservation at 10 °C and 25 °C: apricot raw material (A), washed fruits (W), after blanching (B), apricots from compote (AC), and syrup from compote (SC), during two different years.

Results are means of 3 determinations \pm standard deviation.

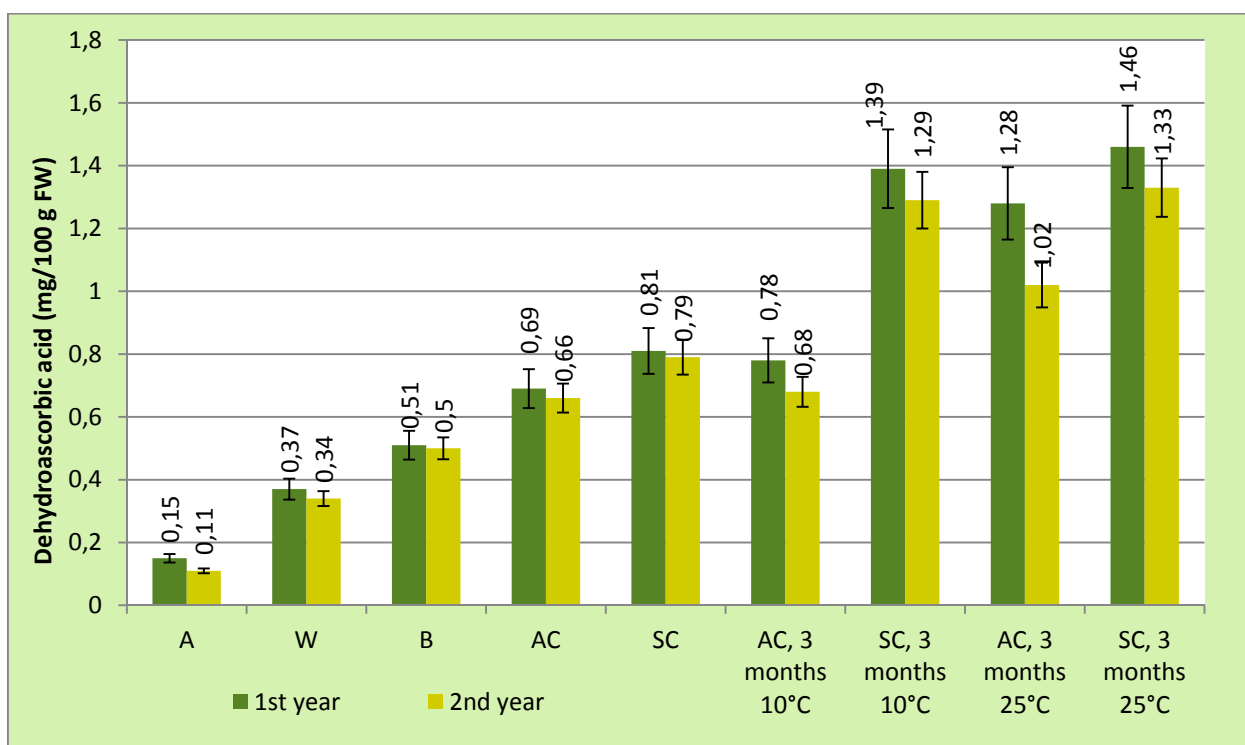


Figure 5. HPLC content of dehydroascorbic acid during the technological flow of apricot compote fabrication and the 3 months preservation at 10 °C and 25 °C: apricot raw material (A), washed fruits (W), after blanching (B), apricots from compote (AC), and syrup from compote (SC), during two different years.

Results are means of 3 determinations \pm standard deviation.

The ascorbate oxidase is the enzyme which catalyses the direct oxidation of ascorbic acid to dehydroascorbic acid. Its activity is strongly inhibited by blanching, being reduced by more than 3 times in both years, and is completely inactivated by pasteurisation

(Table 1). In fact, the enzymes inactivation, as well as the microbial destruction are the main goals of the technologies used for fruits industrialisation. This inactivation of enzymes justifies the good preservation and the stability of AA in the compote, which is proved by light decrease of ascorbic acid and also, light increase of dehydroascorbic acid during the 3 months of conservation at both studied temperatures.

Table 1

Ascorbat oxidase activity ($\mu\text{M/g}\cdot\text{min}$) during 3 phases of the technological flow of apricot compote fabrication, during two different years*

	1 st year		2 nd year		
	after blanching (B)	apricots from compote (AC)	apricot raw material (A)	after blanching (B)	apricots from compote (AC)
apricot raw material (A)	2.15±0.35	0.00±0.00	7.56±1.30	2.25±0.36	0.00±0.00

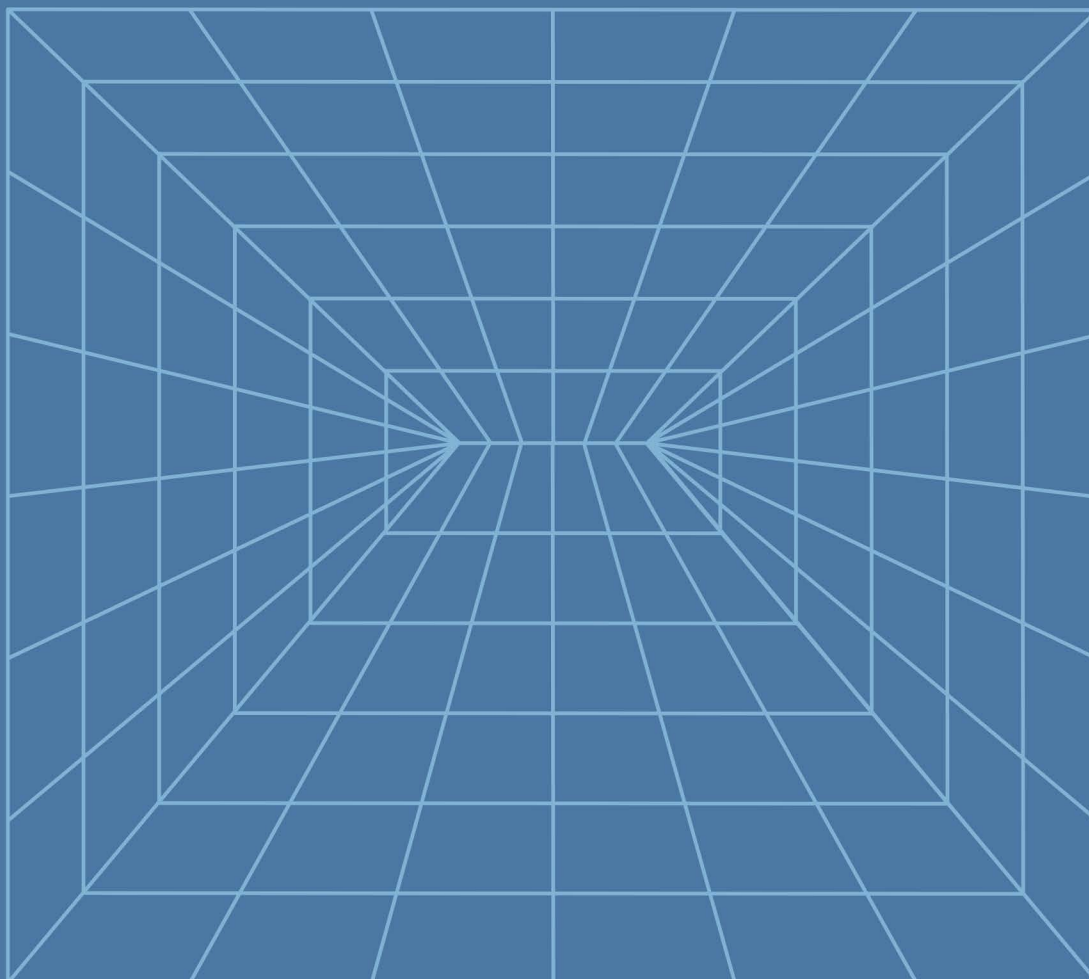
* Results are means of 3 determinations±standard deviation.

Conclusions

During the technological flow of compote fabrication, only the thermal processes seriously decreased the ascorbic acid content and increased the dehydroascorbic acid and these transformations are more important when the temperature and the duration of the process are more important. The 3 months preservation at both temperatures has slight influence on the content of ascorbic acid, but at 25 °C the diminution of ascorbic acid and the increase of dehydroascorbic acid were more significant than at 10 °C. These results confirmed the previous knowledges and brought new information about the exact values of the contents in ascorbic and dehydroascorbic acids after specific technological processes and after preservation in certain conditions.

References

- Alexe C., Vintilă M., Caplan I., Lămureanu G., Chira L. Comparative study of processed products from cultivars of the native apricot. *Scientific Papers-Series B, Horticulture*, 2017, 61, pp. 27-32.
- Rahović, D., Čolić, S., Bakić, I., Stanković, S., Tepić, A. Suitability of Novi Sad Apricot Cultivars and Selections for Compotes. *Contemporary Agriculture*, 2017 66 (3-4), pp. 1-7.
- Gherghi A., Burzo I., Bibicu M., Mărgineanu L., Bădulescu L., *Biochimia și fiziologia legumelor și fructelor*, Editura Academiei Române, București, 2001.
- Cuciureanu R. *Igiena alimentului*, Editura Performantica, Iași, 2010.
- Agar, I.T., Streif, J., Bangerth, F. Effect of high CO₂ and controlled atmosphere on the ascorbic and dehydroascorbic acid content of some berry fruits. *Postharvest Biology and Technology*, 1999, 11, pp. 47–55.
- Cuciureanu R. *Elemente de igiena mediului și a alimentației*, Editura Junimea, Iași. 2002.
- Beceanu D. *Tehnologia prelucrării legumelor și fructelor*, Editura Ion Ionescu de la Brad, Iași. 2009.
- Deutsch, J. C. Ascorbic acid and dehydroascorbic acid interconversion without net oxidation or reduction. *Analytical biochemistry*, 1997, 247 (1). pp. 58-62.
- Rodica Sturza. Principii moderne de analiză a alimentelor. *Ch.: UTM*, 2006.- 310 p.
- Rodica Sturza, Olga Deseatnicova, Valentin Gudumac. Carența de fier în alimentație și modalități de eradicare. *Ch.: UTM*, 2008.- 223 p.
- Standard de stat al R.România - ISO 6557-2: 1984, 1984.
- Standard de stat al R.România - ISO 6557-1: 1986, 1986.
- Eberhardt M.V., Lee C.Y., Liu R.H., Nutrition: antioxidant activity of fresh apples. *Nature*, 2000, 405 (6789), pp. 903-904.
- Oberbacher, M. F., Vines, H. M. Spectrophotometric assay of ascorbic acid oxidase. *Nature*, 1963, 197 (4873), pp. 1203-1204.



PRINT

ISSN 2587-3474



9 772587 347007



ONLINE

ISSN 2587-3482



9 772587 348004